E-ISSN 2228-8082

Volume 74, Number 5, May 2022

SMJ

Siriraj Medical Journal

The world-leading biomedical science of Thailand

MONTHLY

ORIGINAL ARTICLE

REVIEW ARTICLE

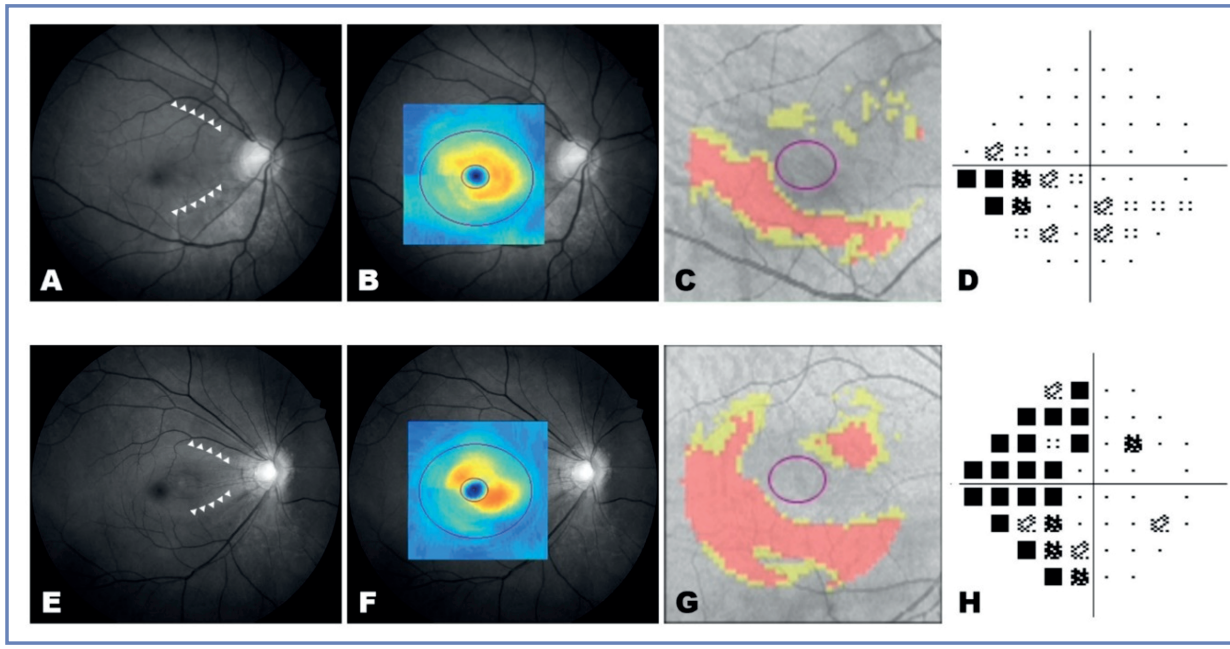

Indexed by

Scopus®

By Anuwat Jiravarnsirikul, et al.

https://he02.tci-thaijo.org/index.php/sirirajmedj/index

E-mail: sijournal92@gmail.com

Siriraj Medical Journal SMJ

Volume 74, Number 5, May 2022

ORIGINAL ARTICLE

REVIEW ARTICLE

SIRIRAJ MEDICAL JOURNAL

www.smj.si.mahidol.ac.th

SIRIRAJ MEDICAL JOURNAL is published bimonthly, 6 issues a year (Jan-Feb, Mar-Apr, May-Jun, Jul-Aug, Sep-Oct and Nov-Dec) and distributed by the end of the last month of that issue.
SIRIRAJ MEDICAL JOURNAL is listed as a journal following the Uniform Requirements for Manuscripts Submitted to Biomedical Journals (URM) by the International Committee of Medical Journal Editors (ICMJE) since 9 July 2010 [http://www.icmje.org/journals.html].

Keratinocyte Culture: Siriraj's Experience

Chongdee Aojanepong, M.D.*, Kongsawate Khaogate, M.D.*, Adisak Wongkajornsilp, M.D., Ph.D., Sunisa Duangsa-ard, Ph.D.**, Kanda Kasetsinsombat, Ph.D.****

**Division of Plastic Surgery, Department of Surgery, **Department of Pharmacology, Faculty of Medicine Siriraj Hospital, Mahidol University, Bangkok 10700, Thailand.*

ABSTRACT

Objective: Cell-based therapy is gaining increasing prominence in medicine, where it has the potential to replace or repair damaged tissue using new engineered cells. Skin cell engineering, also known as keratinocyte culture or cultured epithelial autograft (CEA), is a promising field in cell-based therapy. CEA is now used in many parts of the world as an alternative treatment for some diseases that require large defects to be covered, such as severe and major burn patients and congenital melanocytic nevus. The use of CEA in conjunction with acellular skin substitution is rapidly expanding.

Materials and Methods: This study is an initiative aimed at supporting the production and use of keratinocyte cultures at Siriraj Hospital. This is the first stage of developing sheet keratinocyte culture *in vitro*.

Results: Our study yielded very promising results. As feeder cells, we used irradiated 3T3 murine fibroblasts, as per the standard protocol for keratinocyte culture. The growth duration was four weeks: 2 weeks for the 3T3 murine fibroblasts and 2 weeks for the keratinocytes. The keratinocytes grew rapidly and formed sheets with irradiated 3T3 murine fibroblasts. The retrieval of the cell sheets was straightforward thanks to the temperature-response cell culture dish and halo-ring cell recovery sheet. Flow cytometry revealed that the cells had a very high viability and purity. H&E staining revealed the sheets comprised two to four layers of stratified epithelial tissue.

Conclusion: From this study, our method of manufacturing the CEA can offer a promising result. This can be use in the treatment which require large skin coverage. However, we aim to initiate animal and human trial phase next.

Keywords: Keratinocyte culture; keratinocyte culture in Siriraj Hospital; cultured epithelium autograft; CEA; cultured epithelium autograft in Siriraj Hospital; CEA in Siriraj Hospital (Siriraj Med J 2022; 74: 274-283)

INTRODUCTION

The treatment workhorse for covering large wounds, such as in burn victims or after cancer resection surgery, is the skin graft. Skin grafts are classified into three categories based on the origin of the tissue: autografts (from the patient), allografts (from another person), and xenografts (from other species, such as pigs).

Generally, using autologous tissue is the best option; however, in some cases, such as severe burns or after the removal of a large tumor, an autologous graft may not be sufficient. As a temporary dressing, an allograft or xenograft may be used, but must be later removed due to graft rejection.

The field of regenerative medicine and tissue engineering has grown in recent years. In North America and some European countries, autologous skin culture (keratinocyte culture) is now commercially available. This keratinocyte culture is extremely useful in covering

Corresponding author: Kongsawate Khaogate
E-mail: kongsawate.kha@gmail.com
Received 23 December 2021 Revised 17 February 2022 Accepted 21 February 2022
ORCID ID: https://orcid.org/0000-0002-0128-7483
http://dx.doi.org/10.33192/Smj.2022.34

large skin defects.[1-3] There are three types of keratinocyte culture[4]: sheet, suspension, and spray. However, none of these cultures are available yet in Thailand.

This study is an initiative to support the production and use of keratinocyte cultures at Siriraj Hospital. This is the first stage of developing sheet keratinocyte culture *ex vivo*. Animal and human phases will follow later.

MATERIALS AND METHODS

This study was conducted at the Plastic and Reconstructive Surgery Unit Department of Surgery, and Department of Pharmacology, Faculty of Medicine Siriraj Hospital, Bangkok, Thailand. This study protocol (Si 122/2020) was approved by Ethics Committee of the Siriraj Institutional Review Board. The subjects understood the protocol and gave informed consent prior to the participation.

Preparation of human skin

After receiving informed consent, the human skin used in this study was obtained from patients who had surgical debridement or from a skin graft that was left over after skin graft transplantation. The skin was harvest from thigh using Zimmer dermatome (Zimmber biomet company, Ohio, USA) with 0.010 inches thickness. The sample skin was cleansed with 100 ml of normal saline and wrapped in a sterile gauze soaked in normal saline. The skin was then transferred to a laboratory room in a sterile plastic bag. The skin was washed in phosphate-buffered saline (PBS) with 50 µg/mL streptomycin and 50 unit/mL penicillin G before being transferred to a new sterile 10.0 cm diameter dish (Fig 1).

Isolation of human skin keratinocytes

The sample skin was finely chopped into small pieces (approximately 2 × 2 mm^2). The pieces were then transferred into a 50 mL tube. The tube was then incubated in a water bath for 20 minutes with 5 mL of 0.25% trypsin-EDTA at 37°C. The mixture was washed twice through centrifuged at 1000 rpm for 5 minutes at room temperature. The supernatant was discarded, and the cell pellets were reconstituted in 5 mL of Keratinocyte culture medium (KCM).

Irradiated 3T3 fibroblast preparation (Feeder cell)

The frozen cryotube of 3T3 fibroblasts (murine fibroblast) was then removed from the cryopreserved tank, and 70% ethanol was used to clean the outside of the tube. The frozen cryotube of 3T3 fibroblasts was thawed in a 37°C water bath. When the cell-preservative medium had nearly completely defrosted, the cell suspension was quickly mixed into 5 ml pre-warmed Fibroblast derived matrix (FDM) in a 15 ml tube. The cell suspension solution (approximately 6 ml) was then divided equally and added to each of the two 75 cm^2 flasks. The next day, the culture medium was changed was completely changed to remove the remaining cryoprotectant (Fig 2). Note, the more 75 cm^2 flasks there are, the larger the cell expansion possible.

All of the cultured cells from the 75 cm^2 flasks were collected and placed in a 50 mL tube after two passages. The tube was transferred for two cycles of 34 Gy radiation. Note, the preparation of the irradiated 3T3 fibroblasts took about one to two weeks, and so must be planned ahead of time when needed.

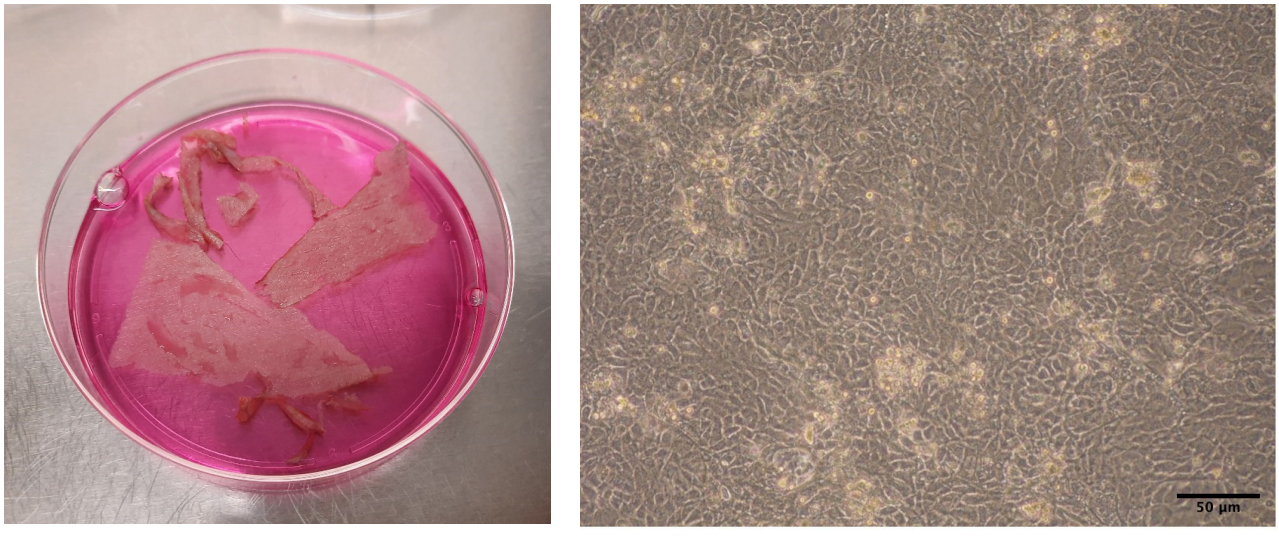

Fig 1. Skin sample was retrieved from a split-thickness skin graft leftover (1A), Primary keratinocytes prepared from the skin samples on day 7 were visualized under 10× objective lens (1B)

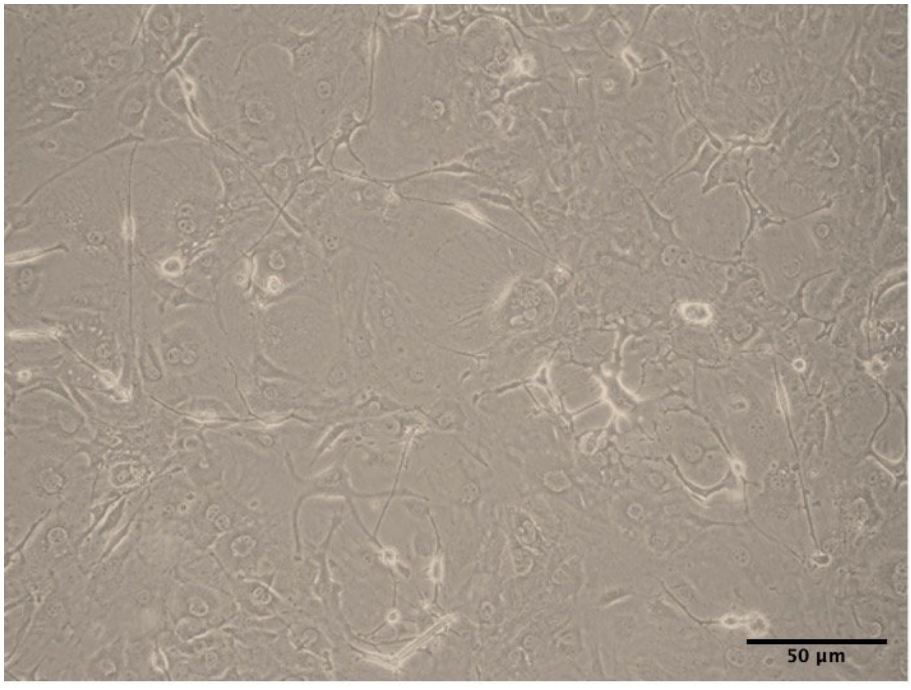

Fig 2. 3T3-murine fibroblasts (feeder cell) were visualized under 10× objective lens.

Plating the human keratinocytes over irradiated 3T3 fibroblasts (Feeder layer)

We used an UpCell dish, which is a specialized culture dish. This UpCell dish has the unique property that when the temperature is reduced, the cultured cells automatically lift off the surface.

Irradiated 3T3 fibroblasts were seeded onto the dish first, covering the entire surface overnight. The irradiated-fibroblasts were then seeded with a suspension of human keratinocytes at concentrations 2.0×10^5 and 4.0×10^5 cells in a 3.5 cm UpCell dish. The dish was then placed in a CO_2 incubator and incubated at 37°C.

Keratinocyte sheet lifting

Every day, the culture medium [keratinocyte medium (KCM)] was changed. Also, the cultured cells were examined every day under a microscope. The keratinocyte sheet was ready to be lifted off once the cell confluence reached 100%, which took about one to two weeks. The keratinocyte sheet was lifted from the dish's surface by lowering the temperature from 37°C to 20°C over 30 minutes. (Fig 3)

A specialized doughnut-shaped paper called a halo-ring cell recovery sheet was used to retrieve the keratinocyte sheet. The halo-ring sheet's outer diameter was smaller than the dish's diameter, so that when the halo-ring sheet was placed over the keratinocyte sheet, the keratinocyte sheet's edge was larger than that of the halo-ring sheet's. Next, by folding the keratinocyte sheet's edge over the edge of the halo-ring sheet, the halo-ring sheet and the keratinocyte sheet could be lifted off the surface of the dish together (Fig 4).

RESULTS

Duration of keratinocyte sheet culture

The preparation of the irradiated 3T3 fibroblasts took about one to two weeks in this study. It then took two weeks from the time the keratinocytes were seeded to the formation of a keratinocyte sheet. As a result, the entire process took three to four weeks overall.

Characteristics of the cultured keratinocyte sheets

Keratinocyte cells were found to grow on irradiated 3T3 fibroblasts in explant culture. At days 5, 7, and 14, the confluence rates were 20%, 80%, and 100%, respectively (Fig 5). Keratinocytes with typical morphological features, such as a polygonal cobblestone shape, were observed to have proliferated.

Histological examination revealed that all the manufactured cell sheets with a 2-4 stratified structure were made up of epithelial cells (Fig 6). The results showed that the keratinocyte cells could be cultured on temperature-responsive cell culture inserts and that the cell sheets could stratify (Table 1).

Lifting the cultured keratinocyte sheets

After 14 days of culture on the temperature-responsive cell culture dish, all the cells were successfully harvested

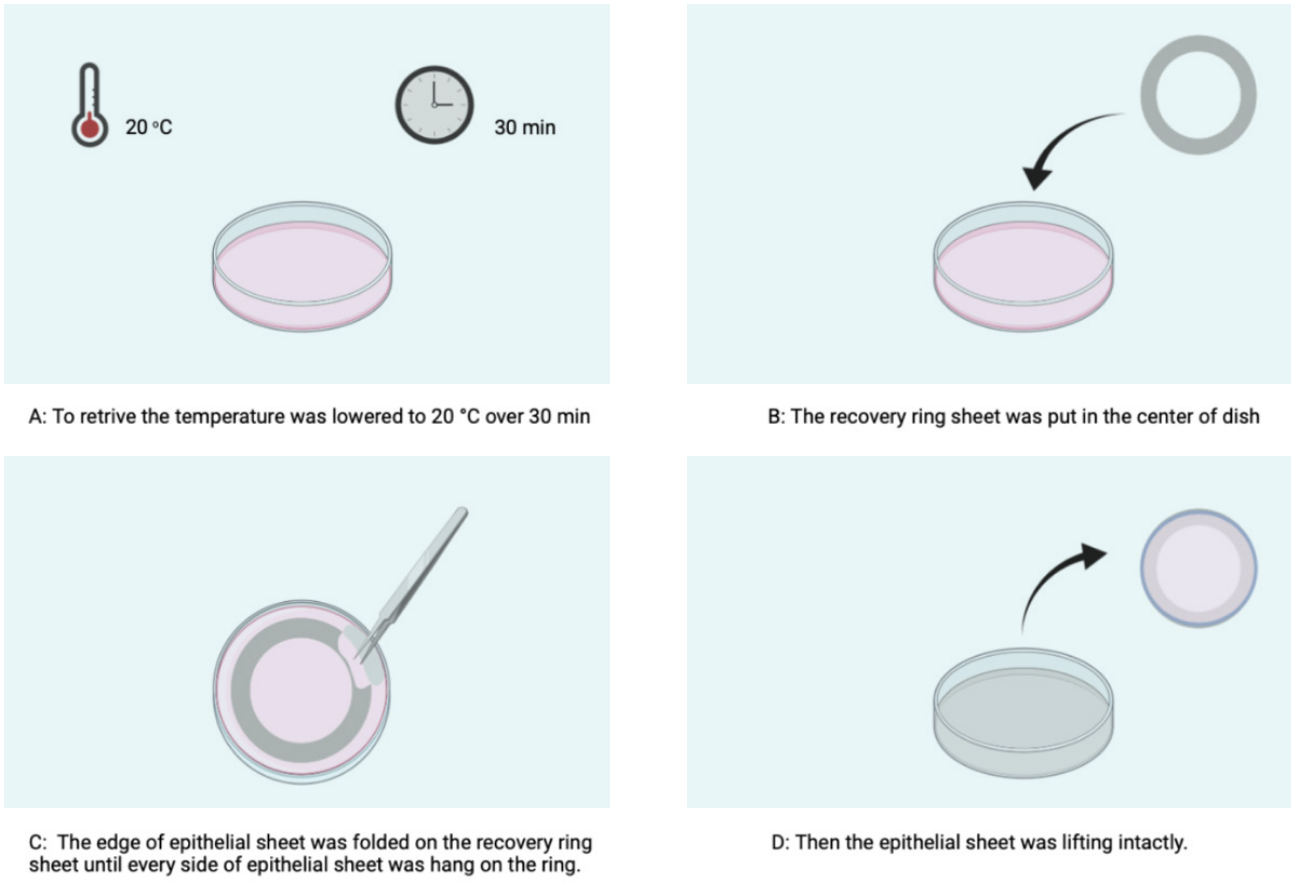

Fig 3. The culture epithelial sheet retrieving method

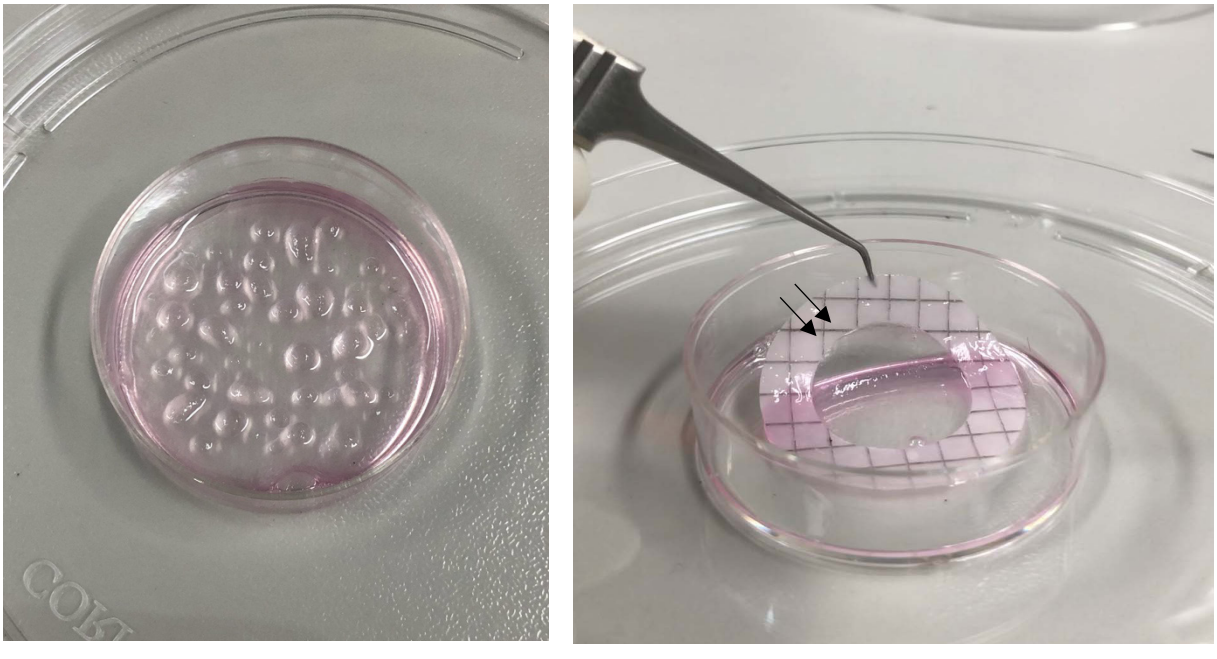

Fig 4. After 14 days, the culture epithelium sheet was growing all over the temperature-responsive UpCell dish (left). For the lifting, the temperature was lowered from 37°C to 20°C over 30 min; then a recovery ring sheet was used for lifting the cultured epithelial cell sheets (right), culture epithelial sheet (arrow).

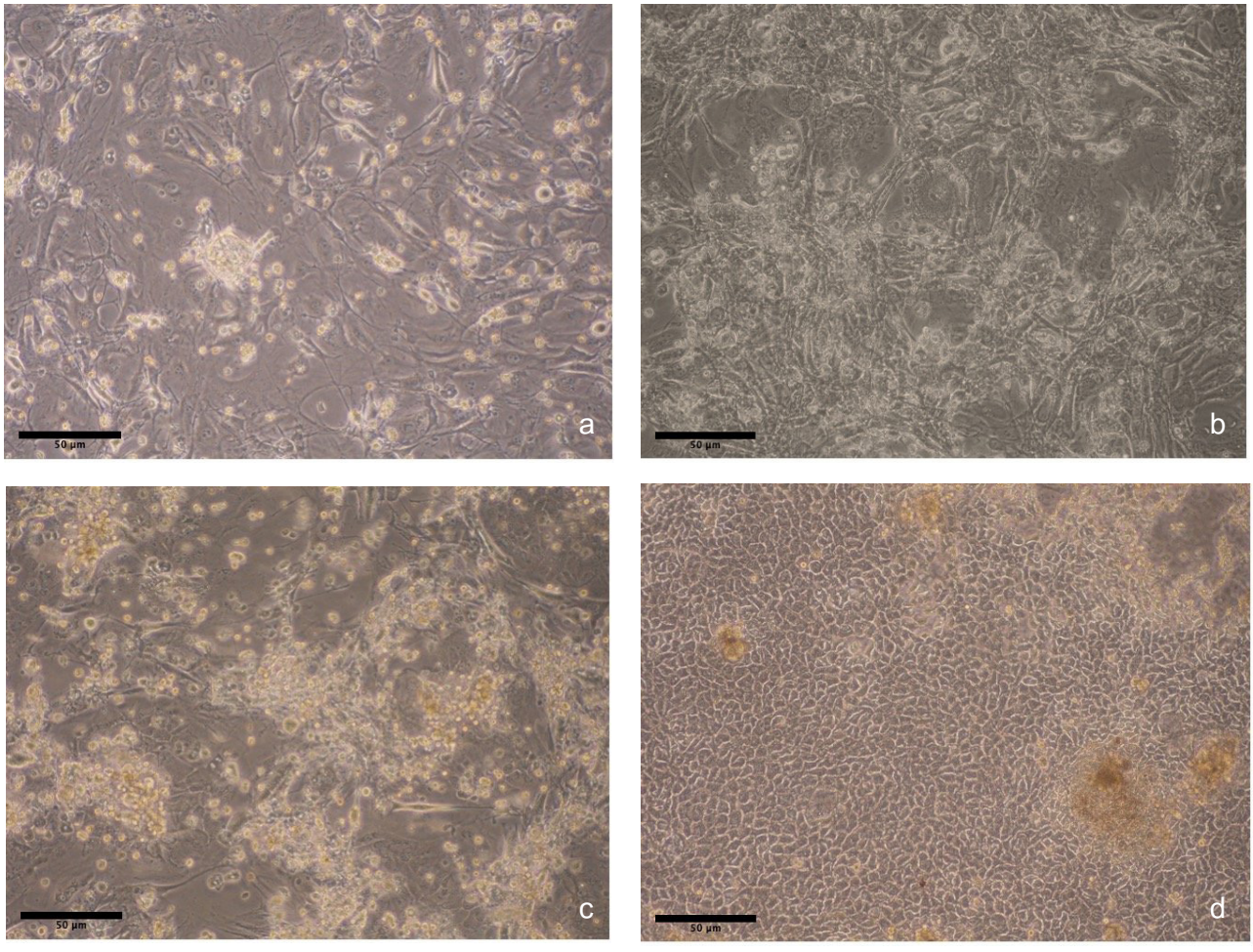

Fig 5. Culture dish at 10x microscopic view on the 1st day showing a low keratinocyte : fibroblast ratio (a). During the culture, the keratinocytes continuously grew in number while the fibroblasts decreased, as can be seen on the 5th day (b), 7th day (c), and finally, on the 14th day, by which time the keratinocytes were confluence. (d)

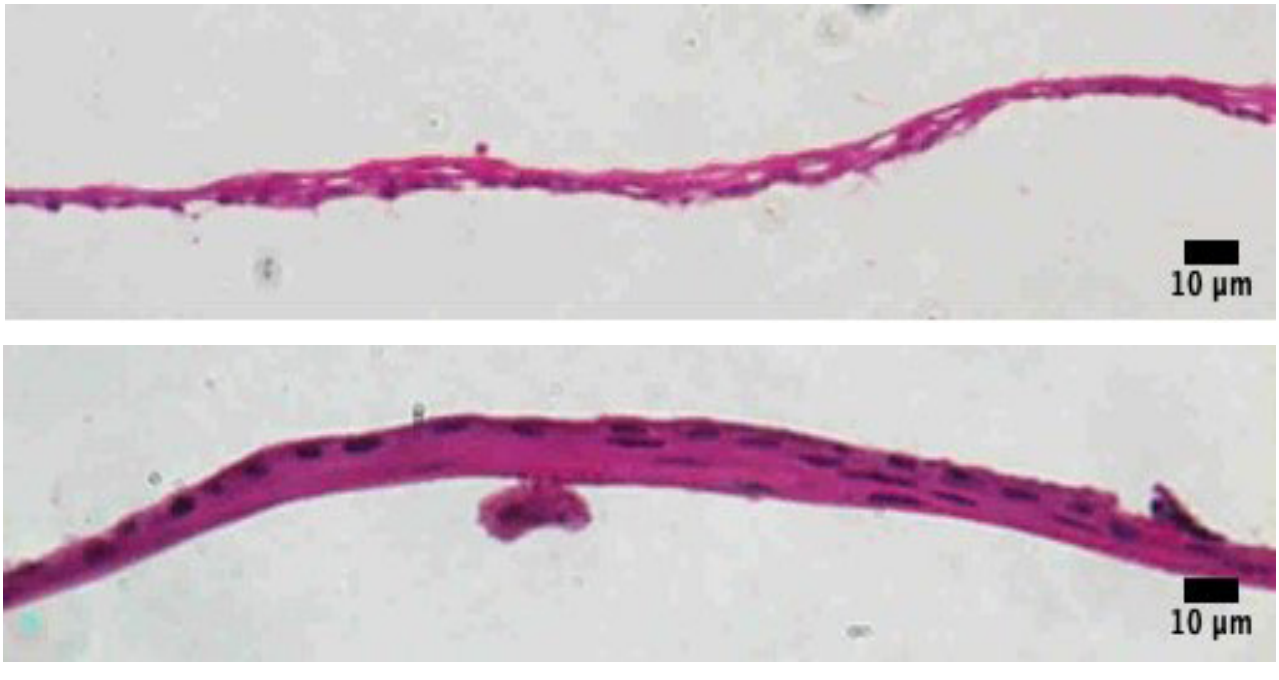

Fig 6. The Cross section of the cell sheet was stained with H&E and viewed under 10× objective lens: keratinocyte at 2.2×10^4 cells/cm^2 (above), and 4.4×10^4 cells/cm^2 (below).

TABLE 1. Physical characteristics of the cultured keratinocyte sheet seeding at 2.2×10^4 cells/cm^2 and 4.4×10^4 cells/cm^2.

Cell sheet		2.2×10^4 cells/cm^2	4.4×10^4 cells/cm^2
Cell morphology	Full confluence keratinocytes and cobble stone-like morphology	Confirmed	Confirmed
Cell sheet recovery	Harvesting w/o any damage	Confirmed	Confirmed
Total cell number	Over 1.0×10^5 cells	8.9×10^5 cells	17.3×10^5 cells
Cell viability	Over 60.0%	92.8%	95.6%
Karatinocytes purity	Over 80.0%	96.5%	98.2%
Degree of stratification	More than 2 layers	More than 2–4 layers	More than 2–4 layers

as contiguous transplantable cell sheets by lowering the incubation temperature from 37°C to 20°C over 30 minutes and by using a halo-ring cell recovery sheet.

Validation of the viability of the culture

Flow cytometry was used to validate the cultured cell sheets. The results showed that the total cell counts in the cell sheets using keratinocyte at cell seedings of 2.0×10^5 (2.2×10^4 cells/cm^2) and 4.0×10^5 (4.4×10^4 cells/cm^2) were 8.9×10^5 and 17.3×10^5 cells, respectively. The viability rates were 92.8% and 95.6%, respectively (Figs 7&8).

Purity of the cultured keratinocyte sheets

Cell purity was 96.5% and 98.2%, respectively, in the above cultures.

DISCUSSION

Cultured epithelial autograft (CEA) was first developed 30 years ago by Green and Rheinwald based on murine 3T3 fibroblasts.[5,6] Because of the high cost and time required for processing, subsequent progress in this field has been very slow.

In the new millennium, cell-based therapy has gained increasing prominence in medicine; particularly in the fields of tissue engineering, regenerative medicine, and stem cell therapy, and is widely recognized to offer the potential to replace or repair damaged tissue using new engineered cells.

Skin cell engineering, also known as keratinocyte culture or cultured epithelial autograft (CEA), is a promising field in cell-based therapy. CEA is now used in many countries as an alternative treatment for large wounds.[1] The indication is still within the controversy, such as major burn greater than 30% of total body surface area.

The lack of skin donor is still a major problem in numerous cases such as severe burn, large post-oncologic resection, or congenital melanocytic nevus in pediatric. In these cases, we can use mesh or meek technique for expand the graft tissue 2 to 6 times. However, the wider mesh/meek is needed to facilitate larger areas of cover, result in the poorer donor site's scar outcome. Re-harvesting of the donor sites normally used, but is associated with a delay overall healing time, as the donor sites require time to heal between procedure. The CEA may play an important role in these cases. This technology has capability to expand the tissue more than the previous strategy we utilized in the past and use fewer tissue donor.

There are currently three types of CEA available: the sheet, suspension, and spray forms.[1,4,7-9]

Morimoto et al.[2,3] demonstrated the use of CEA for accelerating wound healing in neonates with complicated wounds.

The ReCELL spray-on skin system[4,10,11] offers the use of a spray form of CEA combined with an animal-derived enzyme for less complicated wounds.

Nowadays, the sheet form of CEA is classified as a skin substitute. Skin substitution is divided into two types: cellular (composed of living cells, such as CEA) and non-cellular or acellular (composed of biocompatible or biodegradable materials). Acellular skin substitution is further subdivided into allogenic (made up of a decellularized extracellular matrix from the

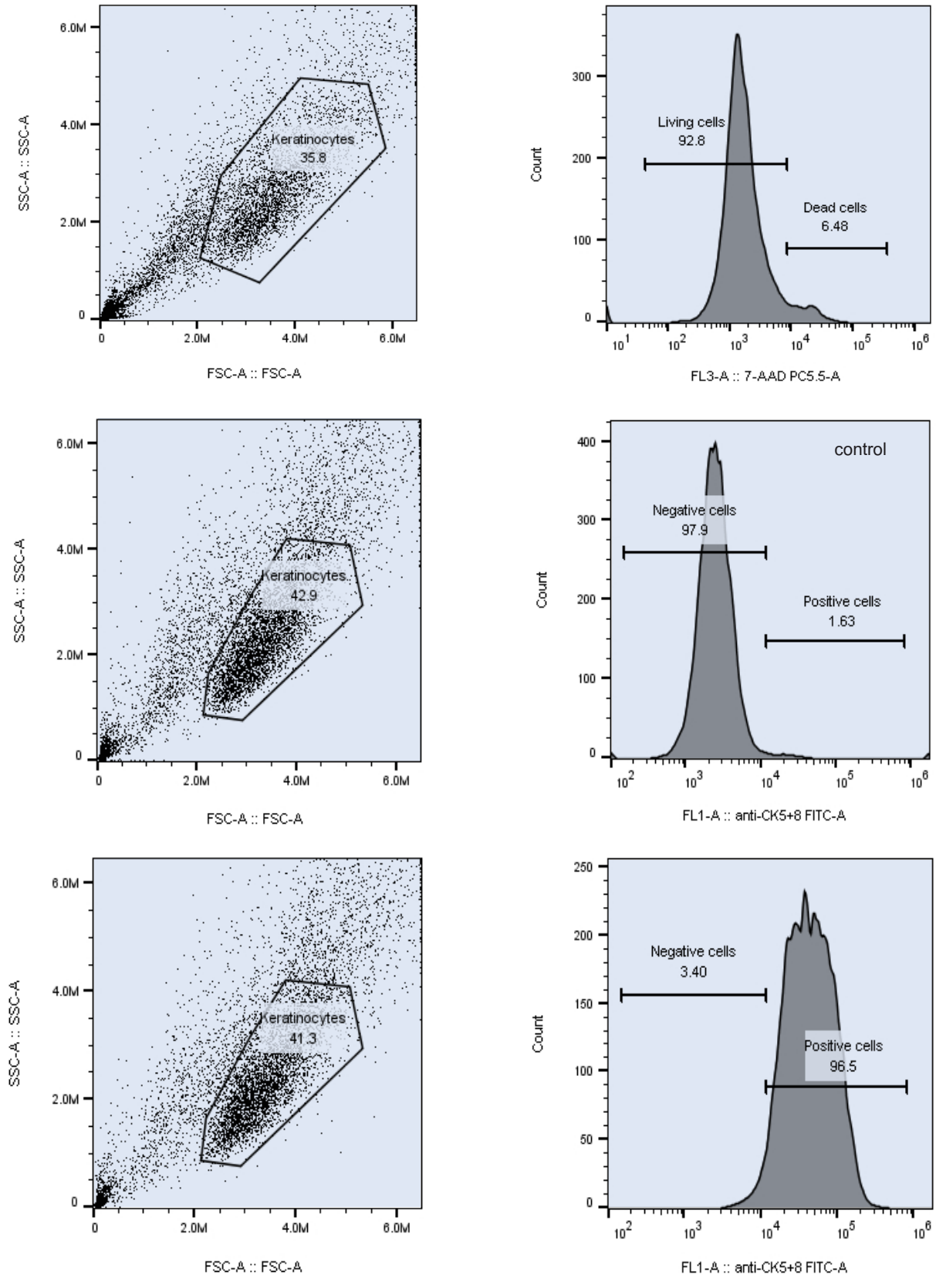

Fig 7. The flow cytometry was used to characterize cultured keratinocytes sheet seeding at 2.2×10^4 cells/cm^2. The cluster of putative keratinocytes was gated based on front scattering and side scattering (left panels). The viability was assessed using 7-amino actinomycin D (7-AAD) assay in PerCP-Cy5.5 channel. The histogram illustrated 92.8% live cells and 6.48% dead cells (top). The purity was assessed using anti-cytokeratin 5 + 8 in FITC (fluorescein isothiocyanate) channel to stain keratinocytes. The histograms illustrated minuscule autofluorescence (1.63%) in the unstained group (middle), and overwhelmingly 96.5% positive cells in the stained group (bottom).

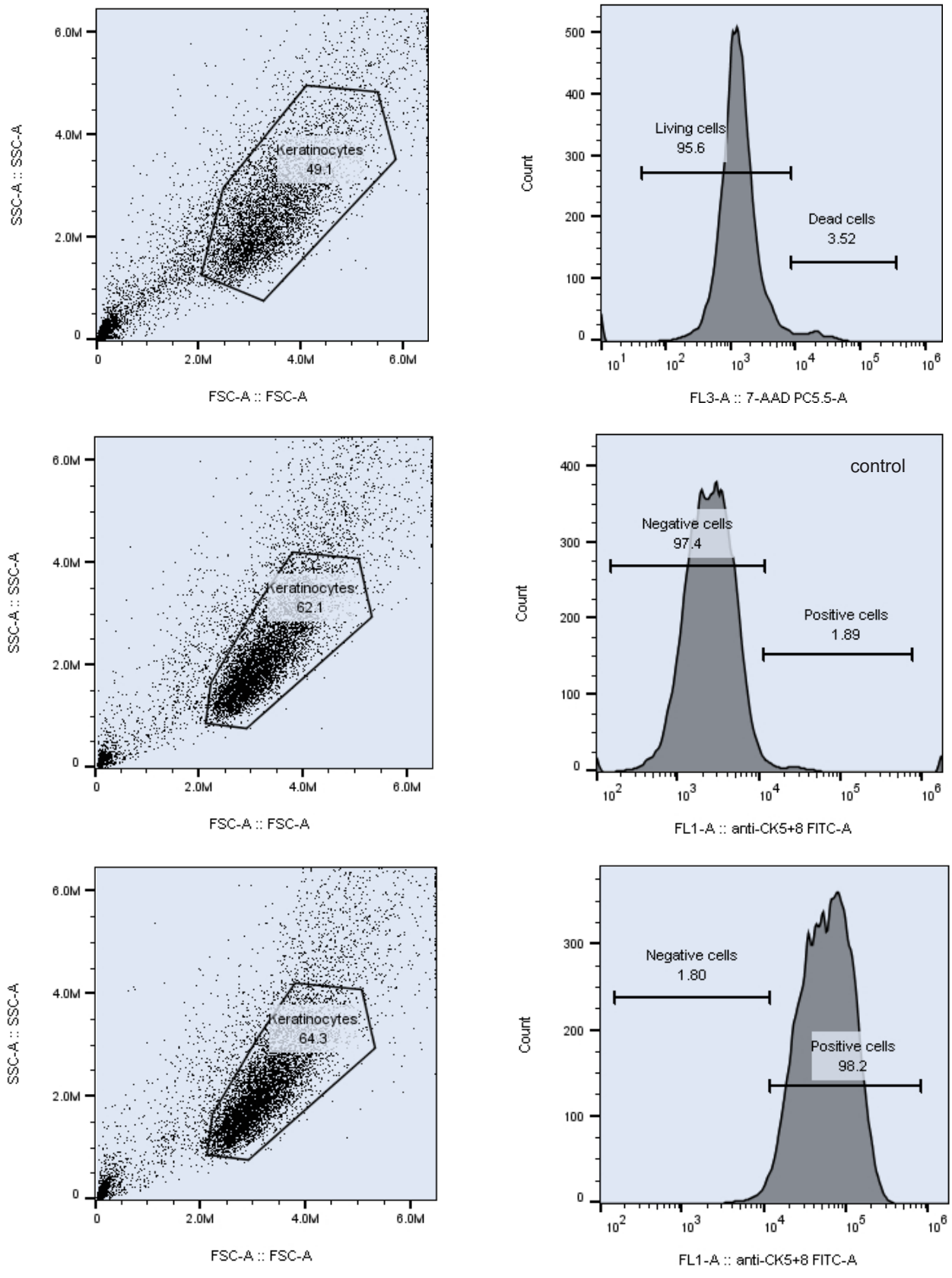

Fig 8. The characteristics of cultured keratinocyte sheet seeding at 4.4×10^4 cells/cm^2 based on flow cytometry were similar to those with lower cell density. There were 95.6% live cells and 3.52% dead cells (top). The autofluorescence in FITC channel was 1.89% (middle). The purity of keratinocytes was 98.2% (bottom).

same species, such as a human cadaver) and xenogenic (composed of a decellularized extracellular matrix from different species, such as bovine or porcine).

The disadvantage of CEA is the thinning of the tissue, as it consists with a couple layers of stratified keratinocyte. In case the wound is deeper to subcutaneous tissue, utilizing this CEA alone will result in loss contour of the area. In the deep wound, acellular skin substitution is very useful, as it is designed to stimulate neodermis formation for 3-4 weeks resulting in the tissue fullness. It can be used as an intermediate step for split- or full-thickness grafting in patients with both small and large defects. Additionally, it can be used in the wound that exposed bone or tendon which cannot be grafted primarily.

There have been numerous reports on these acellular skin substitutes being used as scaffolds in conjunction with the sheet form of CEA for complex wounds.[7,12-15] Matsumura et al.[16] reported the successful use of combined CEA and acellular skin substitution in severe burn patients.

Our research yielded very promising results. As feeder cells, we used irradiated 3T3 murine fibroblasts, as per the standard protocol for keratinocyte culture. In our protocol, we use partial thickness of skin (around 0.010 inches) for isolate human keratinocytes instead of full thickness skin donor. We found out that it can shorten time in cell isolation process and reducing cell damage, as normally it must use thermolysin and incubation overnight for separating epidermis from dermis. The overall growth duration was four weeks: 2 weeks for the 3T3 murine fibroblasts and 2 weeks for the keratinocytes. The keratinocytes grew rapidly and formed sheets with irradiated 3T3 murine fibroblasts. In the retrieval of the cell sheets, we used the temperature-response cell culture dish and halo-ring cell recovery sheet. Normally, enzymatic treatment (for example: dispase) is typically used in the collection of epithelial keratinocyte sheets, but it tends to break the adhesion and basement membrane proteins. We assume that using harvesting technique by temperature dish can lowering cell damage result in improve the survival outcome of epithelial sheet. The flow cytometry revealed that the cells had very high viability and purity. H&E staining revealed two to four layers of stratified epithelial tissue. Following these promising results, animal and human trial phases will be initiated.

In our practice, we usually use acellular skin substitutes in conjunction with the split-thickness skin graft especially in cosmetic area or exposed bone or tendon wound. It will take times approximately 3-4 week for the tissue to be vascularized and good adhere to wound bed. Next, the patient will undergo the second operation for skin grafting. In our perspective, this research is giving more benefit to the patient. During the time for waiting the revascularized process, we aim to prepare the culture keratinocyte sheet and utilize for the second stage operation.

CONCLUSION

The future of CEA is very promising in the treatment of some diseases that require large defects to be covered, such as severe and major burn patients and congenital melanocytic nevus. The use of CEA in conjunction with acellular skin substitution is rapidly expanding globally, and will hopefully be an option in Thailand soon too.

ACKNOWLEDGEMENTS

This work was funded by Aojanepong C. We would like to express sincere gratitude to Siriraj's Laboratory for supporting the equipment of this study.

REFERENCES

1. Chrapusta A, Nessler MB, Drukala J, Bartoszewicz M, Madry R. A comparative analysis of advanced techniques for skin reconstruction with autologous keratinocyte culture in severely burned children: own experience. Postepy Dermatol Alergol 2014;31(3):164-9. DOI: 10.5114/pdia.2014.43190.
2. Morimoto N, Kakudo N, Kako A, et al. A case report of the first application of culture epithelial autograft (JACE((R))) for giant congenital melanocytic nevus after its approval in Japan. J Artif Organs 2018;21(2):261-264. DOI: 10.1007/s10047-017-1007-0.
3. Morimoto N, Jinno C, Sakamoto M, Kakudo N, Yamaoka T, Kusumoto K. An Exploratory Clinical Trial of a Novel Treatment for Giant Congenital Melanocytic Nevi Combining Inactivated Autologous Nevus Tissue by High Hydrostatic Pressure and a Cultured Epidermal Autograft: Study Protocol. JMIR Res Protoc 2016;5(3):e162. DOI: 10.2196/resprot.6195.
4. Ter Horst B, Chouhan G, Moiemen NS, Grover LM. Advances in keratinocyte delivery in burn wound care. Adv Drug Deliv Rev 2018;123:18-32. DOI: 10.1016/j.addr.2017.06.012.
5. Green H, Rheinwald JG, Sun TT. Properties of an epithelial cell type in culture: the epidermal keratinocyte and its dependence on products of the fibroblast. Prog Clin Biol Res 1977;17:493-500. (https://www.ncbi.nlm.nih.gov/pubmed/928463).
6. Rasmussen C, Thomas-Virnig C, Allen-Hoffmann BL. Classical human epidermal keratinocyte cell culture. Methods Mol Biol 2013;945:161-75. DOI: 10.1007/978-1-62703-125-7_11.
7. Kljenak A, Tominac Trcin M, Bujic M, et al. Fibrin gel as a scaffold for skin substitute - production and clinical experience. Acta Clin Croat 2016;55(2):279-89. DOI: 10.20471/acc.2016.55.02.15.
8. Gerlach JC, Johnen C, Ottomann C, Bräutigam K, Plettig J, Belfekroun C, et al. Method for autologous single skin cell isolation for regenerative cell spray transplantation with non-cultured cells. Int J Artif Organs 2011;34(3):271-9. DOI: 10.5301/ijao.2011.6508.
9. Ramos MG, Ramos DG, Ramos CG. Evaluation of treatment response to autologous transplantation of noncultured melanocyte/keratinocyte cell suspension in patients with stable vitiligo. An Bras Dermatol 2017;92(3):312-318. DOI: 10.1590/abd1806-

4841.20175700.
10. Holmes JHt, Molnar JA, Shupp JW, Hickerson WL, King BT, Foster KN, et al. Demonstration of the safety and effectiveness of the RECELL((R)) System combined with split-thickness meshed autografts for the reduction of donor skin to treat mixed-depth burn injuries. Burns 2019;45(4):772-82. DOI: 10.1016/j.burns.2018.11.002.
11. Peirce SC, Carolan-Rees G. ReCell((R)) Spray-On Skin System for Treating Skin Loss, Scarring and Depigmentation after Burn Injury: A NICE Medical Technology Guidance. Appl Health Econ Health Policy 2019;17(2):131-41. DOI: 10.1007/s40258-018-00457-0.
12. Haldar S, Sharma A, Gupta S, Chauhan S, Roy P, Lahiri D. Bioengineered smart trilayer skin tissue substitute for efficient deep wound healing. Mater Sci Eng C Mater Biol Appl 2019;105:110140. DOI: 10.1016/j.msec.2019.110140.
13. Cubo N, Garcia M, Del Canizo JF, Velasco D, Jorcano JL. 3D bioprinting of functional human skin: production and in vivo analysis. Biofabrication 2016;9(1):015006. DOI: 10.1088/1758-5090/9/1/015006.
14. Horch RE, Wagner G, Bannasch H, Kengelbach-Weigand A, Arkudas A, Schmitz M. Keratinocyte Monolayers on Hyaluronic Acid Membranes as "Upside-Down" Grafts Reconstitute Full-Thickness Wounds. Med Sci Monit 2019;25:6702-6710. DOI: 10.12659/MSM.915649.
15. Matsumura H, Gondo M, Imai R, Shibata D, Watanabe K. Chronological histological findings of cultured epidermal autograft over bilayer artificial dermis. Burns 2013;39(4):705-13. DOI: 10.1016/j.burns.2012.10.004.
16. Matsumura H, Matsushima A, Ueyama M, Kumagai N. Application of the cultured epidermal autograft "JACE((R))") for treatment of severe burns: Results of a 6-year multicenter surveillance in Japan. Burns 2016;42(4):769-76. DOI: 10.1016/j.burns.2016.01.019.

Ganglion Cell-inner Plexiform Layer Thickness Measured by Cirrus High-definition Optical Coherence Tomography Enhances Glaucoma Diagnosis in Patients with Moderate or High Myopia

Anuwat Jiravarnsirikul, M.D., Ngamkae Ruangvaravate, M.D., Chaovaporn Ubolviroj, M.D., Yuwared Chattagoon, M.D., Sakaorat Petchyim, M.D.

Department of Ophthalmology, Faculty of Medicine Siriraj Hospital, Mahidol University, Bangkok 10700, Thailand.

ABSTRACT

Objective: To assess the diagnostic ability of Cirrus high-definition optical coherence tomography (HD-OCT) parameters in patients with moderate or high myopia for detecting glaucoma, and to compare the thickness of the macular ganglion cell-inner plexiform layer (GC-IPL) in glaucomatous and normal eyes in both types of myopia.

Materials and Methods: This prospective study enrolled moderately (spherical equivalent -3.00 to -6.00 diopters) and highly (spherical equivalent ≤ -6.00 diopters) myopic patients without (controls) and with (study) glaucoma. Cirrus HD-OCT was used to determine the thickness of the peripapillary retinal nerve fiber layer (RNFL) and the GC-IPL. The area under the receiver operating characteristic curve was analyzed to evaluate the glaucoma detection capability of each Cirrus HD-OCT parameter.

Results: Seventy eyes (31 moderate myopia, 39 high myopia) were included. The parameters with the best diagnostic ability were minimum GC-IPL, inferior RNFL and average RNFL thickness in moderately myopic eyes, and average RNFL, inferior RNFL and inferotemporal GC-IPL thickness in highly myopic eyes. All parameters were thinner in glaucomatous than in normal eyes in both groups.

Conclusion: Although macular GC-IPL thickness demonstrated high ability to detect glaucoma in patients with moderate or high myopia, it should be used in combination with other structural imaging and functional assessments for diagnosing glaucoma.

Keywords: Ganglion cell-inner plexiform layer thickness; glaucoma; myopia; Cirrus high-definition optical coherence tomography (Siriraj Med J 2022; 74: 284-293)

INTRODUCTION

Glaucoma was reported to be the major cause of irreversible blindness and the second most prevalent cause of moderate and severe visual impairment.[1,2] Numerous risk factors lead to the development of glaucoma, and myopia is one of them.[3] Globally, myopia prevalence is increasing, and approximately 5 billion people will be affected by 2050, especially in East and Southeast Asia. In addition to uncorrected myopia itself, pathologic ocular complications from myopia or its comorbidities, such as myopic macular degeneration, choroidal neovascularization, and glaucoma, can lead to increased medical and economic

Corresponding author: Ngamkae Ruangvaravate
E-mail: ngamkae1@gmail.com
Received 15 November 2021 Revised 2 February 2022 Accepted 9 February 2022
ORCID ID: https://orcid.org/0000-0002-4342-0174
http://dx.doi.org/10.33192/Smj.2022.35

burden.[4,5] A previous study reported that myopic eyes had a two to three times higher risk of having glaucoma[6], and high myopic eyes had a nearly six-fold increased risk of having primary open-angle glaucoma.[7] Thus, early detection and treatment of glaucoma in myopia is crucial for preventing disease progression.[8]

Previous study reported that detection of structural abnormalities, i.e., retinal nerve fiber layer (RNFL) defects, may develop four to six years before the onset of visual field abnormalities.[9] As a consequence, recent advances in ocular imaging, especially spectral-domain optical coherence tomography (SD-OCT), which is a frequently used structural imaging, may greatly contribute to the early detection and treatment of glaucoma. Previous studies used peripapillary RNFL thickness as a measurement of RGC axon loss to detect glaucoma, and since approximately 50% of RGCs are located in the macular region, and the inner retinal layers are preferentially affected by glaucomatous damage[10,11], further studies have assessed macular parameters to aid in glaucoma diagnosis. Previous studies demonstrated that the thickness of macular ganglion cell complex (GCC) generated by an RTVue SD-OCT (Optovue, Fremont, CA, USA), and the thickness of macular ganglion cell-inner plexiform layer (GC-IPL) by Cirrus high-definition optical coherence tomography (HD-OCT) with ganglion cell analysis (GCA) algorithm (Carl Zeiss Meditec, Jena, Germany) yielded glaucoma detection ability similar to peripapillary RNFL thickness; however, they found GC-IPL thickness measurement not be confounded by the variation in RNFL.[10-14]

Evaluation of RGC loss using various techniques of structural imaging has been continuously improved to achieve more accuracy in glaucoma detection, and with better reproducibility. However, diagnosing glaucoma in myopic eyes is still difficult since anatomical distortion of the optic nerve head (ONH) (e.g., tilted disc, large peripapillary atrophy) can mystify ophthalmologists to differentiate between glaucomatous damage and myopia-related optic disc changes. Therefore, objective structural quantification may have a role in diagnosing glaucoma in myopia.[15-17] Leung, *et al.* reported that, when using Cirrus HD-OCT, temporally converged superior and inferior RNFL bundles were detected in myopic eyes, which resulted in abnormal RNFL measurement.[18] Additionally, a previous study concluded that optic disc and cup margin detection errors were likely to be found in myopic eyes.[15] Thus, particular care must be taken when interpreting RNFL thickness map and neuroretinal rim measurement obtained by SD-OCT in myopic eyes. Analysis of macular parameters has been proposed as an alternative method for diagnosing glaucoma to avoid misdiagnosis of glaucoma via the influence of optic disc variation in myopia.

The thickness of the GC-IPL is a macular parameter that has been studied in various research. Choi, *et al.* demonstrated that in highly myopic eyes, GC-IPL has a diagnostic potential for glaucoma that is comparable to RNFL thickness.[19] In a previous study, the inferotemporal GC-IPL thickness was found to have the largest area under the receiver operating characteristic (AuROC) curve, suggesting that it might be utilized as an effective preperimetric glaucoma detection parameter in myopia.[20]

Since the normative databases in SD-OCT do not include data from highly myopic subjects, diagnosis of glaucoma in these patients is still somewhat difficult.[21] Moreover, differences in the severity of myopia can affect the GC-IPL thickness measurement. Seo, *et al.* concluded that GC-IPL in all sectors were thinner in high myopes compared to low and moderate myopes.[22] Akashi, *et al.* reported that GC-IPL thickness had a high AuROC curve value for distinguishing highly myopic glaucomatous eyes from normal eyes in patients with and without high myopia (spherical equivalent (SE) ≤ -6.00 diopters).[23] Accordingly, this study aimed to determine the diagnostic capability of Cirrus HD-OCT parameters for diagnosing glaucoma in patients with moderate (SE -3.00 to -6.00 diopters) or high myopia (SE ≤ -6.00 diopters), and to compare macular GC-IPL thickness between glaucomatous and normal eyes in both types of myopia.

MATERIALS AND METHODS

This prospective, comparative cross-sectional study was conducted at Siriraj Hospital, was approved by the Committee for the Protection of Human Participants in Research of the Faculty of Medicine Siriraj Hospital, Mahidol University, Bangkok, Thailand [EC 103/2014], and was registered in the Thai Clinical Trials Registry (identification number TCTR20210726001). This study followed to the tenets of the Declaration of Helsinki. Each subject provided a written informed consent before enrollment.

This study was performed in the ophthalmology outpatient clinic of Siriraj Hospital during February 2014 to December 2018. Patients aged older than 20 years with SE ≤ -3.00 diopters (D) and best spectacles-corrected visual acuity of 20/40 or better were eligible for inclusion. Subjects with retinal or macular pathology, vision-associated systemic or neurologic diseases, receiving drugs known to affect the macula (e.g., chloroquine, ethambutol), previous intraocular surgery or laser within 1 month, inability to cooperate with the examination,

and/or having an allergic reaction to the eye drops used in the study protocol were excluded. Participants visiting the ophthalmology outpatient clinic who met these criteria were enrolled in this study with written informed consent. Only one eye was randomly selected in the final analysis if both eyes met all research eligibility criteria.

All recruited patients underwent a complete ophthalmic examination, which consisted of assessment of visual acuity (VA), refractive error measured by autorefractor (ARK-530A; NIDEK, Aichi, Japan) and recorded as spherical equivalents (SE), intraocular pressure (IOP) measurement obtained with Goldmann applanation tonometry, slit-lamp and dilated fundus examination, gonioscopy, axial length obtained using a biometer (IOL Master 500; Carl Zeiss Meditec), OCT RNFL and GC-IPL parameter measurement by Cirrus HD-OCT software version 6.0.0.599 (Carl Zeiss Meditec), and visual field test by Humphrey visual field analyzer (Carl Zeiss Meditec) using the 24-2 Swedish interactive threshold algorithm (SITA) strategy.

Enrolled subjects were classified into either the moderately or highly myopic groups. Moderate and high myopia were defined as SE -3.00 D to -6.00 D and ≤ -6.00 D, respectively. Within each of those two groups, patients were further subdivided into either glaucoma (study) or normal (control) groups. Using the reference standard[24], glaucomatous eyes were defined as eyes with glaucomatous optic neuropathy with corresponding abnormal visual field tests. Glaucomatous optic neuropathy was defined as enlarged cupping ≥ 0.5 vertical cup/disc (C/D) ratio or an asymmetrical vertical C/D ratio greater than 0.2. Glaucomatous visual field defect was defined as any one of the following: a cluster of ≥ 3 non-edge adjacent points in one hemifield of pattern deviation plot with a probability < 5%, and including at least 1 point with a probability < 1%; a pattern standard deviation (PSD) showing a probability < 5%; or, a glaucoma hemifield test (GHT) showing outside normal limits. Normal subjects were moderately and highly myopic patients who visited ophthalmology outpatient clinic with mild cataract, dry eyes or eye check up and without glaucoma, which defined as those with an IOP ≤ 21 mmHg, no glaucomatous optic neuropathy, and without detectable visual field defect. The visual field of the normal group must not meet any of the aforementioned criteria for glaucomatous visual field defect and a GHT showing within normal limits, a mean deviation (MD) and PSD within the 95% confidence limit. OCT measurements are not considered as part of the examinations to include a patient in the normal control group.

Cirrus HD-OCT measurement

Two scans were obtained through a dilated pupil, one peripapillary RNFL scan and one macular scan (optic disc cube 200x200 protocol and macular cube 512x128 protocol, respectively). Macular scan measured GC-IPL thickness within a 6x6x2 mm cube centered at the fovea using the GCA algorithm, and the measurements were generated into the minimum, average, and 6 sectorial parameters (Inferotemporal, inferior, inferonasal, superonasal, superior and superotemporal). The optic disc cube protocol measured peripapillary RNFL thickness through a 6x6x2 mm cube, after which the measurements were analyzed into the average and the 4 quadrant thicknesses (temporal, superior, nasal, and inferior). Scans with a signal strength lower than 6 on either macular GC-IPL or peripapillary RNFL scan, visible eye movement, decentration, artifacts from blinking, and/or image distortion from anatomical abnormalities were discarded. Measurement values were analyzed via comparison with the device's normative database, and the results were visually described as a color-coded significance map with the colors green, yellow, and red indicating normal, borderline, and abnormal, respectively. There was no cutoff point of OCT value to define glaucoma, but it was used in combination with structural and functional tests to enhance glaucoma diagnosis.

Statistical analysis

Patient characteristics are reported as mean plus/minus standard deviation (SD) for normally distributed continuous data, and as frequency and percentage for categorical variables. Peripapillary RNFL and GC-IPL thicknesses were compared between the glaucoma and normal groups using unpaired *t*-test, and were compared among 4 groups using 1-way analysis of variance (ANOVA) by Tukey HSD or Games-Howell. The ability of a factor to detect glaucoma was assessed by the AuROC curve. All statistical analyses were performed using PASW Statistics software version 26. A p-value < 0.05 indicates statistically significant.

RESULTS

Subjects

Seventy eyes were included and categorized into 4 groups, as follows: moderately myopic normal group (n=16), highly myopic normal group (n=16), moderately myopic glaucomatous group (n=15), and highly myopic glaucomatous group (n=23). Patient demographic and baseline characteristics compared between glaucomatous and normal eyes in the moderate and high myopia groups

are presented in Table 1. The mean age of the moderately myopic group was 47.55±14.51 years (range from 22 to 68 years), and 19 were female (61.29%). The mean age of the highly myopic group was 45.69±15.02 years (range from 21 to 70 years), and 22 were female (56.41%). No significant differences were found in age, VA, IOP, or SE between normal and glaucomatous eyes in both the moderate and high myopia groups.

Cirrus HD-OCT measurement

Macular GC-IPL and peripapillary RNFL thicknesses as evaluated by Cirrus HD-OCT compared between glaucomatous and normal eyes in the moderate and high myopia groups are demonstrated in Table 2. No patients were excluded for poor quality scans. In both groups, all of the RNFL thickness parameters, except for the nasal region in both groups (moderate myopia p=0.700, and high myopia p=0.831) and the temporal region in the highly myopic group (p=0.118), were significantly thinner in glaucomatous than in the normal eyes (all p<0.05).

Comparison of macular GC-IPL thickness between glaucomatous and normal eyes in both the moderate and high myopia groups revealed statistically significant differences in minimum, average, and all sectors of macular GC-IPL thickness (all p<0.05), except for the superonasal GC-IPL sector in both the moderate and high myopia groups (p=0.282 and 0.614, respectively), and the superior GC-IPL sector in the high myopia group (p=0.443).

Diagnostic ability

All of the AuROC values of macular GC-IPL and peripapillary RNFL thickness in both the moderate and high myopia groups were above 0.5 (Table 3). In the moderately myopic group, the best parameters for distinguishing glaucomatous eyes from normal eyes were minimum GC-IPL, inferior RNFL, and average RNFL thicknesses (AuROC: 0.963, 0.925 and 0.919, respectively) (Fig 1). In the highly myopic eyes, average RNFL, inferior RNFL, and inferotemporal GC-IPL thicknesses (AuROC: 0.980, 0.962 and 0.905, respectively) demonstrated the best diagnostic ability for differentiating glaucoma from normal eyes (Fig 2).

TABLE 1. Patient demographic and baseline characteristics compared between normal and glaucomatous eyes in the moderate and high myopia groups.

	Moderately myopic group (n = 31)			Highly myopic group (n = 39)		
	Normal (n =16)	Glaucoma (n =15)	*P* value*	Normal (n =16)	Glaucoma (n =23)	*P* value†
Female, n (%)	11 (68.8)	8 (53.3)	0.38	12 (75)	10 (43.5)	0.10
Age, years	43.56 (13.47)	51.80 (14.80)	0.53	42.50 (15.19)	47.91 (14.83)	0.82
VA, logMAR	0.07 (0.09)	0.11 (0.11)	0.85	0.09 (0.10)	0.10 (0.10)	1.00
IOP, mmHg	15.69 (1.85)	14.33 (2.38)	0.55	14.56 (2.94)	13.65 (2.48)	0.82
SE, D	-4.39 (0.87)	-4.57 (0.99)	1.00	-7.61 (1.14)	-8.40 (4.79)	0.95
AL, mm	25.51 (0.89)	25.14 (1.25)	0.95	26.42 (0.81)	27.69 (1.49)	<0.01
MD, dB	-0.87 (1.49)	-5.10 (4.20)	<0.01	-1.35 (0.99)	-6.27 (3.56)	<0.01
PSD, dB	1.47 (0.25)	5.25 (3.65)	<0.01	1.67 (0.56)	5.60 (3.64)	<0.01

Data are given as mean (SD).

Abbreviations: VA; visual acuity, IOP; intraocular pressure, SE; spherical equivalent, AL; axial length, MD; mean deviation, PSD; pattern standard deviation

* Value for comparison of normal and glaucomatous eyes in moderately myopic group

† Value for comparison of normal and glaucomatous eyes in highly myopic group

TABLE 2. Peripapillary RNFL and macular GCIPL thickness as measured by Cirrus HD-OCT compared between normal and glaucomatous eyes in the moderate and high myopia groups.

	Moderately myopic group (n = 31)			Highly myopic group (n = 39)		
	Normal (n =16)	Glaucoma (n =15)	*P* value*	Normal (n =16)	Glaucoma (n =23)	*P* value†
RNFL thickness parameters, μm						
Average	97.31 (8.13)	72.73 (14.00)	<0.001	89.81 (7.07)	70.96 (7.38)	<0.001
Superior	119.75 (16.18)	89.13 (18.50)	<0.001	103.50 (16.74)	81.39 (14.03)	<0.001
Nasal	68.63 (9.17)	63.20 (11.01)	0.700	65.63 (12.38)	61.48 (12.01)	0.831
Inferior	120.19 (20.87)	77.67 (21.23)	<0.001	114.13 (15.86)	74.13 (15.02)	<0.001
Temporal	80.50 (11.17)	61.27 (17.26)	0.001	75.69 (8.06)	65.74 (13.65)	0.118
Macular GC-IPL parameters, μm						
Average	80.88 (6.64)	71.33 (8.02)	0.004	75.88 (4.26)	67.17 (9.13)	0.004
Minimum	79.44 (6.73)	61.87 (8.73)	<0.001	73.19 (7.48)	58.52 (12.06)	<0.001
ST	80.50 (6.28)	71.33 (8.73)	0.019	76.25 (4.12)	67.78 (10.99)	0.015
S	81.69 (7.29)	70.40 (9.83)	0.047	77.44 (4.79)	71.13 (16.82)	0.443
SN	83.00 (7.04)	75.60 (10.31)	0.282	78.19 (5.91)	73.22 (14.42)	0.614
IN	82.00 (6.19)	71.93 (8.56)	0.001	74.56 (6.06)	67.04 (6.53)	0.007
I	78.50 (6.97)	66.47 (8.08)	0.001	73.50 (4.18)	61.04 (10.37)	<0.001
IT	79.88 (6.87)	66.00 (9.51)	<0.001	75.69 (5.00)	62.96 (8.49)	<0.001

Data are given as mean (SD).
Abbreviations: ST; superotemporal, S; superior, SN; superonasal, IN; inferonasal, I; inferior, IT; inferotemporal
* Value for comparison of normal and glaucomatous eyes in moderately myopic group
† Value for comparison of normal and glaucomatous eyes in highly myopic group

DISCUSSION

This study aimed to demonstrate the diagnostic performance of OCT parameters, including peripapillary RNFL and macular GC-IPL thickness obtained by Cirrus HD-OCT, to detect glaucoma in moderately and highly myopic patients. We found the capability of macular GC-IPL thickness parameters for discriminating between glaucomatous and normal eyes to be high and comparable to peripapillary RNFL thickness in both myopia severity groups.

Diagnosing glaucoma in myopic patients can be a challenge due to anatomical variations in the optic disc and retina, such as tilted disc, nasal elevation, temporal flattening, rotation, posterior staphyloma, and large peripapillary atrophy, can make it difficult for clinicians to distinguish between structural damage from glaucoma and anatomical changes due to myopia.[15,16] In addition to the difficulties in making a clinical diagnosis by direct visualization of ONH or optic disc photographs, structural evaluation via peripapillary RNFL parameters obtained by SD-OCT can also demonstrate inaccuracies of measurement. Hwang, *et al.* reported that neuroretinal rim measurement errors were observed in myopic patients when using Cirrus HD-OCT.[15] Leung, *et al.* concluded that increasing

TABLE 3. The AuROC value (SE) for each Cirrus HD-OCT parameter, which indicates the strength of that parameter for distinguishing between normal and glaucomatous eyes, in the moderate and high myopia groups.

	Moderately myopic group (n = 31)	Highly myopic group (n = 39)
RNFL thickness parameters, μm		
Average	0.919 (0.057)	0.980 (0.018)
Superior	0.892 (0.058)	0.855 (0.064)
Nasal	0.648 (0.108)	0.548 (0.093)
Inferior	0.925 (0.045)	0.962 (0.027)
Temporal	0.850 (0.077)	0.795 (0.076)
Macular GC-IPL parameters, μm		
Average	0.842 (0.073)	0.887 (0.058)
Minimum	0.963 (0.031)	0.897 (0.065)
ST	0.810 (0.086)	0.891 (0.057)
S	0.838 (0.075)	0.760 (0.079)
SN	0.756 (0.091)	0.758 (0.082)
IN	0.823 (0.077)	0.832 (0.074)
I	0.881 (0.059)	0.904 (0.054)
IT	0.894 (0.055)	0.905 (0.053)

Data are given as AUROC (SE).
Abbreviations: ST; superotemporal, S; superior, SN; superonasal, IN; inferonasal, I; inferior, IT; inferotemporal

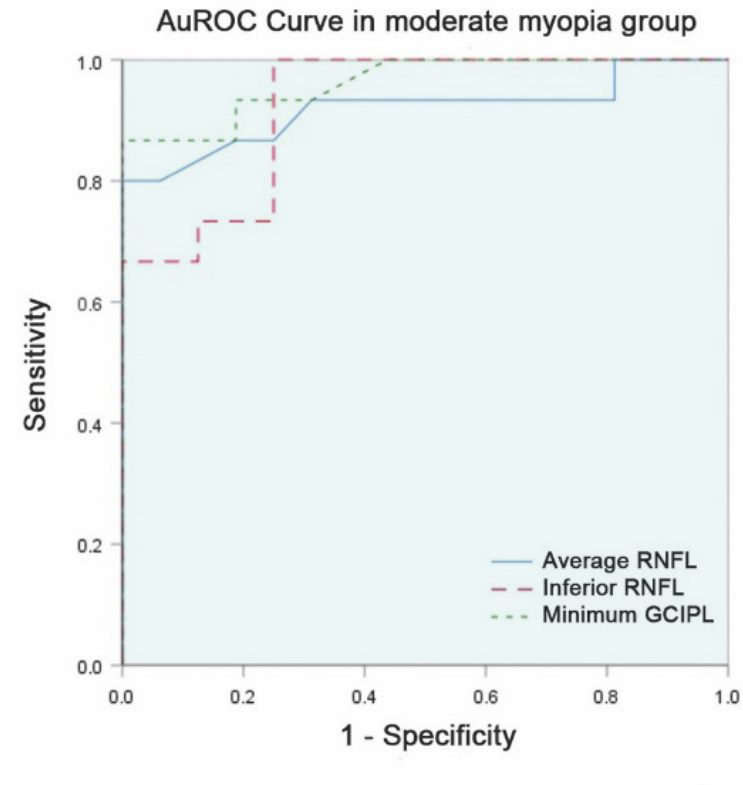

Fig 1. The area under the receiver operating characteristic (AuROC) curve for the 3 best parameters by Cirrus HD-OCT for distinguishing between normal and glaucomatous eyes in the moderate myopia group.
Abbreviations: RNFL; peripapillary retinal nerve fiber layer, GCIPL; macular ganglion cell-inner plexiform layer.

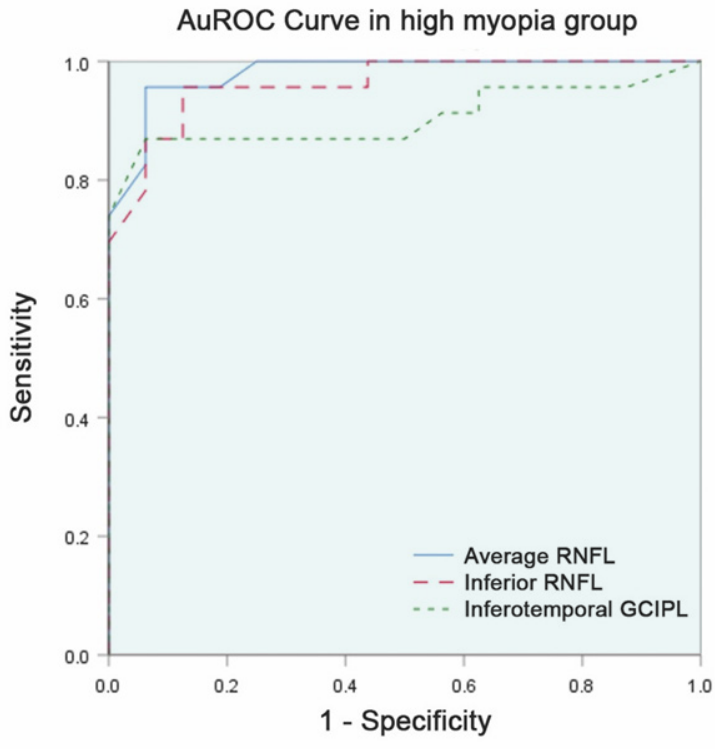

Fig 2. The area under the receiver operating characteristic (AuROC) curve for the 3 best parameters by Cirrus HD-OCT for distinguishing between normal and glaucomatous eyes in the high myopia group.
Abbreviations: RNFL; peripapillary retinal nerve fiber layer, GCIPL; macular ganglion cell-inner plexiform layer.

severity of myopia associated with temporally converged superotemporal and inferotemporal bundles of RNFL, which led to abnormal measurement of RNFL.[18] Kim, *et al.* reported that in healthy eyes, false-positive OCT RNFL findings were influenced by smaller disc areas and longer axial lengths, and these factors are usually found in myopic eyes.[25]

In contrast to the limitations of RNFL measurement for diagnosing glaucoma in myopic patients, macular parameters, which are less affected by the optic nerve head variations found in myopia, have good diagnostic ability and their application has been reported in several studies.[14,19,20,23,26-28] Kim, *et al.* reported the effectiveness of using GCC thickness, composed of inner plexiform layer, ganglion cell layer, and RNFL, measured by RTVue SD-OCT for diagnosing glaucoma in myopic eyes to be similar to the diagnostic results obtained from using peripapillary RNFL thickness.[27] Previous study found that global loss volume from GCC algorithm was the best parameter for differentiating between highly myopic glaucoma and nonglaucoma subjects.[28] Despite its advantages, recent study showed the RNFL in myopic eyes to be thinner than the RFNL in normal eyes[23], so the results of macular GCC thickness may be confounded by these variations of RNFL in myopic subjects.

When excluding RNFL measurement, another macular parameter, GC-IPL thickness, was introduced. Previous study reported that in highly myopic subjects, macular GC-IPL thickness demonstrated a similar capability to identify glaucoma as the RNFL thickness. In the highly myopic group (SE -6.00 to -20.00 D), they found the SD-OCT parameters with the highest AuROC values to be inferior RNFL and inferotemporal GC-IPL thicknesses (AuROC: 0.906, 0.852, respectively). In the non-highly myopic eyes (SE -0.25 to -6.00 D), the best AuROC values were average RNFL (AuROC: 0.920) and minimum GC-IPL thicknesses (AuROC: 0.908).[19] Seol, *et al.* found GC-IPL thickness at inferotemporal sector to be the best parameter for detecting preperimetric glaucoma in both the non-highly myopic (SE -0.50 to -6.00 D; AuROC: 0.747) and highly myopic groups (SE ≤ -6.00 D; AuROC: 0.737).[20] These results are consistent with our findings. In our study, minimum GC-IPL, inferior RNFL, and average RNFL thicknesses (AuROC: 0.963, 0.925, and 0.919, respectively) were the parameters with the best diagnostic performance in the moderately myopic group. In the highly myopic group, average RNFL, inferior RNFL, and inferotemporal GC-IPL thicknesses (AuROC: 0.980, 0.962, and 0.905, respectively) were the best parameters for detecting glaucoma.

The parameters that demonstrated the greatest AuROC in the moderately myopic eyes (mean SE: -4.48 ± 0.92 D) in our study were similar to those identified in the non-highly myopic group (mean SE: -2.46 ± 1.69 D) in previous study[19]; however, greater AuROC values were found in our study. Since increasing severity of myopia temporally converges the inferior and superior RNFL bundles and brings them closer to the macula[18], using macular parameters may be an appropriate tool for detecting glaucomatous damage in eyes with a higher severity of myopia. Moreover, previous study reported the glaucoma diagnostic ability of macular GCA to be

influenced by the angular distance between the RNFL defect and the fovea, which means that defects located far from the fovea may be difficult to detect with GCA maps.[29] In the moderately myopic group, the AuROC for minimum GC-IPL thickness was the highest in our study, and higher than that reported from previous study, and this may be due to a greater degree of myopia, as discussed above.

In the high myopia group, we found average RNFL, inferior RNFL, and inferotemporal GC-IPL thickness to have the greatest AuROC values, which is consistent with previous studies.[19,20] However, among all of the SD-OCT parameters, the RNFL parameters showed the best AuROC values. Despite the higher degree of myopia, it remains unclear why the RNFL parameters have superior diagnostic ability. Of interest, recent studies reported several factors specific to highly myopic eyes that may reduce the reliability of GC-IPL measurements. Kim, *et al*. reported that in eyes with myopic tilted disc, increasing degree of optic disc torsion corresponded with distortion of the posterior pole contour[30], which may imply that GC-IPL measurement in high myopes could be influenced by anatomical misalignment in the macular area. Furthermore, although GC-IPL thickness assessments in highly myopic eyes demonstrated satisfying long-term reproducibility, various factors, such as retinal thinning caused by chorioretinal atrophy and posterior staphyloma from myopia-related changes, may significantly influence reproducibility.[31] In addition to thinning of the macular region from stretching of the posterior globe, abnormal macular thickening or macular retinoschisis may also develop in highly myopic eyes.[32] These factors will eventually confound GC-IPL evaluation, so caution must be exercised when interpreting GC-IPL thickness in high myopia.

The current study demonstrated that all of the parameters obtained by SD-OCT were thinner in glaucomatous than in normal eyes in both moderately and highly myopic patients. Among the normal eyes, RNFL and GC-IPL thickness parameters were both lower in high myopes than in moderate myopes. In contrast to our findings, Seo, *et al*. reported that temporal RNFL thickness analyzed by Cirrus HD-OCT was significantly greater in highly myopic normal eyes than moderately myopic normal eyes, which could be attributed to the temporalization of RNFL when the degree of myopia and axial length increase.[22] Further studies that include more normal subjects in both groups may confirm these hypotheses. Thinning of RNFL and GC-IPL thicknesses in higher severity myopia could be artifactual findings due to the ocular magnification effect. A recent study showed that the significant negative correlation found between OCT parameters (GC-IPL and RNFL thicknesses) and axial length was the result of ocular magnification effect since the area scanned by OCT was greater in elongated globes.[33,34] Therefore, further study using magnification correction factors is needed to remedy this limitation, and to avoid misdiagnosis of glaucoma in patients with myopia.

Since the prevalence of myopia is increasing globally, and especially in Asia[17], data collection from various population groups is needed to construct normative databases for myopia, which will enhance our ability to diagnose glaucoma in myopic patients. Previous studies were mainly conducted in Korean, Japanese, and Chinese participants.[14,18-20,22,23,26] To the best of our knowledge, this is the first study to investigate the common structural imaging parameters and their diagnostic abilities in different severities of myopia in Thai population. These results from different ethnic groups provide clinically useful data that can be used to develop myopia-specific normative databases for general population. One of the strengths of this study is that we enrolled normal subjects in both myopia severity groups so that AuROC values could be generated to satisfactorily detect glaucoma among myopic patients. However, according to the Hodapp, Parish, and Anderson criteria[35], the glaucomatous eyes included in this study were classified as having early to moderate defects, which means that our findings may not be applicable to eyes with greater or lesser severity of glaucoma damage. Future study evaluating the diagnostic performance of these parameters for differentiating different severities of glaucoma is warranted.

Limitations

There are certain limitations to this study that should be mentioned. First, the study population size was relatively small, and this may have given our study insufficient statistical power to identify all statistically significant differences and associations between groups. Additional studies in a larger number of participants may be needed confirm and/or improve the validity of our results. Second, GC-IPL thinning in myopic glaucoma patients was not necessarily detected by HD-OCT measurement. Because the Cirrus HD-OCT equipment utilized in this research assessed macular GC-IPL thickness inside a 6x6x2 mm cube centered at the fovea, the presence of any glaucomatous defect away from this area might not be detected by this algorithm, as shown in Fig 3. Measurement of a larger field of the macula may optimize the glaucoma diagnosis, even in patients with myopia.

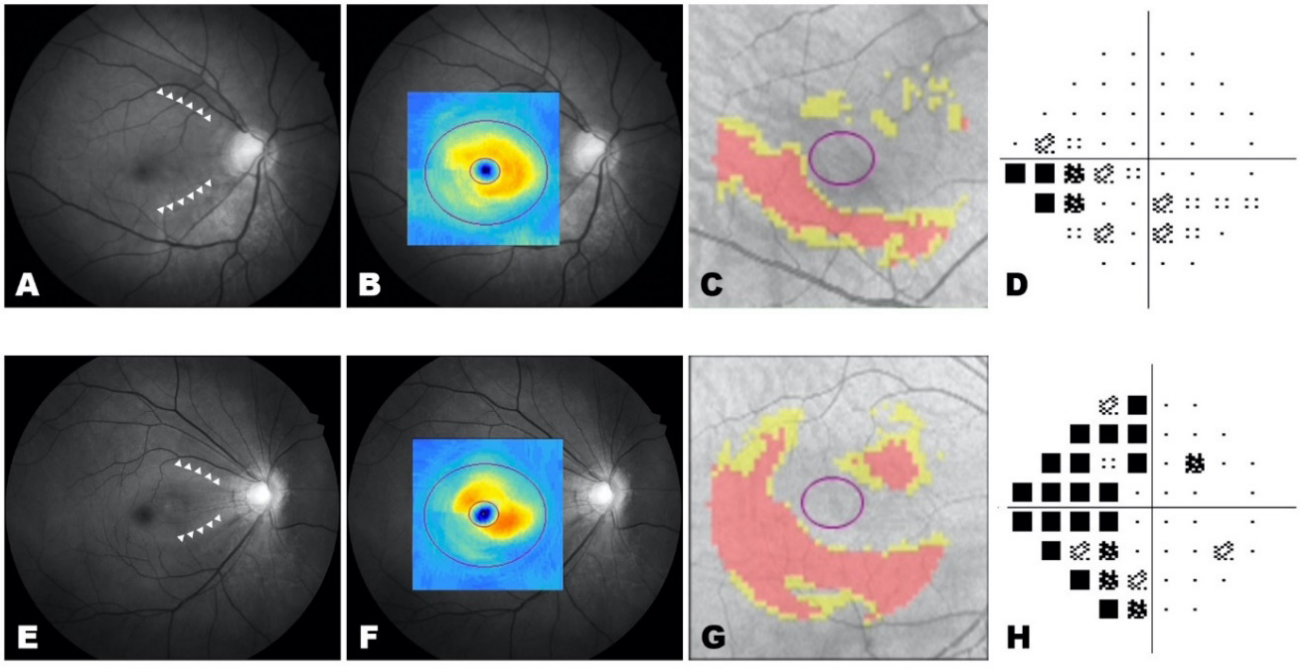

Fig 3. An example of a moderate myopia patient, and a high myopia patient.
Moderately myopic patient (A-D). Right eye; SE -5.00 D, AL 26.68 mm, HVF MD -2.00 dB.
(A) Red-free fundus photograph showed multiple RNFL defects (arrow heads). Generalized RNFL thinning in the inferior retina was observed as the choroidal vessels became clearly visible, so the RNFL defect was more easily detected in the superior hemifield than in the inferior hemifield.
(B) Detection of inferior defect on GCIPL thickness map indicated that the superior defect was located away from the macular area, thus the scanned area of the GCIPL thickness map was unable to include the superior defect into the analysis.
(C) The GCIPL deviation map was consistent with the thickness map.
(D) HVF pattern deviation map showed inferior arcuate scotoma and early superior nasal step both of which correspond with the RNFL defects. Of note, GCA could not detect abnormality in the superior hemifield despite mild inferior field loss.
Highly myopic patient (E-H). Right eye; SE -6.00 D, AL 27.23 mm, HVF MD -7.20 dB.
(E) Red-free fundus photograph showed multiple RNFL defects (arrow heads) in both the superior and inferior hemifields.
(F) The GCIPL thickness map was able to detect both superior and inferior hemifield defect, and the inferior defect was much more severe than superior defect.
(G) The findings of the GCIPL deviation map were consistent with those of the GCIPL thickness map.
(H) HVF pattern deviation map showed double arcuate scotomas, and severe defect was found in the superior visual field, which corresponds with the observed RNFL defects and GCA.

CONCLUSION

Macular GC-IPL thickness demonstrated high ability to detect glaucoma in patients with moderate or high myopia and thus can enhance glaucoma diagnosis in both groups of myopic patients. However, it should be utilized in conjunction with a comprehensive clinical examination, additional structural imaging modalities, and functional assessments to elucidate a more precise diagnosis of glaucoma in myopia.

ACKNOWLEDGEMENTS

The authors gratefully acknowledge the patients that generously agreed to participate in this study, and Assistant Professor Chulaluk Komoltri, DrPH (Biostatistics) from the Office for Research and Development, Faculty of Medicine Siriraj Hospital, Mahidol University, for assistance with statistical analysis.

Conflict of interest declaration

All authors declare no personal or professional conflicts of interest, and no financial support from the companies that produce and/or distribute the drugs, devices, or materials described in this report.

Funding disclosure

This was an unfunded study.

REFERENCES

1. Adelson JD, Bourne RRA, Briant PS, Flaxman SR, Taylor HRB, Jonas JB, et al. Causes of blindness and vision impairment in 2020 and trends over 30 years, and prevalence of avoidable blindness in relation to VISION 2020: the Right to Sight: an analysis for the Global Burden of Disease Study. Lancet Glob Health. 2021;9(2):e144-e60.
2. Foster A, Resnikoff S. The impact of Vision 2020 on global blindness. Eye. 2005;19(10):1133-5.

3. McMonnies CW. Glaucoma history and risk factors. J Optom. 2017;10(2):71-8.
4. Holden BA, Fricke TR, Wilson DA, Jong M, Naidoo KS, Sankaridurg P, et al. Global Prevalence of Myopia and High Myopia and Temporal Trends from 2000 through 2050. Ophthalmology. 2016;123(5):1036-42.
5. Pan CW, Ramamurthy D, Saw SM. Worldwide prevalence and risk factors for myopia. Ophthalmic Physiol Opt. 2012;32(1): 3-16.
6. Mitchell P, Hourihan F, Sandbach J, Wang JJ. The relationship between glaucoma and myopia: the Blue Mountains Eye Study. Ophthalmology. 1999;106(10):2010-5.
7. Pan CW, Cheung CY, Aung T, Cheung CM, Zheng YF, Wu RY, et al. Differential associations of myopia with major age-related eye diseases: the Singapore Indian Eye Study. Ophthalmology. 2013;120(2):284-91.
8. Weinreb RN, Khaw PT. Primary open-angle glaucoma. The Lancet. 2004;363(9422):1711-20.
9. Sommer A, Katz J, Quigley HA, Miller NR, Robin AL, Richter RC, et al. Clinically detectable nerve fiber atrophy precedes the onset of glaucomatous field loss. Arch Ophthalmol. 1991;109(1): 77-83.
10. Curcio CA, Allen KA. Topography of ganglion cells in human retina. J Comp Neurol. 1990;300(1):5-25.
11. Tan O, Chopra V, Lu AT, Schuman JS, Ishikawa H, Wollstein G, et al. Detection of macular ganglion cell loss in glaucoma by Fourier-domain optical coherence tomography. Ophthalmology. 2009;116(12):2305-14.e1-2.
12. Guedes V, Schuman JS, Hertzmark E, Wollstein G, Correnti A, Mancini R, et al. Optical coherence tomography measurement of macular and nerve fiber layer thickness in normal and glaucomatous human eyes. Ophthalmology. 2003;110(1):177-89.
13. Mwanza JC, Oakley JD, Budenz DL, Chang RT, Knight OJ, Feuer WJ. Macular ganglion cell-inner plexiform layer: automated detection and thickness reproducibility with spectral domain-optical coherence tomography in glaucoma. Invest Ophthalmol Vis Sci. 2011;52(11):8323-9.
14. Kim KE, Park KH. Macular imaging by optical coherence tomography in the diagnosis and management of glaucoma. Br J Ophthalmol. 2018;102(6):718-24.
15. Hwang YH, Kim YY, Jin S, Na JH, Kim HK, Sohn YH. Errors in neuroretinal rim measurement by Cirrus high-definition optical coherence tomography in myopic eyes. Br J Ophthalmol. 2012; 96(11):1386-90.
16. Chang RT, Singh K. Myopia and glaucoma: diagnostic and therapeutic challenges. Curr Opin Ophthalmol. 2013;24(2):96-101.
17. Tan NYQ, Sng CCA, Jonas JB, Wong TY, Jansonius NM, Ang M. Glaucoma in myopia: diagnostic dilemmas. Br J Ophthalmol. 2019;103(10):1347-55.
18. Leung CK-S, Yu M, Weinreb RN, Mak HK, Lai G, Ye C, et al. Retinal Nerve Fiber Layer Imaging with Spectral-Domain Optical Coherence Tomography: Interpreting the RNFL Maps in Healthy Myopic Eyes. Invest Ophthalmol Vis Sci. 2012; 53(11):7194-200.
19. Choi YJ, Jeoung JW, Park KH, Kim DM. Glaucoma Detection Ability of Ganglion Cell-Inner Plexiform Layer Thickness by Spectral-Domain Optical Coherence Tomography in High Myopia. Invest Ophthalmol Vis Sci. 2013;54(3):2296-304.
20. Seol BR, Jeoung JW, Park KH. Glaucoma Detection Ability of Macular Ganglion Cell-Inner Plexiform Layer Thickness in Myopic Preperimetric Glaucoma. Invest Ophthalmol Vis Sci. 2015;56(13):8306-13.
21. Knight ORJ, Girkin CA, Budenz DL, Durbin MK, Feuer WJ, Cirrus OCT Normative Database Study Group ft. Effect of Race, Age, and Axial Length on Optic Nerve Head Parameters and Retinal Nerve Fiber Layer Thickness Measured by Cirrus HD-OCT. Arch Ophthalmol. 2012;130(3):312-8.
22. Seo S, Lee CE, Jeong JH, Park KH, Kim DM, Jeoung JW. Ganglion cell-inner plexiform layer and retinal nerve fiber layer thickness according to myopia and optic disc area: a quantitative and three-dimensional analysis. BMC Ophthalmol. 2017;17(1):22.
23. Akashi A, Kanamori A, Ueda K, Inoue Y, Yamada Y, Nakamura M. The Ability of SD-OCT to Differentiate Early Glaucoma With High Myopia From Highly Myopic Controls and Nonhighly Myopic Controls. Invest Ophthalmol Vis Sci. 2015;56(11):6573-80.
24. European Glaucoma Society Terminology and Guidelines for Glaucoma, 5th Edition. Br J Ophthalmol. 2021;105(Suppl 1): 1-169.
25. Kim KE, Jeoung JW, Park KH, Kim DM, Kim SH. Diagnostic classification of macular ganglion cell and retinal nerve fiber layer analysis: differentiation of false-positives from glaucoma. Ophthalmology. 2015;122(3):502-10.
26. Kim YK, Yoo BW, Jeoung JW, Kim HC, Kim HJ, Park KH. Glaucoma-Diagnostic Ability of Ganglion Cell-Inner Plexiform Layer Thickness Difference Across Temporal Raphe in Highly Myopic Eyes. Invest Ophthalmol Vis Sci. 2016;57(14):5856-63.
27. Kim NR, Lee ES, Seong GJ, Kang SY, Kim JH, Hong S, et al. Comparing the ganglion cell complex and retinal nerve fibre layer measurements by Fourier domain OCT to detect glaucoma in high myopia. Br J Ophthalmol. 2011;95(8):1115-21.
28. Shoji T, Sato H, Ishida M, Takeuchi M, Chihara E. Assessment of Glaucomatous Changes in Subjects with High Myopia Using Spectral Domain Optical Coherence Tomography. Invest Ophthalmol Vis Sci. 2011;52(2):1098-102.
29. Hwang YH, Jeong YC, Kim HK, Sohn YH. Macular ganglion cell analysis for early detection of glaucoma. Ophthalmology. 2014;121(8):1508-15.
30. Kim YC, Moon J-S, Park H-YL, Park CK. Three Dimensional Evaluation of Posterior Pole and Optic Nerve Head in Tilted Disc. Sci Rep. 2018;8(1):1121.
31. Lee M-W, Park K-S, Lim H-B, Jo Y-J, Kim J-Y. Long-term reproducibility of GC-IPL thickness measurements using spectral domain optical coherence tomography in eyes with high myopia. Sci Rep. 2018;8(1):11037.
32. Benhamou N, Massin P, Haouchine B, Erginay A, Gaudric A. Macular retinoschisis in highly myopic eyes. Am J Ophthalmol. 2002;133(6):794-800.
33. Francisconi CLM, Freitas AM, Wagner MB, Ribeiro RVP. Effects of axial length on retinal nerve fiber layer and macular ganglion cell-inner plexiform layer measured by spectral-domain OCT. Arquivos Brasileiros de Oftalmologia (Online). 2020;83(4):269-76.
34. Huang D, Chopra V, Lu AT-H, Tan O, Francis B, Varma R, et al. Does optic nerve head size variation affect circumpapillary retinal nerve fiber layer thickness measurement by optical coherence tomography? Invest Ophthalmol Vis Sci. 2012;53(8): 4990-7.
35. Hodapp E, Parrish RK, Anderson DR. Clinical decisions in glaucoma: Mosby Incorporated; 1993.

Implementation of Viscoelastic Hemostatic Assay-guided Therapy to Evaluate and Manage Trauma-related Bleeding: A Pilot Study from a Level 1 Trauma Center in Bangkok, Thailand

Tongporn Wannatoop, M.D.*, Janejira Kittivorapart, M.D. Ph.D., Kulvara Kittisares, M.D.**, Warit Werawatakul, M.D.*, Theera Ruchutrakool, M.D.***, Parichart Permpikul, M.D.**, Sunanta Chobpluk, B.Sc.****

**Division of Trauma Surgery, Department of Surgery, **Department of Transfusion Medicine, ***Division of Hematology, Department of Medicine, Faculty of Medicine Siriraj Hospital, Mahidol University, Bangkok 10700, Thailand.*

ABSTRACT

Objective: To evaluate the effectiveness of viscoelastic hemostatic assay (VHA)-guided therapy for assessing and managing trauma-related bleeding using a multidisciplinary team approach at a level 1 trauma center.

Materials and Methods: This retrospective pilot study included trauma-related hemorrhagic patients who underwent rotational thromboelastometry (ROTEM) during September 2019-May 2020. ROTEM trace results were compared with those of conventional coagulation tests (CCT).

Results: Thirteen patients (median age: 29.1 years; male: 76.92%) were included. The median (range) days of ventilator support, ICU length of stay, and hospital length of stay was 4 [0-65], 5 [1-65], and 6 [1-83], respectively. ROTEM-guided therapy was applied 26 times, and was repeated in 7 cases. Of those, four cases were repeated to correct coagulopathy. The median time-to-confirmed hemostasis for ROTEM was substantially shorter than for CCT (92 minutes [70-110] vs. 287 minutes [204-354], respectively). The coagulation results from 26 ROTEM tests were also compared between those requiring and not requiring a massive transfusion protocol (MTP). MTP with ROTEM-guided therapy was activated in 6/13 cases. Following the resuscitation endpoints in traumatic shock, four of those had their median serum lactate levels decreased from 10.9 d/L (2.1-16.8) to 3.9 d/L (1.7-17.7). ROTEM traces detected cases with low fibrinogen that only required cryoprecipitate transfusion, and red blood cell and fresh frozen plasma use was less in ROTEM than in conventional MTP.

Conclusion: VHA-guided therapy was shown to effectively facilitate goal-directed hemostatic resuscitation and efficient blood product use during resuscitation, definitive treatment, and postoperative intensive care.

Keywords: Implementation; viscoelastic hemostatic assay-guided therapy; trauma-related bleeding; rotational thromboelastometry; trauma-induced coagulopathy (Siriraj Med J 2022; 74: 294-304)

INTRODUCTION

Preventable death due to exsanguination is a leading cause of death in trauma patients. This means that improvements in patient care can improve patient survival.[1] Consistent with this premise, advancements in damage control resuscitation (DCR), including improvements in methods for assessing and managing trauma-related bleeding, have been adopted and implemented with very

Corresponding author: Tongporn Wannatoop
E-mail: tongporn.wan@mahidol.ac.th
Received 27 November 2021 Revised 31 December 2021 Accepted 4 January 2022
ORCID ID: https://orcid.org/0000-0002-9331-9218
http://dx.doi.org/10.33192/Smj.2022.36

favorable results.[2,3] The DCR concept comprises three aspects, including balanced resuscitation, hemostatic resuscitation, and bleeding control. Hemostatic resuscitation requires advanced understanding of trauma-induced coagulopathy (TIC) that is guided by a goal-directed resuscitation approach.[4-8] This is essentially important because several previous studies reported TIC to be associated with 4- to 6-fold higher mortality.[4,9-13]

Another important death-related factor in hemorrhaging patients is time, including time to hemostasis, time-to-treat, and time to activation of a massive transfusion protocol (MTP).[14] Therefore, a rapid and reliable method is needed that can detect and correct TIC during efforts to achieve surgical control at the bleeding site.[10,15] In a trauma setting, conventional coagulation tests (CCT), such as prothrombin time (PT), activated partial thromboplastin time (APTT), international normalized ratio (INR), platelet count, and fibrinogen level, have limited ability to evaluate for TIC due to their ability to accurately reflect the real physiologic dynamic changes that occur during the coagulation process.[3,16] Moreover, these tests consume too much of the 'golden hour' that is so crucial to patient survival in a trauma setting.[17]

To remedy these treatment-related concerns, technological innovations for detecting coagulopathy were introduced to improve advanced resuscitation. Viscoelastic hemostatic assay (VHA), such as rotational thromboelastometry (ROTEM) (TEM Innovations GmbH, Munich, Germany) and thromboelastography (TEG) (Haemonetics Corp, Niles, IN, USA), is a tool that has the ability to detect and report global hemostasis, including all stages of the coagulation cascade from initiation of clot formation to clot lysis.[3,18] Several clinical trials, reported significant advantages of VHA-guided MTP in trauma patients relative to both decreased mortality and reduced use of blood components during resuscitation.[19-23]

The VHA technique was first introduced by Hellmut Hartert in 1948.[24] During the early period, VHA was used during liver transplantation and cardiac surgery.[3,25-27] It was first applied in trauma care in 1997 to study its ability to detect and improve the management of TIC.[28] VHA-guided MTP was then evaluated their superior benefit than standard MTP for use in trauma patients in 2013.[29] The VHA instrument that is available at our center is a ROTEM sigma machine (TEM Innovations GmbH, Munich, Germany), so this study evaluated the effectiveness of this device compared to conventional MTP. This cartridge-based device delivers dynamic run-through coagulation information in trace, including clot initiation, clot propagation, clot firmness, and clot lysis.

Even though the management of trauma patients in Thailand continues to improve and evolve, certain factors, such as TIC, continue to delay treatment, which reduces the likelihood of a favorable outcome. Moreover, genetic variations may exert variable influence on the pathophysiology of TIC, and data specific to this condition in Thai population remains scarce. Accordingly, the aim of this pilot study was to evaluate the effectiveness of VHA-guided therapy for assessing and managing trauma-related bleeding using a multidisciplinary team approach at our level 1 trauma center, which is a major university-based medical center.

MATERIALS AND METHODS

Study design and patients

This retrospective pilot study included trauma-related hemorrhagic patients who underwent ROTEM testing during September 2019 to May 2020. Patients with trauma-related bleeding caused by penetrating injury or blunt force injury, and patients who required blood transfusion were eligible for inclusion. Our institution's massive transfusion protocol with rotational thrombolelastometry (ROTEM)-guided coagulation management algorithm (Fig 1) was designed and implemented by hematologists and blood bank specialists. ROTEM trace results were compared with those of CCT and interpreted by trained personnel in a multidisciplinary team that included the trauma surgeons, hematologists, and the transfusion team. The primary outcome was 24-hour survival. The secondary outcomes were the number of ventilator days, the number of hospital days, the number of intensive care days, and clinical progression until hospital discharge. Time-to-confirmed hemostasis in this study was defined as the duration from the drawing of the initial blood sample to be sent to the ROTEM machine and the laboratory with subsequent correction of any reported coagulopathy to the time point when repeat results reported the achievement of hemostasis after receiving guided-therapy. The protocol for this study was approved by our center's institutional review board, and written informed consent was not obtained due to our study's anonymous retrospective design.

Brief overview of the use and function of the ROTEM sigma VHA

The ROTEM sigma system is a reagent cartridge-based fully automated system. Blood is added into a cup that is fixed, and a pin is moved by a counterspring (Fig 2). The pin is stabilized by a ball bearing avoid artifacts caused by shock and vibration, which facilitates mobile use of the device. With increasing viscoelastic forces due

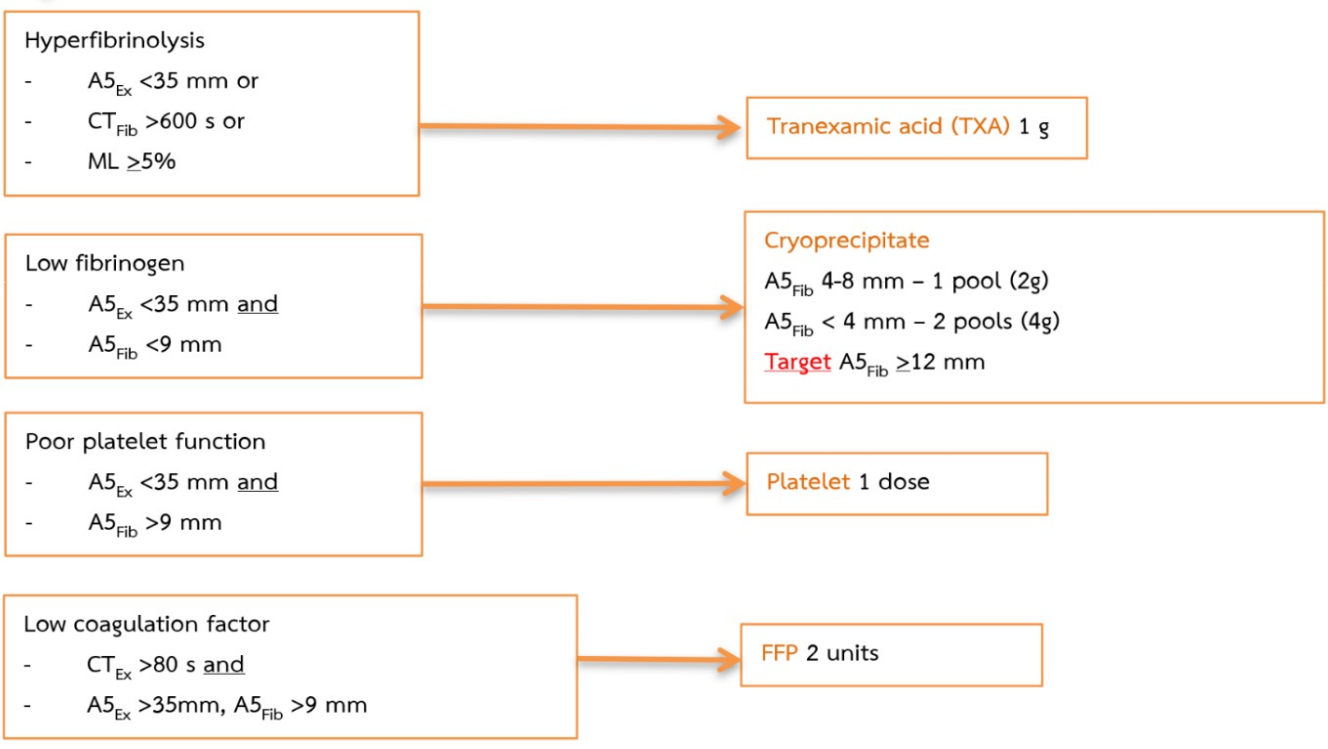

Fig 1. Siriraj massive transfusion protocol with rotational thrombolelastometry (ROTEM)-guided coagulation management algorithm. $A5_{EX}$, clot amplitude 5 min after CT on EXTEM assay; CT_{FIB}, clotting time (CT) on FIBTEM assay; ML, maximum lysis; $A5_{FIB}$, clot amplitude 5 min after CT on FIBTEM assay; CT_{EX}, CT on EXTEM assay; FFP, fresh frozen plasma.

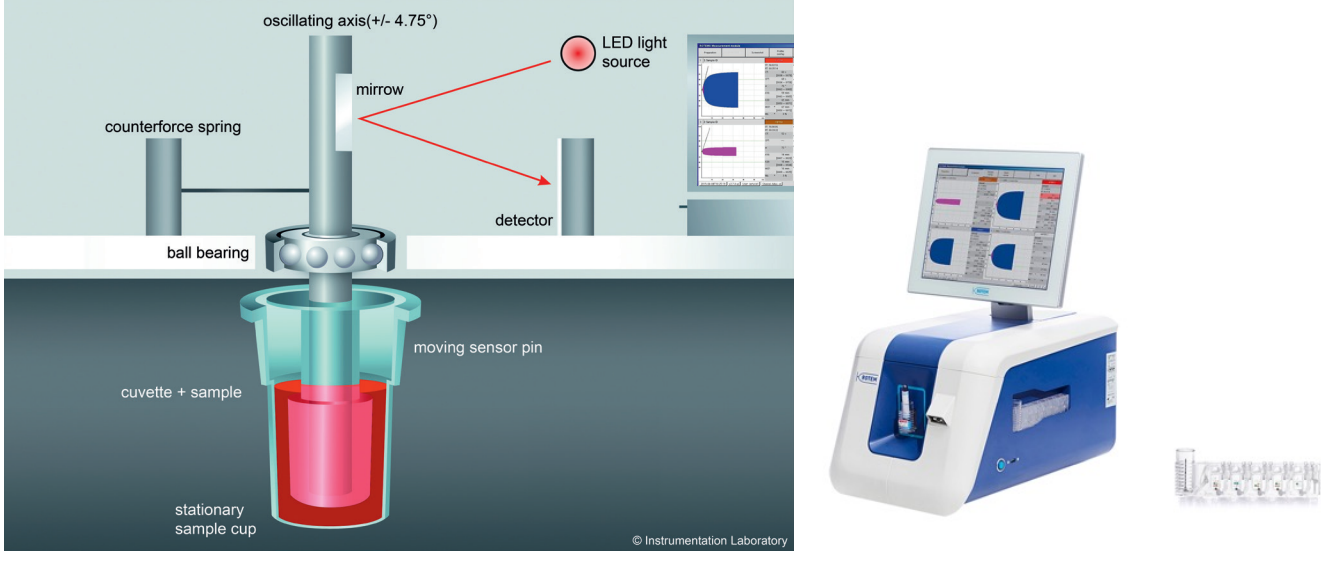

Fig 2. Operational principle of rotational thromboelastometry (ROTEM). (Left image) The ROTEM sigma system is a reagent cartridge-based fully automated system. Blood that is pre-warmed to 37°C is added into a cup that is fixed, and a pin is moved by a counterspring. The pin is stabilized by a ball bearing avoid artifacts caused by shock and vibration, which facilitates mobile use of the device. With increasing viscoelastic forces due to fibrin polymerization and fibrin-platelet interaction, the movement of the pin is reduced, which is detected contact-free by an LED light-mirror-optical detector system. The ROTEM software transforms this signal to a graphical result/signature waveform called a temogram. (Right image) The ROTEM sigma machine. (Figure provided courtesy of TEM Innovations GmbH, Munich, Germany)

to fibrin polymerization and fibrin-platelet interaction, the movement of the pin is reduced, which is detected contact-free by an LED light-mirror-optical detector system. The ROTEM software transforms this signal to a graphical result/signature waveform called a temogram (Fig 3). Clot initiation, propagation, strength, and lysis are displayed in time tracing patterns. The essential initial results for correcting TIC are fibrinolysis, fibrinogen level, platelet quantity, and platelet function because these factors influence initiation and propagation of blood clotting. ROTEM output data can be reliable interpreted within 5 minutes after clotting time (CT) (A5 = amplitude of clot firmness 5 minutes after CT) for fibrinogen polymerization and clot formation. These findings help to determine the stage of the dynamic process of coagulopathy, and facilitate correction via goal-directed therapy.[23,30-32]

Statistical analysis

Descriptive statistics were used to summarize patient demographic and clinical characteristics. Microsoft Excel® spreadsheet and data analysis software was used to manage and analyze the data. The data are presented as number and percentage for categorical variables, and as median and range for continuous data.

RESULTS

Patient characteristics

A total of 13 patients with trauma-related bleeding were included. The median age of patients was 29.1 years (range: 15-75), most were men (10/13, 76.92%), and most had sustained blunt force trauma (11/13, 84.6%). One of the two patients with a penetrating injury was referred to our center with cardiac tamponade and clinically compensated shock at 4 hours after the injury. Three

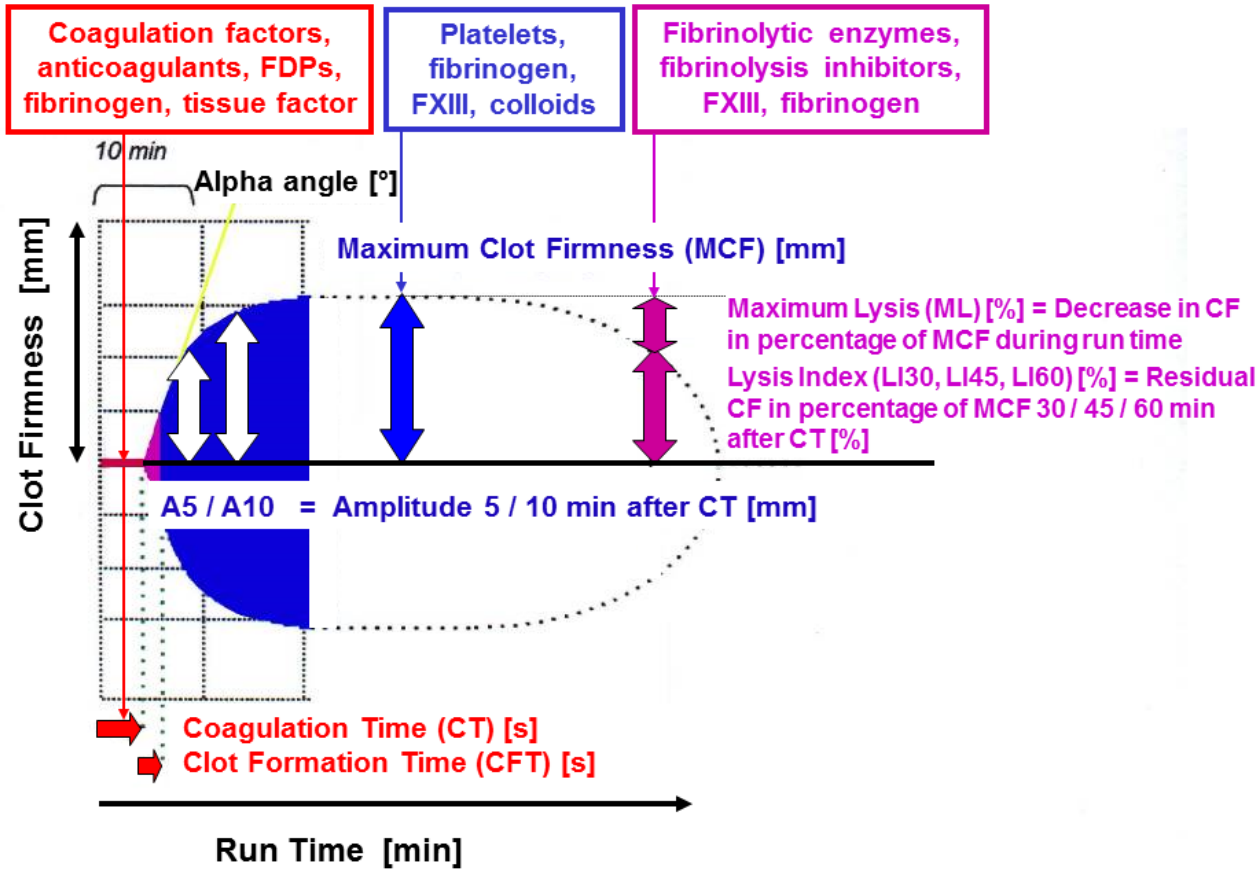

Fig 3. ROTEM traces 4 main clot parameters. **1. Clot initiation**: Coagulation time (CT) is defined as the time from initiation of clot formation to fibrin aggregation **2. Clot propagation:** Clot formation time (CFT) and alpha-angle are used to determine the speed of growth in clot firmness due to fibrin polymerization and fibrin-platelet interaction. **3. Clot strength:** Amplitude (A) 5 minutes (A5) and 10 minutes (A10) after CT and maximal clot firmness (MCF) result from fibrinogen and platelet contribution. We normally used the amplitude at 5 minutes after CT (A5) fibrinogen trace (ROTEM – FIBTEM) as POC for early correction of fibrinogen concentration during resuscitation. [27-29] **4. Clot lysis:** Maximal lysis (ML) and clot lysis index at 30 and 60 minutes after CT (LI30 and LI60, respectively) are related to fibrinolysis. If hyperfibrinolysis is present, antifibrinolytic agents, such as tranexamic acid (TXA) will be administered to correct this pathology that is commonly associated with TIC. [7, 13, 15] (Figure provided courtesy of Dr. Klaus Görlinger, Munich, Germany)

patients were on heparinization, antiplatelet therapy or anticoagulants for post-injury related conditions. Among all cases, the median Injury Severity Score (ISS) was 26 (range: 10-43), and the Revised Trauma Score (RTS) was 7.84 (range: 0-7.84).

Two patients were diagnosed with severe traumatic brain injury (TBI), which was defined as a Glasgow Coma Scale (GCS) score <8, and a head Abbreviated Injury Scale (AIS) score >2. Among all patients, the median systolic blood pressure (SBP) was 118 mmHg (range: 0-154), and the heart rate (HR) was 110 beats per minute (range: 0-158). Patient body temperature data was not recorded in all cases, so that information is not presented here. During critical stage assessment, the median base deficit (BD) was -8.2 mEq/L (range: -16 to 0), and the serum lactate level was 6.5 d/L (range: 1.1-16.8). After VHA-guided therapy, seven patients underwent immediate further surgery in the operating room, and the remaining patients were transferred to the intensive care unit (ICU) (Table 1). In our study group, five cases were transported directly to our trauma center (not transferred from another hospital), and tranexamic acid (TXA) was administrated after drawing the blood sample.

Twelve of 13 patients survived to at least 24 hours after treatment for a survival rate of 92.3%. The one patient who did not survive had sustained an unsurvivable TBI, and also had preexisting terminal cancer. The median number of days of ventilatory support, ICU admission, and length of hospital stay was 4 (range: 0-65), 5 (range: 1-65), and 6 (range: 1-83), respectively.

ROTEM-guided therapy

A total of 26 ROTEM tests were performed among the 13 study participants. The indications for ROTEM activation were, as follows: (1) MTP activation (13 tests in 6 patients), (2) evaluation of clinical correlation (4 tests in 3 patients), and (3) evaluation of efforts to achieve hemostasis (9 tests in 4 patients). These ROTEM tests were performed during hemorrhagic shock in 12 patients. The locations where the decision was made to employ ROTEM-guided therapy were, as follows: resuscitation room (6 cases), ICU (13 cases), and the perioperative care unit (7 cases). Due to the limited number of cartridges available at the beginning of implementation, ROTEM testing was applied more than once in only 7 cases. Of those, four cases had repeat ROTEM testing immediately after blood component transfusion to correct coagulopathy.

TABLE 1. Patient characteristics on admission or during initiation of viscoelastic hemostatic assay (VHA)-guided therapy and patient outcomes (N=13).

Parameters	n (%) or median [range]
Age (years)	29.1 [15-75]
Gender (male)	10 (76.92%)
Type of injury: Blunt force trauma	11 (84.62%)
Severe traumatic brain injury (cases)	2 (15.38%)
Injury Severity Score (ISS)	26 [10-43]
Revised Trauma Score (RTS)	7.84 [0-7.84]
Systolic blood pressure (mmHg)	118 [0-154]
Heart rate (beats per minute)	110 [0-158]
Base deficit (mEq/L)	-8.2 [-16 to 0]
Serum lactate (d/L)	6.5 [1.1-16.8]
Survival rate after 24-hour	12 (92.31%)
Intensive care unit outcomes	
Duration of ventilatory support (days)	4 [0-65]
Intensive care unit admission (days)	5 [1-65]
Length of hospital stay (days)	6 [1-83]

The median time-to-confirmed hemostasis was markedly shorter in the ROTEM group (92 minutes; range: 70-110) than in the CCT group (287 minutes; range: 204-354).

ROTEM trace results and conventional coagulation test results compared between the massive transfusion protocol (MTP) and non-MTP groups are shown in Table 2. An initial study in three cases found normal coagulation status. One case had no further resuscitation plan after a family discussion due to non-survivable TBI with pre-coexisting terminal cancer. The other two cases were reassessed in the ICU after resuscitation, and both were found to have achieved hemostasis. Four cases that were treated according to the ROTEM-guided coagulation management algorithm, demonstrated good response to resuscitation with a median decrease in serum lactate level from 10.9 d/L (range: 2.1-16.8) to 3.9 d/L (range: 1.7-17.7).

Blood and blood component utilization

MTP with ROTEM-guided coagulation management algorithm was activated in 6 of 13 cases (Table 2). Our institutional conventional MTP comprises 3 different sets of blood and blood components. The first set, which is transfused into patients with an unknown ABO blood group, consists of 4 units of group 'O' RBCs, and two units of group "AB" fresh frozen plasma (FFP). This set was transfused into five patients. The second set consists of 4 units of RBCs, 4 units of FFP, and 1 adult dose of platelets. The third set consists of 4 units of RBCs, 4 units of FFP, and 12 units of cryoprecipitate. There were 4 patients who required set 2, and only 1 patient received set 3. The blood package was no longer used after ROTEM results were reported.

This study analyzed the blood and blood components used within 6 hours pre- and post-ROTEM application by categorizing their use into following 3 phases: (1) pre-ROTEM, which was defined as 6 to 1 hour before testing; (2) peri-ROTEM, which was defined as 1 hour before testing to 3 hours after testing; and, (3) post-ROTEM, which was defined as 3 hours to 6 hours after testing. This description of the distribution of blood and blood products makes clearer the benefit of ROTEM testing data and the types of blood products needed during different phases of treatment (Fig 4).

TABLE 2. Indications for rotational thromboelastometry (ROTEM) activation, and ROTEM trace results and conventional coagulation test results compared between the massive transfusion protocol (MTP) and non-MTP groups.

Indications for ROTEM activation	N=13 cases, 26 tests	
Massive transfusion protocol, n	6	
Clinical correlation, n	3	
Evaluation of efforts to achieve hemostasis, n	4	
	MTP (n=6, 13 tests)	**Non-MTP (n=7, 13 tests)**
ROTEM trace results		
Low fibrinogen	6	1
Low coagulation factor	3	4
Poor platelet	1	1
Hyperfibrinolysis	0	1
Normal study	0	3
Conventional coagulation tests when ROTEM was run (data presented as median)		
Fibrinogen level (mg/dL)	186.13	229.64
Platelets (/μL)	171,667	162,667
Prothrombin time (seconds)	16.02	15.08
Activated partial thromboplastin time (seconds)	35.05	28.94

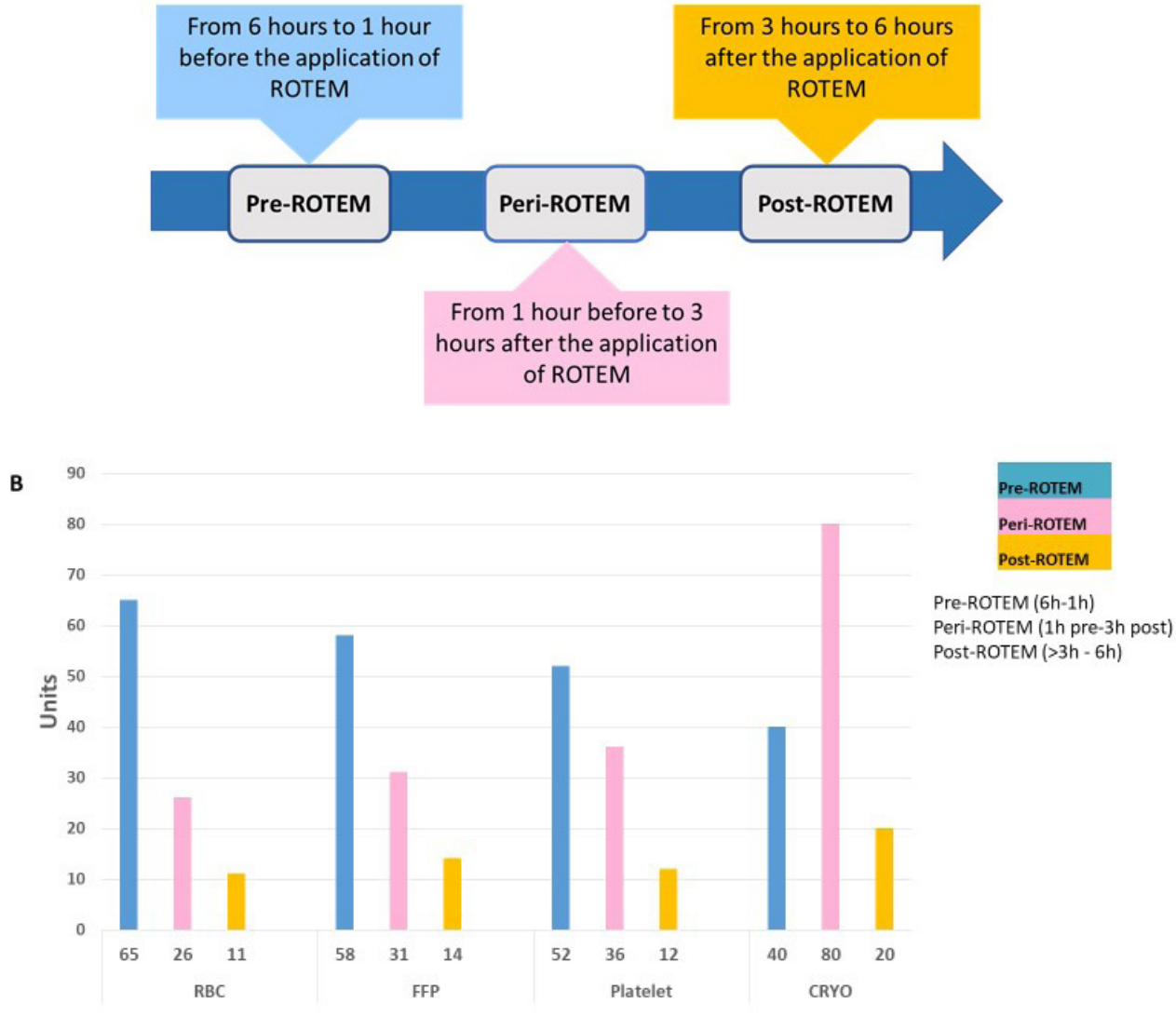

Fig 4. Flow diagram defining the time of evaluation for the before, during, and after phases of rotational thromboelastometry (ROTEM) application (A). Units of blood products given during the before, during, and after phases of ROTEM application among the 13 study patients (B).
Abbreviations: RBC; red blood cell product, FFP; fresh frozen plasma, CRYO; cryoprecipitate

The total number of units of transfused blood products among the 13 patients in this study were, as follows: RBCs 102 units, FFP 103 units, platelets 100 units (25 adult doses), and cryoprecipitate 140 units. A patient who had multiple active conditions, including reoperation for laparotomy and thoracotomy with extracorporeal membrane oxygenation (ECMO) support received a blood transfusion during ROTEM testing that included the following products: RBC 12 units, FFP 14 units, platelet 2 doses, and cryoprecipitate 54 units. Of the four products, RBCs, FFP, and platelets were mainly used during the pre-ROTEM phase for a phase total of 65, 58, and 52 units, respectively. The ratio of MT during the resuscitation phase before applying ROTEM was 1 to 0.9 to 1.12 for FFP, platelets, and RBCs. Cryoprecipitate was given either as part of the 3rd blood product combination MTP set or as needed according to the result of ROTEM testing. The number of units of cryoprecipitate used in the pre-, peri-, and post-ROTEM phases was 40, 80, and 20 units, respectively.

To non-statistically evaluate the benefit of ROTEM-guided therapy as a point-of-care testing (POCT) modality, we evaluated 6 cases that were included in this study that met the activation criteria for conventional MTP. That analysis revealed that we administered 24 units of RBCs and 20 units of FFP less than the number called for using the conventional MTP protocol.

DISCUSSION

Trauma resuscitation in an actively hemorrhagic patient is a challenge, especially in patients with a non-compressible torso hemorrhage (NCTH) because these patients require more time to stabilize, and surgical interventions are commonly needed to control the bleeding. Improved understanding of the pathophysiology of TIC has improved DCR in trauma patients.[2,4-6,9,10,19] The incidence of TIC was reported to range from 25% to 35% in civilian and military trauma-related bleeding patients.[4,9]

Prior to the introduction of VHA-guided therapy, CCT was used for coagulation-guided therapy in patients with TIC; however, these tests are time-consuming and they are limited in their ability to dynamically assess the coagulation cascade.[3,19,28] VHA as a POCT for coagulation assessment was implemented in many countries to overcome these limitations.[5,6,8,10,33,34] Even though there is limited evidence and varied outcomes among studies, several studies reported the benefit of VHA-guided therapy for the management of bleeding in trauma, liver transplantation, cardiothoracic surgery, and obstetric patients.[3,5,8,22,34-36]

Moreover, this technology continues to rapidly evolve and improve. From recent study, the fastest reliable result for the FIBTEM assay was the 5-minute result (the A5 FIBTEM).[30-32]

The benefits of VHA are essential in trauma care, especially during resuscitation and the critical phase, which is associated with many factors that can cause or contribute to TIC. Previous studies that investigated the efficacy of VHA applied in trauma care reported a decrease in mortality from as high as 36% to as low as 17%.[5,18,19,22,23] In the present study, the median ISS among our study subjects was 26, and our 24-hour survival rate was 92.3%. The only death occurred in a patient with non-survivable TBI with coexisting terminal cancer.

TIC incidence

ROTEM analysis of 6 unstable trauma patients upon arrival revealed TIC in all patients (incidence 100%). When comparing between MTP and non-MTP patients, we found a far higher number of patients with low fibrinogen in the MTP group (85.7% vs. 16.67%, respectively), which was defined as a fibrinogen level <200 mg/dL or A5 FIBTEM <9 mm. (Table 2). These results are consistent with the known mechanisms of TIC, especially the importance of fibrinogen concentration, which strongly influences the initial phase of the coagulation cascade. Base on the principle of early fibrinogen and coagulation factor deficiency in TIC, the evolution of VHA as a POCT was developed to deliver faster results so that the speed of care could be accelerated in this vulnerable patient population. These advantages encourage hospitals to provide both VHA-guided therapy and specific coagulation therapy (fibrinogen concentration, prothrombin complex concentrate) to improve patient care to the level currently being provided in several countries around the world.[3,5,8,20,21,37,38]

Interestingly, no patients in the MTP group showed hyperfibrinolysis as a result of ROTEM testing. However, it is possible that cases that were transferred to our trauma center from other hospitals could have received TXA prior to transfer. At present, the CRASH-2 trial and many clinical practice guidelines recommend administration of tranexamic acid (TXA), which is an antifibrinolytic drug, for patients with trauma-related bleeding to correct hyperfibrinolysis in TIC.[4,33,39,40] Our pilot data suggests this as a potentially important topic of further study because TXA administration may help to improve trauma care in developing countries.

ROTEM-related clinical considerations

In addition to the benefits of faster point-of-care testing to determine hemodynamic status, bleeding status, and lactate acidosis or base excess, ROTEM-guided test data also helped us differentiate between medically controllable bleeding and bleeding that required surgical intervention. Two cases that required extensive resuscitation had their treatment plan changed to surgical intervention after our review of ROTEM test results. One patient in our cohort presented with clinically profound shock and was unresponsiveness to resuscitation. Hemorrhagic shock was excluded in that patient after negative result from evaluation by both clinical examination and full-body computed tomography scan. The ROTEM result was also normal, so further investigation revealed a non-survivable TBI with neurogenic shock and no additional strategies for correcting the patient's condition. We also used VHA to evaluate the coagulation status of 3 patients who were on heparinization, antiplatelet therapy or anticoagulants for post-injury related conditions. The first case was on ECMO support for post-traumatic acute respiratory distress syndrome (ARDS), the second had post-vascular bypass with prosthetic graft, and the third was on anticoagulant to treat thrombosis.

Transfusion of blood components

Blood transfusion is one of the mainstay treatments for hemorrhagic trauma patients, especially in those requiring massive transfusion (MT). There are several definitions of MT. MT was defined as a requirement for

more than 4 RBC units or death within the first hour after injury.[5,6] In this study, there were 6 patients who received MT therapy.

Early initiation of blood and blood component transfusion combined with close monitoring of hemostasis is needed to correct TIC. In this study, we evaluated the use of blood and blood components before, during, and after ROTEM measurement. A target MTP ratio of 1:1:1 or 1:1:2 is achieved during the resuscitation process before applying ROTEM. We observed that the use of RBCs, FFP, and platelets was decreased during and after ROTEM testing compared to the pre-ROTEM phase. A previous randomized controlled trial also reported less use of plasma and platelets, but not RBC units, in patients who received MT in the VHA arm.[19] Since the first and second sets of MTP consist of RBC, FFP, and platelet, the higher numbers of blood products used before the application of ROTEM than the post-ROTEM period possibly account for the component consisting in the conventional MTP and a requirement of volume resuscitation in an initial phase. After administration of ROTEM, blood and components would be transfused based on the ROTEM results. This result is in agreement with what we observed that in the VHA arm, the total of 24 units of RBC and 20 units of FFP was spared when compared with the conventional MTP.

In contrast, cryoprecipitate was the only component that was increasingly transfused during the peri-and post-ROTEM phases. The increasing requirement for cryoprecipitate after ROTEM testing suggests that ROTEM is an effective tool for identifying hypofibrinogenemia, and that fibrinogen is an important factor in hemorrhagic trauma patients. This result strongly correlates with the pathophysiology of massive bleeding condition.[5,37,38,41] These results emphasize the importance of fibrinogen level and plasma replacement in an early phase of resuscitation.

Time-to-confirmed hemostasis of coagulation assessment

Time-to-confirmed hemostasis depends on the consistency of VHA-guided initiation, institutional protocol, and team activation. Time-to-confirmed hemostasis in this study was defined as outlined in the Methods section, and included the turnaround time (TAT) duration, which was defined as the time from the blood draw to the reporting of the results. The current European guideline for the management of major bleeding and coagulopathy following trauma states that VHA as a POCT can reduce the TAT by 30-60 minutes when compared to CCT.[5] A multicenter study reported the median TAT in CCT to be 88 minutes with a maximum TAT of up to 235 minutes.[17] The our study found a markedly decreased time-to-confirmed hemostasis between ROTEM and CCT (92 minutes [70-110] vs. 287 minutes [204-354], respectively). Moreover, we are confident that the time-to-confirmed hemostasis by ROTEM can be further decreased once an institutional protocol is established, learned, and refined.

Limitations

This study has some limitations that need to be addresses. First, the inherent weaknesses of the retrospective study design include missing and/or incomplete data, a tendency towards certain types of biases, and an inability to prove causation. For example, body temperature data was not available in all cases, so that data could not be reported in this study. Second, the size of our study population was small because this is a newly implemented technique at our center, and we set forth in this study to evaluate its effectiveness since its introduction. Third, the small number of cases in each group limited our ability to perform sophisticated statistical analyses. However, we analyzed and compared several important related parameters to assess the performance of ROTEM testing compared to non-VHA-guided therapy, and we found marked improvement between techniques for all evaluated parameters. Fourth, since this is a new technique at our center, no standard protocol has been established, which means that heterogeneity in practice management should be assumed. Fifth, since we were limited by the number of available cartridges for VHA testing, repeat ROTEM testing was only performed in 7 of 13 patients. The results of this study suggest the value of full implementation of ROTEM testing in this trauma setting, and that an established ROTEM practice protocol be established within a multidisciplinary team framework. From the beginning of full implementation, a pilot study should be conducted to confirm the results of this study. Our patients and our center will benefit from the improvements in patient survival and more efficient use of blood products that were both demonstrated in this study.

CONCLUSION

The findings of this pilot study strongly suggest the value of VHA-guided therapy for facilitating goal-directed hemostatic resuscitation and efficient blood product use during resuscitation, definitive treatment, and postoperative intensive care. The median time-to-confirmed hemostasis for ROTEM was markedly shorter than for CCT. Among the 6 cases that had MTP activated via ROTEM-guided therapy, four who adhere the protocol had their median lactate levels substantially decreased.

Regarding blood product use, ROTEM detected cases with low fibrinogen that only required cryoprecipitate transfusion, and red blood cell and fresh frozen plasma use was less in ROTEM than in conventional MTP. This point-of-care test platform reduces the time to treat trauma-induced coagulopathy in patients with trauma-related bleeding resulting in improved survival outcome. These results support full implementation of this technique in Thailand to improve survival among patients with trauma-related bleeding.

Funding disclosure

This was an unfunded study.

Authors' contributions

TW and JK conceived and designed the study, performed the literature review, collected the data, analyzed and interpreted the data, and drafted the article. KK designed the study and critically reviewed the manuscript. WW and SC collected, analyzed, and interpreted the data. PR and TR critically reviewed the manuscript for important intellectual content. All authors have read and approved the version of the manuscript submitted for journal publication.

ACKNOWLEDGEMENTS

The authors thank Dr. Klaus Görlinger for his review and providing knowledge of viscoelastic-hemostatic assays (VHA) and rotational thromboelastometry (ROTEM).

Conflict of interest declaration

All authors declare no personal or professional conflicts of interest, and no financial support from the companies that produce and/or distribute the drugs, devices, or materials described in this report. However, it is herewith declared that laboratory reagents were provided free of charge by TEM International GmbH during the early phase of VHA implementation at our center.

REFERENCES

1. Eastridge B, Holcomb J, Shackelford S. Outcomes of traumatic hemorrhagic shock and the epidemiology of preventable death from injury. Transfusion. 2019;59(S2):1423-8.
2. Mizobata Y. Damage control resuscitation: a practical approach for severely hemorrhagic patients and its effects on trauma surgery. J Intensive Care. 2017;5(1):4.
3. Bugaev N, Como JJ, Golani G, Freeman JJ, Sawhney JS, Vatsaas CJ, et al. Thromboelastography and rotational thromboelastometry in bleeding patients with coagulopathy: Practice management guideline from the Eastern Association for the Surgery of Trauma. J Trauma Acute Care Surg. 2020;89(6):999-1017.
4. Brohi K, Singh J, Heron M, Coats T. Acute traumatic coagulopathy. J Trauma. 2003; 54:1127–30.
5. Spahn D, Bouillon B, Cerny V, Duranteau J, Filipescu D, Hunt B, et al. The European guideline on management of major bleeding and coagulopathy following trauma: 5th edition. Crit Care. 2019;23(1):98.
6. Moore EE, Moore BH, Kornblith LZ, Neal MD, Hoffman M, Mutch NJ, et al. Trauma-induced coagulopathy. Nat Rev Dis Primers. 2021.29;7(1):30.
7. Inaba K, Rizoli S, Veigas PV, Callum J, Davenport R, Hess J, et al. Viscoelastic Testing in Trauma Consensus Panel. 2014 Consensus conference on viscoelastic test-based transfusion guidelines for early trauma resuscitation: Report of the panel. J Trauma Acute Care Surg. 2015;78(6):1220-9.
8. Görlinger K, Pérez-Ferrer A, Dirkmann D, Saner F, Maegele M, Calatayud ÁAP, et al. The role of evidence-based algorithms for rotational thromboelastometry-guided bleeding management. Korean J Anesthesiol. 2019;72(4):297-322.
9. MacLeod JB, Lynn M, McKenney MG, Cohn SM, Murtha M. Early coagulopathy predicts mortality in trauma. J Trauma. 2003; 55:39–44.
10. Brill J, Cotton B, Brenner M, Duchesne J, Ferrada P, Horer T, et al. The Role of TEG and ROTEM in Damage Control Resuscitation. Shock. 2021;56(1S):52-61.
11. Maegele M, Lefering R, Yucel N, Tjardes T, Rixen D, Paffrath T, et al. Early coagulopathy in multiple injury: an analysis from the German Trauma Registry on 8724 patients. Injury. 2007;38(3): 298-304.
12. Niles SE, McLaughlin DF, Perkins JG, Wade CE, Li Y, Spinella PC, Holcomb JB. Increased mortality associated with the early coagulopathy of trauma in combat casualties. J Trauma. 2008; 64(6):1459-63.
13. Brohi K, Cohen MJ, Ganter MT, Matthay MA, Mackersie RC, Pittet JF. Acute traumatic coagulopathy: initiated by hypoperfusion: modulated through the protein C pathway? Ann Surg. 2007; 245(5):812-8.
14. Chang R, Kerby JD, Kalkwarf KJ, Van Belle G, Fox EE, Cotton BA, et al. PROPPR Study Group. Earlier time to hemostasis is associated with decreased mortality and rate of complications: Results from the Pragmatic Randomized Optimal Platelet and Plasma Ratio trial. J Trauma Acute Care Surg. 2019;87(2):342-9.
15. Meyer DE, Vincent LE, Fox EE, O'Keeffe T, Inaba K, Bulger E, et al. Every minute counts: Time to delivery of initial massive transfusion cooler and its impact on mortality. J Trauma Acute Care Surg. 2017;83(1):19-24.
16. Gonzalez E, Moore E, Moore H. Management of Trauma-Induced Coagulopathy with Thrombelastography. Critical Care Clinics. 2017;33(1):119-34.
17. Toulon P, Ozier Y, Ankri A, Fleron MH, Leroux G, Samama CM. Point-of-care versus central laboratory coagulation testing during haemorrhagic surgery. A multicenter study. Thromb Haemost. 2009;101(2):394-401.
18. Da Luz L, Nascimento B, Shankarakutty A, Rizoli S, Adhikari N. Effect of thromboelastography (TEG®) and rotational thromboelastometry (ROTEM®) on diagnosis of coagulopathy, transfusion guidance and mortality in trauma: descriptive systematic review. Crit Care. 2014;18(5):518.
19. Gonzalez E, Moore EE, Moore HB, Chapman MP, Chin TL, Ghasabyan A, et al. Goal-directed Hemostatic Resuscitation of Trauma-induced Coagulopathy: A Pragmatic Randomized Clinical Trial Comparing a Viscoelastic Assay to Conventional Coagulation Assays. Ann Surg. 2016;263(6):1051-9.

20. Schochl H, Nienaber U, Hofer G, Voelckel W, Jambor C, Scharbert G, et al. Goal-directed coagulation management of major trauma patients using thromboelastometry (ROTEM)-guided administration of fibrinogen concentrate and prothrombin complex concentrate. Crit Care. 2010;14(2):R55.
21. Schochl H, Nienaber U, Maegele M, Hochleitner G, Primavesi F, Steitz B, et al. Transfusion in trauma: thromboelastometry-guided coagulation factor concentrate-based therapy versus standard fresh frozen plasma-based therapy. Crit Care. 2011; 15(2):R83.
22. Wikkelsø A, Wetterslev J, Møller A, Afshari A. Thromboelastography (TEG) or thromboelastometry (ROTEM) to monitor haemostatic treatment versus usual care in adults or children with bleeding. Cochrane Database of Systematic Reviews. 2016;2016(8):CD007871.
23. Stein P, Kaserer A, Sprengel K, Wanner G, Seifert B, Theusinger O, et al. Change of transfusion and treatment paradigm in major trauma patients. Anaesthesia. 2017;72(11):1317-26.
24. Hartert H. Blutgerinnungsstudien mit der Thrombelastographie; einem neuen Untersuchungs verfahren [Blood clotting studies with Thrombus stressography; a new Investigation procedure]. Klin Wochenschr. 1948;26(37-38):577-83. [Article in German]
25. De Nicola P, Mazzetti GM. Evaluation of thrombelastography. Am J Clin Pathol. 1955;23(4):447-52.
26. Von Kaulla KN, Weiner M. Studies of coagulation and fibrinolysis by new technic of continuous recording. Blood. 1955; 10(4):362–9.
27. Von Kaulla KN, Swan H. Clotting deviations in man during cardiac bypass: fibrinolysis and circulating anticoagulant. J Thorac Surg. 1958;36(4):519-30.
28. Kaufmann CR, Dwyer KM, Crews JD, Dols SJ, Trask AL. Usefulness of thrombelastography in assessment of trauma patient coagulation. J Trauma. 1997;42(4):716-20; discussion 720-2.
29. Tapia N, Chang A, Norman M, Welsh F, Scott B, Wall M, et al. TEG-guided resuscitation is superior to standardized MTP resuscitation in massively transfused penetrating trauma patients. J Trauma Acute Care Surg. 2013;74(2):378-85.
30. Blayney A, McCullough J, Wake E, Walters K, Campbell D, Ho D, et al. Substitution of ROTEM FIBTEM A5 for A10 in trauma: an observational study building a case for more rapid analysis of coagulopathy. Eur J Trauma Emerg Surg. 2022;48(2): 1077-84.
31. de Vries JJ, Veen CSB, Snoek CJM, Kruip MJHA, de Maat MPM. FIBTEM clot firmness parameters correlate well with the fibrinogen concentration measured by the Clauss assay in patients and healthy subjects. Scand J Clin Lab Invest. 2020;80(7):600-5.
32. Olde Engberink R, Kuiper G, Wetzels R, Nelemans P, Lance M, Beckers E, et al. Rapid and Correct Prediction of Thrombocytopenia and Hypofibrinogenemia With Rotational Thromboelastometry in Cardiac Surgery. J Cardiothorac Vasc Anesth. 2014;28(2):210-216.
33. American College of Surgeons, editor. Massive transfusion in trauma - facs.org [Internet]. Trauma Quality Programs. American College of Surgeons; 2014 [cited 2021 Oct 25]. Available from: https://www.facs.org/-/media/files/quality-programs/trauma/tqip/transfusion_guildelines.ashx;
34. Curry N, Davenport R, Pavord S, Mallett S, Kitchen D, Klein A, et al. The use of viscoelastic haemostatic assays in the management of major bleeding. Br J Haematol. 2018;182(6): 789-806.
35. American Society of Anesthesiologists Task Force on Perioperative Blood Management. Practice guidelines for perioperative blood management: an updated report by the American Society of Anesthesiologists Task Force on Perioperative Blood Management. Anesthesiology. 2015;122(2):241-75.
36. Santos AS, Oliveira AJF, Barbosa MCL, Nogueira JLDS. Viscoelastic haemostatic assays in the perioperative period of surgical procedures: Systematic review and meta-analysis. J Clin Anesth. 2020;64:109809.
37. Ziegler B, Bachler M, Haberfellner H, Niederwanger C, Innerhofer P, Hell T, et al. FIinTIC study group. Efficacy of prehospital administration of fibrinogen concentrate in trauma patients bleeding or presumed to bleed (FIinTIC): A multicentre, double-blind, placebo-controlled, randomised pilot study. Eur J Anaesthesiol. 2021;38(4):348-57.
38. Innerhofer N, Treichl B, Rugg C, Fries D, Mittermayr M, Hell T, et al. On Behalf of the RETIC Study Group. First-Line Administration of Fibrinogen Concentrate in the Bleeding Trauma Patient: Searching for Effective Dosages and Optimal Post-Treatment Levels Limiting Massive Transfusion - Further Results of the RETIC Study. J Clin Med. 2021;10(17):3930.
39. CRASH-2 trial collaborators, Shakur H, Roberts I, Bautista R, Caballero J, Coats T, et al. Effects of tranexamic acid on death, vascular occlusive events, and blood transfusion in trauma patients with significant haemorrhage (CRASH-2): a randomised, placebo-controlled trial. Lancet. 2010;376(9734):23-32.
40. Wang IJ, Park SW, Bae BK, Lee SH, Choi HJ, Park SJ, et al. FIBTEM Improves the Sensitivity of Hyperfibrinolysis Detection in Severe Trauma Patients: A Retrospective Study Using Thromboelastometry. Sci Rep. 2020;10(1):6980.
41. Simmon JW, Pittet JF, Pierce B. Trauma-induced coagulopathy. Curr Anesthesiol Rep. 2014;4(3):189–99.

Accumulation of Advanced Glycation End Products Independently Increases the Risk of Hospitalization Among Hemodialysis Patients

Chalothorn Taesilapasathit, M.D.*, Ittikorn Spanuchart, M.D., Supawadee Suppadungsuk, M.D.*, Napun Sutharattanapong, M.D.**, Kotcharat Vipattawat, M.D.***, Sethanant Sethakarun, M.D.***, Kanin Thammavaranucupt, M.D.***

**Chakri Naruebodindra Medical Institute, Faculty of Medicine Ramathibodi Hospital, Mahidol University, Samut Prakan 10540, Thailand, **Department of Medicine, Faculty of Medicine Ramathibodi Hospital, Mahidol University, Bangkok 10400, Thailand, ***Bhumirajanagarindra Kidney Institute Hospital, Bangkok 10400, Thailand.*

ABSTRACT

Objective: To determine the association between AGE accumulation detected by skin-autofluorescence (SAF) and hospitalization among ESKD patients.

Materials and Methods: 196 ESKD patients from two hemodialysis (HD) units in Bangkok were enrolled in this retrospective study from November 2015 to March 2016. Before HD treatment, AGEs were measured with the SAF device on the area with intact skin on the volar surface of the non-fistula arm. The study concluded in December 2020, and the number of and causes of hospitalization were reviewed. A logistic regression model was used to determine the association between SAF level and patient hospitalization.

Results: Of the 196 patients enrolled in the study, SAF was measured in 165 patients with a mean (SD) age of 69.2 (13.0) years. Most of the participants were non-smokers who had hypertension and diabetes and were on high-flux dialyzers. The average weekly spKt/V was 2.1, and the mean (SD) SAF was 3.05 (0.81) AU. The group with high SAF consisted of older patients and had a higher proportion of diabetics and smokers, but this was not statistically significant when compared to the low SAF group. In the multivariable analysis model, SAF greater or equal to 3.05 AU (OR = 2.28; 95% CI, 1.05–4.94; $P < 0.05$) and increased age (OR = 1.05; 95% CI, 1.01–1.09; $P < 0.05$) were associated with an increased risk of hospitalization.

Conclusion: Higher values of age and SAF were independently associated with increased risk of hospitalization among ESKD patients.

Keywords: Hospitalization; skin autofluorescence; advanced glycation end-products; end-stage kidney disease (Siriraj Med J 2022; 74: 305-313)

INTRODUCTION

End-stage kidney disease (ESKD) is recognized as one of the leading non-communicable diseases worldwide. The global prevalence of ESKD patients requiring renal replacement therapy is estimated to be between 4.9 and 7.1 million[1], and the total number of affected patients has been steadily increasing. Progression of chronic kidney disease (CKD) are associated with an increased risk of morbidity, mortality, and decreased quality of life.[2,3] Moreover, ESKD causes a substantial financial burden

Corresponding author: Kanin Thammavaranucupt
E-mail: geng103@hotmail.com
Received 30 January 2022 Revised 13 March 2022 Accepted 14 March 2022
ORCID ID: https://orcid.org/0000-0002-9873-3848
http://dx.doi.org/10.33192/Smj.2022.37

on the patients, and its treatment requires an immense amount of human resources.[4]

Compared with the general population and non-dialysis CKD patients, dialysis patients have higher hospitalization and in-hospital mortality rates.[5,6] With the elevated cardiovascular risk that is related to ESKD, cardiovascular disease (CVD) is the major cause of hospitalization among these patients.[7] Hospitalization of ESKD patients is associated with an increased risk of hospital-acquired infection, malnutrition, depression, and impaired quality of life, and it often results in higher overall costs.[8,9] Strategies for preventing the hospitalization of ESKD patients are yet to be determined.

In the general population, hypertension, diabetes mellitus, dyslipidemia, age, and tobacco use are known risk factors for developing CVD. Non-traditional risk factors contributing to CVD among patients with ESKD include anemia, mineral bone disease from the accumulation of calcium and phosphorous levels, and uremic toxins.[10] In recent times, greater evidence shows markedly increased levels of advanced glycation end-products (AGEs) in ESKD patients, leading to atherosclerosis-one of the established risk factors for CVD.[11]

AGEs are medium-sized uremic toxin molecules[12] that are formed as by-products of non-enzymatic reactions between the glucose and amino groups in proteins and nucleic acids. AGEs can also be formed through the oxidation of lipid-derived intermediates, resulting in advanced lipid oxidation products.[13,14] Moreover, ingestion of processed food and smoking habits are exogenous sources of AGEs. As AGEs are mainly excreted in the urine, AGE accumulation can be found in patients with ESKD. AGEs accumulate in tissues and affect protein structures, leading to the stiffness of tissues and blood vessels. Further, the binding of AGEs to AGE receptors (RAGE) activates the intracellular transduction mechanisms, resulting in cytokine release and oxidative stress. These can cause further tissue damage and accelerate the atherosclerotic process.[15,16] Previous studies have reported that AGE accumulation in tissues is associated with an increased risk of CVD.[17,18] However, to date, the association between AGE accumulation and hospitalization has never been conducted in a formal study.

There are several techniques of AGE measurement. Plasma AGEs are easier to detect, but the plasma levels in patients on dialysis keep fluctuating and is less reliable; this is because dialysis may result in some types of AGEs being removed.[13] Tissue AGEs can be measured via tissue biopsy, but the process is invasive, time-consuming, less specific, and poorly reproducible. Recently, a novel AGE measurement technique with skin autofluorescence (SAF) has been developed. Compared to other methods, SAF is non-invasive and reproducible. The tissue levels measured using this method tend to be more constant and reliable despite the patient undergoing regular dialysis.[18,19] To address the gap in the literature, this study aimed to evaluate the association between tissue AGE accumulation measured by SAF and the incidence of all-cause hospitalization among ESKD patients.

MATERIALS AND METHODS

Participants

We enrolled ESKD patients from Ramathibodi Hospital and Bhumirajanagarindra Kidney Institute Hospital, Bangkok, Thailand. The enrollment period was from November 2015 to March 2016. The participants aged 18-90 years who had received regular chronic hemodialysis (HD) for more than one week, signed the informed consent form, and completed AGE measurements using the SAF device at the enrollment were included in this study. The patients were dialyzed twice or thrice weekly using high-flux HD or hemodiafiltration. Unfractionated heparin was administered as an anticoagulant during HD sessions. Pre-HD blood chemistry was obtained and processed using a standard central laboratory analyzer. Patients hospitalized for elective surgery were excluded. Those participants were followed until December 31st, 2020 when the study concluded.

Ethics

The present study was approved by the Human Research Ethics Committee from the Faculty of Medicine Ramathibodi Hospital, Mahidol University (the approval number MURA2021/1052, dated December 29, 2021) and from Bhumirajanagarindra Kidney Institute Hospital (the approval number Ref. no. 1/2016, dated January 14, 2016).

Study design

This study was a retrospective cohort study. The patients' baseline characteristics, dialysis profiles, and laboratory parameters were collected through interviews and from their electronic medical records. Patient-identifying information was removed. The SAF measurements were performed at the time the participants were initially enrolled between November 2015 and March 2016. Those participants were followed until December 31st, 2020 for hospitalization events.

Measurement of tissue AGEs

Trained nurses were designated to perform AGE measurement as standard instruction. Tissue AGEs were

measured using the skin autofluorescence ultraviolet technique (AGEs reader, DiagnOptics, The Netherlands). The device has been clinically validated and shown to be highly correlated with tissue AGEs that are histologically measured from a skin biopsy.[20] The area with intact skin on the volar surface of the non-fistula arm was examined while the patient was in a seated position. Blemishes and hairy areas were avoided. An additional light source was used for naturally pigmented skin color.[21] Before an HD treatment session, tissue AGEs were measured three times consecutively with the SAF device, calculated using the AGE reader software, and reported in arbitrary units (AU). The mean of the three measurements was used for the statistical analyses. The SAF measurements are nonoperator-dependent, reliable, not fluctuating between pre- and post-dialysis, and highly reproducible.[18,19] To the best of our knowledge, there are no standard criteria for defining high SAF values. Therefore, we divided the patients into two groups, high and low SAF, using the mean SAF from our study as the cut-off point.

Primary outcome of all-cause hospitalization

The term 'Hospitalization' was defined as the event when the patient was hospitalized due to any causes at least once except elective surgery. Multiple rehospitalizations in the same participant would be counted as one.

Statistical analysis

The baseline characteristics of the patients, including their demographic data, underlying diseases, and laboratory results, were reported as mean and standard deviation (SD) or median (interquartile range, IQR) values for continuous variables and as frequencies (%) for categorical variables. Student's *t* test and the Wilcoxon rank sum test were used to compare the means and medians of the two SAF groups, while the chi-square test was used to analyze the categorical variables.

The event of hospitalization was analyzed using a logistic regression model from the time of AGE measurement to the first hospitalization. To test the associations between AGE accumulation and ESKD patient hospitalization, factors that might affect hospitalization were also analyzed using a logistic regression model and reported as odds ratios (OR) with a 95% confidence interval (CI). Variables identified by univariate analysis with *P* value less than .1 were subsequently analyzed using a multivariable analysis model.

A scatter diagram was formed to depict hospitalization, SAF, and any other interesting factors. Two-tailed *P* values less than .05 were considered statistically significant. All the statistical analyses were performed using IBM SPSS Statistics for Windows, Version 24.0 (Armonk, NY: IBM Corp).

RESULTS

Of 196 enrolled, 165 patients met the inclusion criteria and were included in the study, with a mean (SD) age of 69.2 (13.0) years. Most of the patients were non-smokers with hypertension and diabetes. 38% had CVD, and 9% had cerebrovascular disease (CVA). Most of the patients were hemodialyzed using a high-flux dialyzer for 4 hours per HD session. The median dialysis vintage was 21.0 (range 1-41) months, and the mean (SD) weekly spKt/V was 2.1 (0.4). The patients' vascular accesses were 44.2% arteriovenous fistula (AVF), 29.1% arteriovenous graft (AVG), and 26.7% tunneled cuffed catheter (TCC). The mean (SD) SAF level was 3.05 (0.81) AU. There was no significant difference between the characteristics of patients with SAF less than 3.05 AU and those with SAF greater or equal to 3.05 AU. The comorbidities, dialysis profiles, and laboratory parameters were similar for both groups of participants (Table 1).

During the 56-month study period, the total number of hospitalizations was 410. Of 165, 20 patients (12.1% of the cohort) had no hospitalization, and 33 patients (20%) had one hospitalization. The causes of hospitalization (Fig 2) were infection (37.3%), cardiovascular disease (22.2%), stroke (2.2%), and malignancy (1.7%). However, up to 36.6% had no clear documentation regarding the cause of hospitalization. During the follow-up period, 48 patients died while hospitalized; 22 patients (25%) in the low SAF group and 26 patients (33.8%) in the high SAF group. One patient in the low SAF group had died before hospitalization due to infection.

Univariate analysis (Table 2) showed that patient hospitalization was associated with different vascular access types, ages, and SAF levels. When compared with arteriovenous fistula (AVF) or arteriovenous graft (AVG), tunneled cuffed catheter (TCC) was associated with an increased risk of hospitalization (OR = 4.49; 95% CI, 1.02–19.77; $P = 0.05$). Greater patient age was associated with increased hospitalization (OR = 1.05; 95% CI, 1.02–1.08; $P = 0.005$). Further, the risk of hospitalization was higher among patients with SAF greater or equal to 3.05 AU (OR = 4.06; 95% CI, 1.29–12.72; $P = 0.02$). These associations were significant even after adjustments for other covariates. The multiple regression model (Table 2) showed that older age groups and SAF greater or equal to 3.05 AU were independently associated with an increased risk of hospitalization, with ORs of 2.28 (95% CI, 1.05–4.94; $P = 0.04$) and 1.05 (95% CI, 1.01–1.09; $P = 0.01$), respectively. The multiple regression analysis

TABLE 1. Baseline characteristics stratified by skin autofluorescence level.

Characteristics	Total (N = 165)	No. (%) SAF < 3.05 AU (n = 88)	SAF ≥ 3.05 AU (n = 77)	*P* value*
Age, mean (SD), y	69.2 (13.0)	68.0 (13.7)	70.4 (12.2)	0.24
Female	96 (58.1)	51 (57.9)	45 (58.4)	0.95
Body mass index, mean (SD), kg/m^2	22.4 (4.3)	22 (4.6)	22.8 (3.9)	0.23
Bodyweight, mean (SD), kg	57.3 (12.4)	56.7 (12.9)	57.9 (11.9)	0.56
Height, mean (SD), cm	159.7 (8.2)	160.4 (8.5)	159 (8.0)	0.27
Hypertension	157 (95)	83 (94)	74 (96)	0.59
Diabetes	95 (57.6)	48 (54.5)	47 (61.0)	0.40
Smoker	32 (19.3)	15 (17)	17 (22)	0.42
Coronary artery disease	54 (38)	28 (32)	26 (38)	0.79
Cerebrovascular disease	15 (9)	8 (9)	7 (9)	0.98
Dialysis vintage, median (IQR), mo	21 (20)	21 (19.2)	27 (21.5)	0.15
Residual urine volume, median (IQR), mL	0 (1100)	0 (1110)	0 (1170)	0.52
Vascular access				0.95
AVF	73 (44.2)	40 (45.4)	33 (42.9)	
AVG	48 (29.1)	25 (28.4)	23 (29.8)	
TCC	44 (26.7)	23 (26.2)	21 (27.3)	
Hemodiafiltration	21 (12.7)	11 (12.5)	10 (13)	0.93
3 times/week dialysis	76 (46)	39 (44.3)	37 (48)	0.63
Time, mean (SD), min	239.2 (4.8)	239.2 (4.9)	239.2 (4.8)	0.98
Hemoglobin, mean (SD), g/dL	11 (1.4)	11 (1.5)	11 (1.3)	0.98
HbA1C, mean (SD), %	6 (5.6)	6 (1.3)	6 (1.1)	0.80
Serum albumin, mean (SD), g/dL	3.7 (0.4)	3.8 (0.4)	3.7 (0.4)	0.40
Serum calcium, mean (SD), mg/dL	9.2 (0.7)	9.2 (0.7)	9.2 (0.7)	0.57
Serum phosphorus, mean (SD), mg/dL	4.6 (1.4)	4.6 (1.4)	4.6 (1.3)	0.90
Serum iPTH, median (IQR), pg/mL	355 (452.9)	382.5 (510.5)	353.0 (366.8)	0.24
Serum B_2-microglobulin, mean (SD), ug/mL	31.2 (10.2)	31.7 (9.7)	30.7 (10.8)	0.57
hsCRP, median (IQR), mg/L	0.16 (0.5)	0.17 (0.51)	0.15 (0.54)	0.63
spKt/V, mean (SD)	2.1 (0.4)	2.1 (0.4)	2.1 (0.4)	0.86
nPCR, mean (SD)	1 (0.3)	1 (0.3)	1 (0.3)	0.61

Abbreviations: AVF; arteriovenous fistula, AVG; arteriovenous graft, hsCRP; high sensitivity C-reactive protein, iPTH; intact parathyroid hormone, nPCR; normalized protein catabolic rate, SAF; skin autofluorescence, spKt/V; single-pool Kt/V, TCC; tunneled cuffed catheter.
* Significance threshold, $P < .05$

revealed no association between vascular access type and hospitalization (OR = 2.70; 95% CI, 0.58–12.61; $P = 0.21$). According to our results, SAF is an independent factor associated with the primary endpoint of hospitalization even after adjustment for age and vascular access types.

The AUROC of SAF for prediction of hospitalization was 0.70 (95% CI, 0.566-0.825). The sensitivity was 50.3% and the specificity was 80%. The scatter plot of SAF-stratified hospitalization and age (Fig 3) shows that increased SAF levels in ESKD patients are associated with hospitalization.

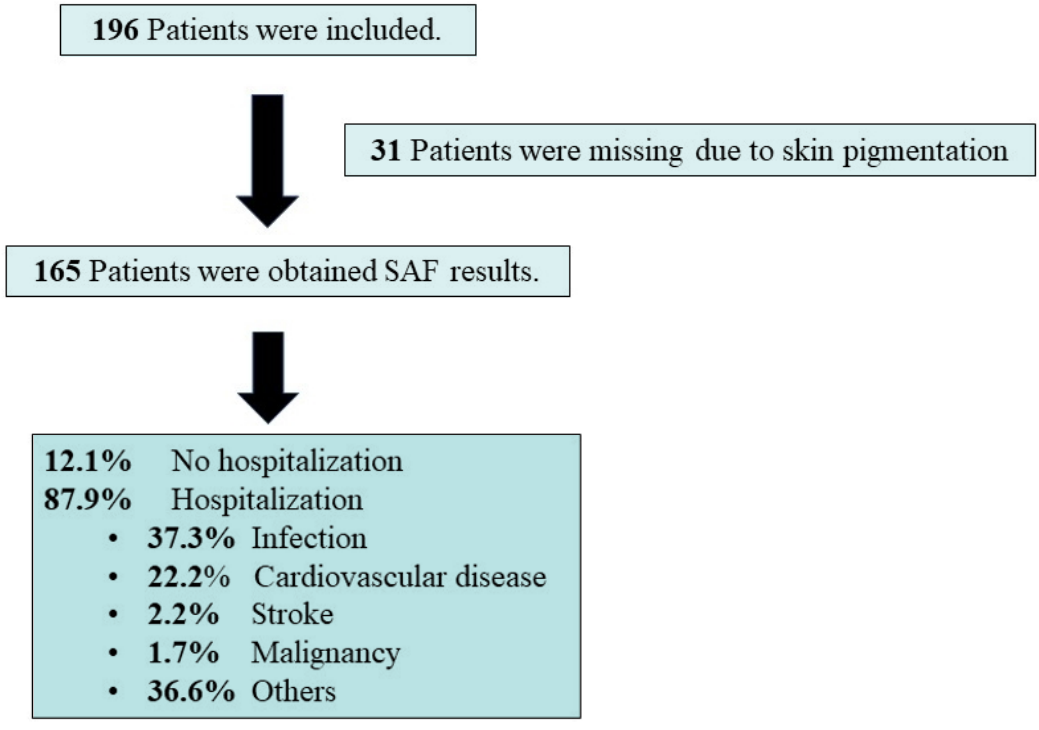

196 Patients were enrolled.
31 Patients were unable to obtain complete SAF results.
165 Patients obtained complete SAF results and were included.
Abbreviation: SAF; skin autofluorescence

Fig 1. Flow chart shows that 196 patients were eligible for the study, and SAF was measured for 165 patients.

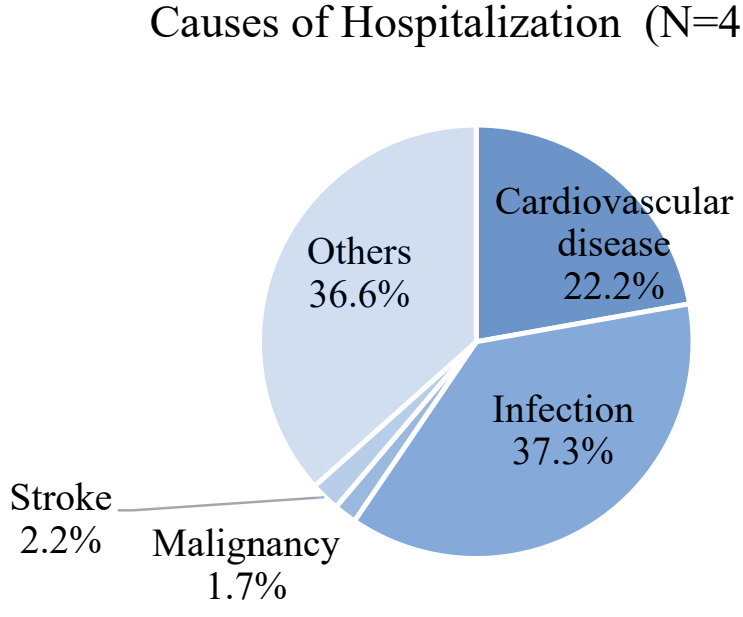

Fig 2. Causes of hospitalization.

TABLE 2. Univariate and multiple logistic regression analyses of factors associated with hospitalization among hemodialysis cohort.

Risk factor	Hospitalization			
	Univariate		Multivariate‡	
	OR (95% CI)	*P* value*	OR (95% CI)	*P* value*
Vascular access				
AVF/AVG	1.00 [Reference]	NA	1.00 [Reference]	NA
TCC	4.49 (1.02–19.77)	0.05	2.70 (0.58–12.61)	0.21
Age	1.05 (1.02–1.08)	0.005*	1.05 (1.01–1.09)	0.01†
SAF ≥ 3.05 AU	4.06 (1.29–12.72)	0.02*	2.28 (1.05–4.94)	0.04†
Female	1.03 (0.44–2.38)	0.95		
Body weight	0.98 (0.95–1.01)	0.22		
Height	0.76 (0.17–3.40)	0.72		
Body mass index	0.94 (0.86–1.03)	0.19		
Hypertension	2.46 (0.62–9.76)	0.20		
Diabetes	1.06 (0.45–2.46)	0.90		
Smoker	0.69 (0.27–1.77)	0.44		
Coronary artery disease	1.32 (0.52–3.34)	0.56		
Dialysis vintage	0.99 (0.98–1.00)	0.25		
Residual urine volume	1.00 (0.99–1.00)	0.24		
Hemodiafiltration	3.73 (0.48–28.92)	0.21		
3 times/week dialysis	0.85 (0.37–1.97)	0.71		
Hemoglobin	0.87 (0.65–1.16)	0.34		
HbA1C	0.90 (0.66–1.22)	0.49		
Serum calcium	1.10 (0.60–2.02)	0.75		
Serum phosphorus	1.06 (0.78–1.44)	0.71		
Serum albumin	0.79 (0.26–2.34)	0.66		
Serum iPTH	1.00 (0.99–1.00)	0.38		
Serum B_2-microglobulin	0.97 (.092–1.01)	0.11		
hsCRP	0.88 (0.59–1.31)	0.53		
spKt/V	1.57 (0.53–4.61)	0.41		
nPCR	1.53 (0.39–5.90)	0.54		

Abbreviations: AVF; arteriovenous fistulae, AVG; arteriovenous graft, CI; confidence intervals, HbA1C; hemoglobin A1c, hsCRP; high sensitivity C-reactive protein, iPTH; intact parathyroid hormone, NA; not applicable, nPCR; normalized protein catabolic rate, OR; odds ratio, SAF; skin autofluorescence, spKt/V; single-pool Kt/V, TCC; tunneled cuffed catheter.

* Significance threshold, $P < 0.05$

‡ Adjusted for age, vascular access, SAF.

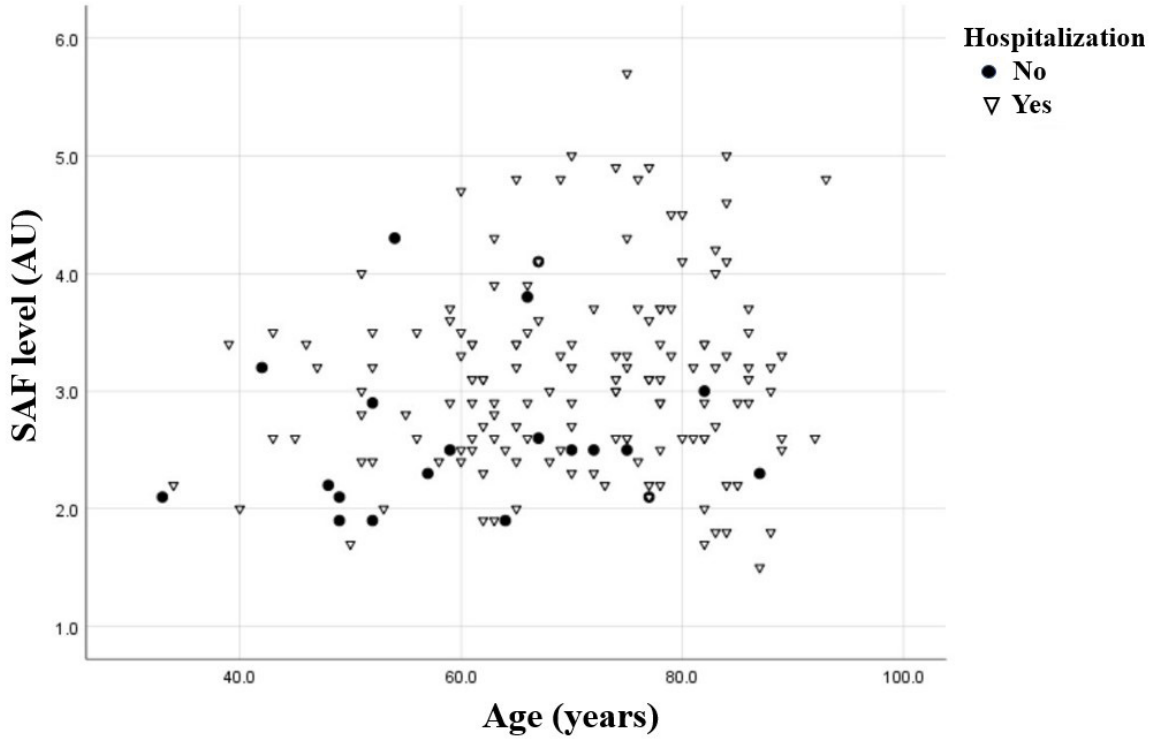

Fig 3. Scatter plot for the hospitalization of ESKD patients stratified by SAF level and age
Abbreviations: ESKD; end-stage kidney disease, SAF; skin autofluorescence.

DISCUSSION

To our knowledge, plasma AGE concentrations fluctuate from one dialysis treatment to another and are affected by dietary intake. In contrast, tissue AGE concentration is relatively constant and likely reflects the chronically elevated plasma AGE level.[22]

SAF measurements, representing tissue AGE accumulation, have been reported to be reliable markers of AGEs and independently associated with overall and cardiovascular mortality among ESKD patients of all ethnicities.[21] Elevated tissue AGEs are associated with advanced age, diabetes, smoking, and inflammatory states. The baseline characteristics of the patients in the present study (Table 1) showed no difference between the higher and lower SAF groups in terms of age, diabetes, smoking status, serum albumin, or CRP, a surrogate marker of inflammation.

The multivariable analysis revealed that SAF level and age are independently associated with hospitalization. The age factor was in agreement with previous studies.[10,23,24] This study reinforces that AGE levels greater or equal to 3.05 AU, measured using SAF, constitute an independent factor associated with an increased risk of hospitalization. While TCC utilization was found to be associated with an increased risk of hospitalization in the univariate analysis model, the effect became statistically insignificant when analyzed in the final multivariable analysis model. This might be due to a preference for using TCC over AVF or AVG in elderly patients with higher risk of CVD or with limited life expectancy.

In this study, the most common causes of hospitalization were infection and cardiovascular disease. Previous studies have indicated that AGE accumulation might increase a patient's susceptibility to infection. Previous observation studies also suggest that AGEs might attenuate the activation of the NLRP3 inflammasome in bone marrow-derived macrophages. Besides, AGEs might dampen innate immune responses, including NLRP3 inflammasome activation and type-I interferon production in macrophages upon infection.[25,26] Therefore, AGEs could impair host NLRP3 inflammasome–mediated innate immune defenses against infection. AGE accumulation not only induces immune system dysregulation but also leads to endothelial dysfunction, arterial stiffness, myocardial changes, and atherosclerosis progression.[27] Previous studies have reported that tissue AGE accumulation measured by SAF is associated with higher prevalence of cardiovascular events, cardiovascular mortality, and all-cause mortality among non-dialysis and dialysis CKD patients.[28] This evidence supports the present study's result of CVD being the second most common cause of hospitalization. Thus, this study emphasizes that high SAF is an independent risk factor for patient hospitalization.

Interestingly, our results showed that the plasma levels of beta-2-microglobulin, one of the middle-molecule uremic toxins similar to AGEs, in the higher and lower SAF did not differ. This discordance between the plasma beta-2-microglobulin level and the tissue AGE level measured by SAF could be from the following reasons. First, plasma uremic toxins could generally be removed with HD more than those accumulated in the tissue.[29] The same principle applies to HD clearance of plasma beta-2-microglobulin compared to tissue AGEs. Second, different kinds of uremic toxins might have different HD clearance properties, even only plasma uremic toxins are considered. Compared to plasma beta-2-microglobulin, plasma AGEs are marginally removed, despite the utilization of a high flux dialyzer or increased dialysate flow rate, given their higher molecular weight of greater than 12 kDa and higher binding affinity to protein. These techniques would not provide any significant effect on the clearance of the solutes.[30-32] Moreover, ingestion of a particular type of food can further increase the accumulation of AGEs whereas beta-2-microglobulin has a lesser correlation with the dietary factor.[33]

Accordingly, measuring AGEs by SAF in ESKD patients may have several clinical applications, including prognosis prediction and possible SAF lowering interventions, such as AGE-rich diet restriction, oral AGE-adsorbent use, or hemodiafiltration. According to our result of the positive association between tissue AGE accumulation and all-cause hospitalization, this may open an avenue for future research in AGE lowering intervention.

To the best of our knowledge, this is the first study that showed the association between AGEs accumulation and hospitalization in ESKD patients. Also, this is the first study that applied SAF to determine dialysis adequacy in Thai populations. Moreover, this study had a long follow-up period to determine study outcome of hospitalization.

However, our study has some limitations. First, this study consisted of a retrospective cohort with a small sample size. Second, since all the participants were of the Asian ethnicity, the results cannot be generalized to the overall population. Third, as the SAF principle is based on the interaction of ultraviolet radiation (UV) irradiation with the AGE chromophore in skin, different skin types may result in different SAF findings. Our study was conducted with Thai patients who normally have Fitzpatrick skin type IV-V, which represents a certain degree of skin pigmentation in response to UV exposure. Thus, our SAF findings may not be applicable to other skin types. Fourth, the SAF cutoff considered was based on the mean SAF value of the study cohort, which may limit the generalizability of results to other ESKD patients. Although classifying the SAF outcome by tertile or quartile is a standard method for non-established cut-off point variable, our study is the early stage with the modest sample size. By this method, the number of sample size in each group is small. Further prospective study in larger number of participants would be appropriate. Last, a large proportion of unidentified causes of hospitalization (36.6%) due to poor documentation in our study might affect the reported outcome.

Although SAF was shown to be an independent risk factor for hospitalization in this study, we can only report an association between increased SAF and hospitalization, not the causality. Nevertheless, our results and AGE measurements by SAF in Thai patients can be considered as preliminary data that would be beneficial for future research.

CONCLUSION

The present study revealed that SAF, as a measurement of tissue AGE deposition, is an independent factor associated with an increased risk of hospitalization.

REFERENCES

1. Lv J-C, Zhang L-X. Prevalence and Disease Burden of Chronic Kidney Disease. Adv Exp Med Biol. 2019;1165:3-15.
2. Thaweethamcharoen T, Sakulbumrungsil R, Vasuvattakul S, Nopmaneejumruslers C. Quality of life and hemoglobin levels of hemodialysis patient at Siriraj Hospital. Siriraj Med J. 2011;63:12-16.
3. Thaweethamcharoen T, Vasuvattakul S, Noparatayaporn P. PUK22 Comparison of Utility Score and Quality of Life Score in Thai Patient Between Twice and Thrice-Weekly Hemodialysis. Siriraj Med J. 2012;64: 94-97.
4. Hill NR, Fatoba ST, Oke JL, Hirst JA, O'Callaghan CA, Lasserson DS, et al. Global Prevalence of Chronic Kidney Disease – A Systematic Review and Meta-Analysis. PLoS One. 2016;11(7): e0158765.
5. Mathew AT, Strippoli GF, Ruospo M, Fishbane S. Reducing Hospital Readmissions in Patients with End-stage Kidney Disease. Kidney Int. 2015;88(6):1250-60.
6. Vareesangthip K. Effect of Ultrafiltration Rate in Long Interdialytic Interval Hemodialysis Session versus Average Weekly Ultrafiltration Rate on Mortality Rate and Adverse Cardiovascular Outcomes in Maintenance Hemodialysis Patients. Siriraj Med J. 2020; 72: 391-8.
7. Jankowski J, Floege J, Fliser D, Böhm M, Marx N. Cardiovascular Disease in Chronic Kidney Disease. Pathophysiological Insights and Therapeutic Options. Circulation. 2021;143(11):1157-72.
8. Lacson E Jr, Bruce L, Li NC, Mooney A, Maddux FW. Depressive Affect and Hospitalization Risk in Incident Hemodialysis Patients. Clin J Am Soc Nephrol. 2014;9(10):1713-9.
9. Sorthananusa A, Sitawarin J, Warasompati P, Seetee T, Chirawong P. Assessment of Nutritional Status in Chronic Hemodialysis Patients at the Galayanivadhana Hemodialysis Unit. Siriraj Hosp Gaz. 2005; 57:19-36.
10. Kundhal K LC. Clinical Epidemiology of Cardiovascular Disease

in Chronic Kidney Disease. Nephron Clin Pract. 2005;101(2):c47-52.
11. Peppa M, Raptis SA. Advanced Glycation End Products and Cardiovascular Disease. Curr Diabetes Rev. 2008;4(2):92-100.
12. Kalousová M, Sulková S, Zima T, Deppisch R, Beck W, Bednarova V, et al.Advanced Glycation End Products in Hemodialyzed Patients with Diabetes Mellitus Correlate with Leptin and Leptin/Body Fat Ratio. Ren Fail. 2003;25(2):277-86.
13. Thornalley PJ. Advanced Glycation End Products in Renal Failure. J Ren Nutr. 2006;16(3):178-84.
14. Thornalley P, Rabbani N. Highlights and Hotspots of Protein Glycation in End-Stage Renal Disease. Semin Dial. 2009;22:400-4.
15. Henle T, Deppisch R, Beck W, Hergesell O, Hänsch GM, Ritz E. Advanced Glycated End-products (AGE) During Haemodialysis Treatment: Discrepant Results with Different Methodologies Reflecting the Heterogeneity of AGE Compounds. Nephrol Dial Transplant. 1999;14(8):1968-75.
16. Nongnuch A, Davenport A. The Effect of On-Line Hemodiafiltration, Vegetarian Diet, and Urine Volume on Advanced Glycosylation End Products Measured by Changes in Skin Auto-Fluorescence. Artif Organs. 2018;42(11):1078-85.
17. Meerwaldt R, Lutgers HL, Links TP, Graaff R, Baynes JW, Gans RO, et al. Skin autofluorescence is a strong predictor of cardiac mortality in diabetes. Diabetes Care. 2007;30:107–12.
18. Meerwaldt R, Hartog JW, Graaff R, Huisman RJ, Links TP, Hollander NC et al. Skin Autofluorescence, A Measure of Cumulative Metabolic Stress and Advanced Glycation End Products, Predicts Mortality in Hemodialysis Patients. J Am Soc Nephrol. 2005;16(12):3687-93.
19. Nongnuch A, Davenport A. Skin Autofluorescence Advanced Glycosylation End Products as an Independent Predictor of Mortality in High Flux Haemodialysis and Haemodialysis Patients. Nephrology (Carlton). 2015;20(11):862-7.
20. Jiang J, Chen P, Chen J, Yu X, Xie D, Mei C, et al. Accumulation of Tissue Advanced Glycation End Products Correlated with Glucose Exposure Dose and Associated with Cardiovascular Morbidity in Patients on Peritoneal Dialysis. Atherosclerosis. 2012;224(1):187-94.
21. McIntyre NJ, Chesterton LJ, John SG, Jefferies HJ, Burton JO, Taal MW, et al. Tissue-advanced Glycation End Product Concentration in Dialysis Patients. Clin J Am Soc Nephrol. 2010;5(1):51-55.
22. Yue X, Hu H, Koetsier M, Graaff R, Han C. Reference Values for the Chinese Population of Skin Autofluorescence as a Marker of Advanced Glycation End Products Accumulated in Tissue. Diabet Med. 2011;28(7):818-23.
23. Furuya F, Shimura H, Takahashi K, Akiyama D, Motosugi A, Ikegishi Y, et al. Skin Autofluorescence is a Predictor of Cardiovascular Disease in Chronic Kidney Disease Patients. Ther Apher Dial. 2015;19(1):40-44.
24. Tanaka K, Tani Y, Asai J, Nemoto F, Kusano Y, Suzuki H, et al. Skin Autofluorescence is Associated with Renal Function and Cardiovascular Diseases in Pre-Dialysis Chronic Kidney Disease Patients. Nephrol Dial Transplant. 2011;26(1):214-20.
25. Stinghen AE, Massy ZA, Vlassara H, Striker GE, Boullier A. Uremic Toxicity of Advanced Glycation End Products in CKD. J Am Soc Nephrol. 2016;27(2):354-70.
26. Juliana C, Fernandes-Alnemri T, Wu J, Datta P, Solorzano L, Yu J-W, et al. Anti-inflammatory Compounds Parthenolide and Bay 11-7082 are Direct Inhibitors of the Inflammasome. J Biol Chem. 2010;285(13):9792-802.
27. Birukov A, Cuadrat R, Polemiti E, Eichelmann F, Schulze MB. Advanced glycation end-products, measured as skin autofluorescence, associate with vascular stiffness in diabetic, pre-diabetic and normoglycemic individuals: a cross-sectional study. Cardiovasc Diabetol. 2021;20(1):110.
28. Shardlow A, McIntyre NJ, Kolhe NV, Nellums LB, Fluck RJ, McIntyre CW, et al. The Association of Skin Autofluorescence with Cardiovascular Events and All-cause Mortality in Persons with Chronic Kidney Disease Stage 3: A Prospective Cohort Study. PLoS Med. 2020;17(7):e1003163.
29. Graaff R, Arsov S, Ramsauer B, Koetsier M, Sundvall N, Engels GE, et al. Skin and plasma autofluorescence during hemodialysis: a pilot study. Artif Organs. 2014;38(6):515-8.
30. Gerdemann A, Lemke HD, Nothdurft A, Heidland A, Munch G, Bahner U, et al. Low-molecular but not high-molecular advanced glycation end products (AGEs) are removed by high-flux dialysis. Clin Nephrol. 2000;54(4):276-83.
31. Deluyker D, Evens L, Bito V. Advanced glycation end products (AGEs) and cardiovascular dysfunction: focus on high molecular weight AGEs. Amino Acids. 2017;49(9):1535-41.
32. Srisuwan, W, Charoensri S, Jantarakana K, Chanchairujira T. Increasing Dialysate Flow Rate over 500 ml/Min for Reused High-Flux Dialyzers Do Not Increase Delivered Dialysis Dose: A Prospective Randomized Cross Over Study. Siriraj Med J. 2022;74:152-60.
33. Nongnuch A, Davenport A. The effect of vegetarian diet on skin autofluorescence measurements in haemodialysis patients. Br J Nutr. 2015;113(7):1040-3.

Evaluation of Oral Hygiene Status, Salivary Fluoride Concentration and Microbial Level in Thalassemic and Hemophilic Patients

Suryasnata Nayak, MDS.*, Shashirekha Govind, MDS.*, Amit Jena, MDS., Priyanka Samal, M.D.***, Naresh Kumar Sahoo, M.D.****, Shakti Rath, Ph.D.*****

Department of Conservative Dentistry and Endodontics, Institute of Dental Sciences, Siksha O Anusandhan Deemed to be University, Bhubaneswar, Odisha, India, **Department of Conservative Dentistry and Endodontics, SCB Dental College, Cuttack, Odisha,*Department of Hematology, IMS & SUM Hospital, Siksha O Anusandhan Deemed to be University, Bhubaneswar, Odisha, India, ****Department of Chemistry, Institute of Technical Education and Research, Sikhsa O Anusandhan Deemed to be University, Bhubaneswar, Odisha, India, *****Central Research Laboratory, Institute of Dental Sciences, Siksha O Anusandhan Deemed to be University, Bhubaneswar, Odisha, India.*

ABSTRACT

Objective: This study aimed to evaluate oral hygiene status, salivary fluoride concentration, and *Streptococcus mutans* and *Lactobacillus* levels in saliva of thalassemic, hemophilic and individuals without any other systemic disorders.

Materials and Methods: A total 162 individuals (44 healthy individuals, 86 thalassemic and 32 hemophilic patients) were selected, and randomly (n=30 in each group), the patients were allocated to Group A: individuals without any systemic condition, Group B: thalassemic patients, and Group C: hemophilic patients. Detailed case history, DMFT/DMFS, and OHI-S index were recorded. An aliquot of 5 ml of saliva was collected from each patient to determine the salivary fluoride concentration and predominant microbial colony in saliva. The data were analyzed by chi-square test of independence and nonparametric Kruskal-Wallis H test.

Results: The mean debris and calculus index among groups A, B, and C was 0.55 ± 0.43, 0.61 ± 0.46, 0.46 ± 0.47 and 0.33 ± 0.48, 0.18 ± 0.34, and 0.15 ± 0.34, respectively. The DMFT score for group A was high (1.93 ± 1.86, 1.67 ± 1.92) compared to groups B (0.40 ± 0.77, 0.67 ± 1.37) and C (0.47 ± 0.68, 0.30 ± 0.54). The fluoride concentrations among three groups (A, B, and C) were 0.06 ± 0.07, 0.12 ± 0.13, and 0.12 ± 0.13 ppm respectively. The number of colony-forming units was highest in the healthy individual>hemophilic>thalassemic and presence of predominant microorganisms showed insignificant association among the groups (p=0.323).

Conclusion: Compared to healthy individuals, thalassemic and hemophilic patients had better oral hygiene.

Keywords: Dental caries; fluorides; hemophilia; thalassemia; saliva; *lactobacillus*; *Streptococcus mutans* (Siriraj Med J 2022; 74: 314-322)

INTRODUCTION

Thalassemia is a genetic blood disorder that can result in the abnormal formation (partial or complete synthesis of α- globin or β- globin chains in hemoglobin, a tetramer of $\alpha_2 \beta_2$) of hemoglobin.[1] The two main types are alpha and beta-thalassemia.[2] The patient becomes thalassemia major if a gene defect is inherited from both parents. If the defect is inherited only from one parent,

Corresponding author: Shashirekha Govind
E-mail: shashirekha123@yahoo.com
Received 29 July 2021 Revised 1 December 2021 Accepted 3 December 2021
ORCID ID: https://orcid.org/0000-0003-4992-3087
http://dx.doi.org/10.33192/Smj.2022.38

it is known as thalassemia minor. Such individuals are carriers of the disease and most of the time remain asymptomatic.[3]

Hemophilia is a rare hereditary condition, resulting in prolonged and uncontrolled bleeding either spontaneously or subsequently after trauma. It inherits an X- linked recessive pattern, which occurs mostly in males. It occurs due to the absence of one or more clotting factors that lead to prolonged clotting time and excessive bleeding that can cause risk to life. The two most common forms are hemophilia A and hemophilia B which are caused by factors VIII and IX deficiency, respectively.[4]

Dental caries is a disease of microbial origin.[5] In addition to *Lactobacillus* and *Actinomyces species*, "*Streptococcus mutans*" (gram-positive facultative anaerobic cocci commonly found in the oral cavity of a human) is the most common pathogen associated with caries.[6,7] According to literature Ora-facial abnormalities (protrusion of maxillary incisors, wide spacing of teeth, occlusion abnormalities, and nasal deformity) are common in thalassemic patient and high caries prevalence in thalasemic and hemophilic patients.[8,9] Authors have observed that the prevalence of caries experienced was low in hemophiliacs.[10] Dental practioners should be aware of the risk associated with the procedures among the aforementioned patients. Early detection and prevention of dental caries is an effective caries-control strategy. Fluoride in saliva promotes tooth remineralization by producing less soluble fluorapatite crystals.[11] As a result, it is essential to determine whether thalassemia and hemophilia patients are more prone to tooth decay than the general population. The purpose of this study was to investigate: a) comparing the oral hygiene status of patients with thalassemia, hemophilia, and healthy individuals, b) determining their salivary fluoride concentration, and c) identifying the predominant microorganism (*S. mutans* and *Lactobacillus*) levels in saliva. The hypothesis for this study was that the categorical variables had no association.

MATERIALS AND METHODS

The study was approved by the Ethics Committee Institute of Medical Sciences (IMS) and Sum Hospital Siksha 'O' Anusandhan Deemed to be University (Ref. No. DMRI IMS. SH/SOA/180319). The research was carried out between 2018 and 2020. G* power software, version 3.1.9 (available at http://www.gpower.hhu.de/en.html) was used to calculate sample size based on the results of previous studies.[12,13] Individual group sample size was n=30, with the level of significance and power of test set at 5% and 80%, respectively (total 90). Sample selection is described in Fig 1. The inclusion criteria were thalassemic or hemophilic patients above the age of 14 years (individuals visiting "Institute of Dental Sciences" and "Institute of Medical Science and SUM Hospital"), healthy individuals without any bleeding disorder or systemic condition, visiting the Institute of Dental Sciences for a dental check-up. The exclusion criteria were: other bleeding or clotting disorders and chronic systemic conditions, hormonal disorders, fluoride therapy patients, medications affecting the salivary flow rate (β-blockers, antihistamines, antipsychotics, anti-inflammatory drugs, etc.), patients below the age of 14 years, and dental fluorosis (according to modified Dean's fluorosis index i.e.:questionable/0.5 to severe/4).

All patients provided written informed consent (in the case of patients below the age of 18, written informed consent was taken from their parents /gaurdian). A sample size of 90 patients (n=30 in each group) was allocated using randomization software (www.radomization.com). Group A [Control group]: Healthy individuals (who did not have any bleeding or clotting disorder and satisfied the exclusion criteria) Group B: Thalassemic patients, Group C: Hemophilic patients. Each patient had a detailed case record and oral hygiene status, which included the DMFT (Decayed- Missed- Filled- Teeth) and (debris & calculus) OHI-S (Oral Hygiene Index- Simplified) indexes. A single dental practitioner performed the patients' dental examinations (Fig 2). Five milliliters of unstimulated saliva was collected from each individual minimum 30 minutes after eating and stored separately in sterile sample collection bottles. Each patient's saliva was collected between 10 a.m. to 3 p.m. (No specific instructions regarding oral hygiene maintenance was advised). Saliva (5 mL) were divided into Part I (4 mL) to determine salivary fluoride concentration and Part II (1 mL) to determine predominant microbiota and colony-forming units (Fig 1).

Measurement of salivary fluoride concentration

The 4 ml of saliva samples were centrifuged at 1500 rpm for 3 min, and the supernatant was stored in close lid containers at 4°C for a maximum of 48 hours. After the readings were standardized using fluoride standard solution, the saliva samples were diluted with TISAB III (Total Ionic Strength Adjustment Buffer- III) reagent (Merck India) and used to quantify salivary fluoride concentration using an Orion Star A 214ASIC pH meter with a fluoride ion-selective electrode. For each sample, the results were acquired three times, and the mean values for each group were recorded individually.

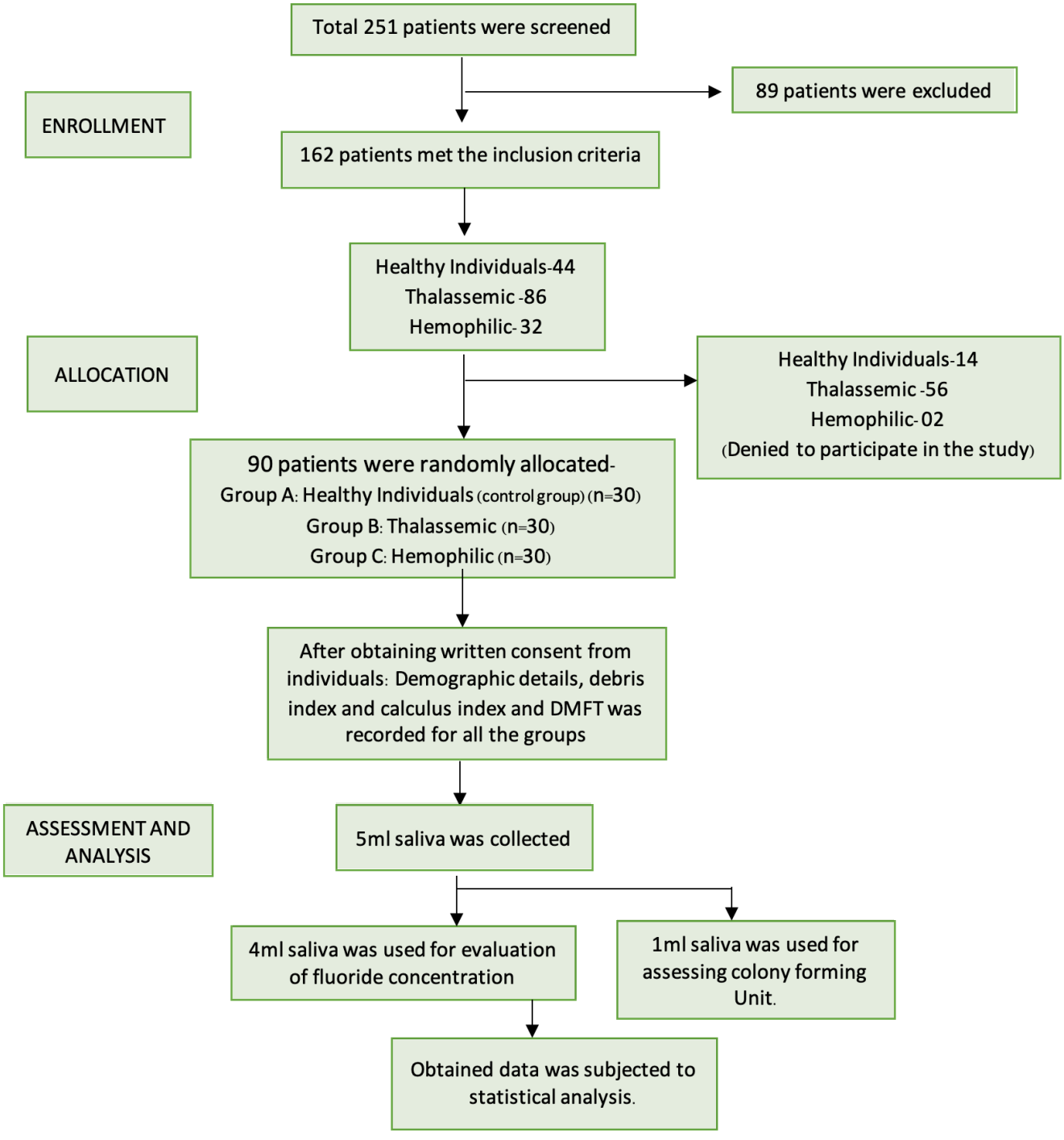

Fig 1. Flow chart of sampling of groups and methodology.

Determination of the salivary microbial level

One milliter of saliva sample was stored in close lid containers at 37°C for a maximum of 48 hours and used for microbiological culture on nutrient agar and blood agar plates. The plates were incubated in a bacterial incubator for 24 hours at 37°C. The predominant colony was identified and subjected to Gram's staining. The stained slides were observed under a microscope (Olympus India) at 40x and 100x magnifications in oil immersion. The predominant microflora for each sample was determined under the microscope. The number of colony-forming units (CFU) was counted for the predominant microflora of each sample. The results were recorded and subjected to statistical analysis.

Statistical analysis

Statistical analysis was performed using IBM SPSS statistics 24.0, South Asia Private Ltd. www.spss.co.in. The

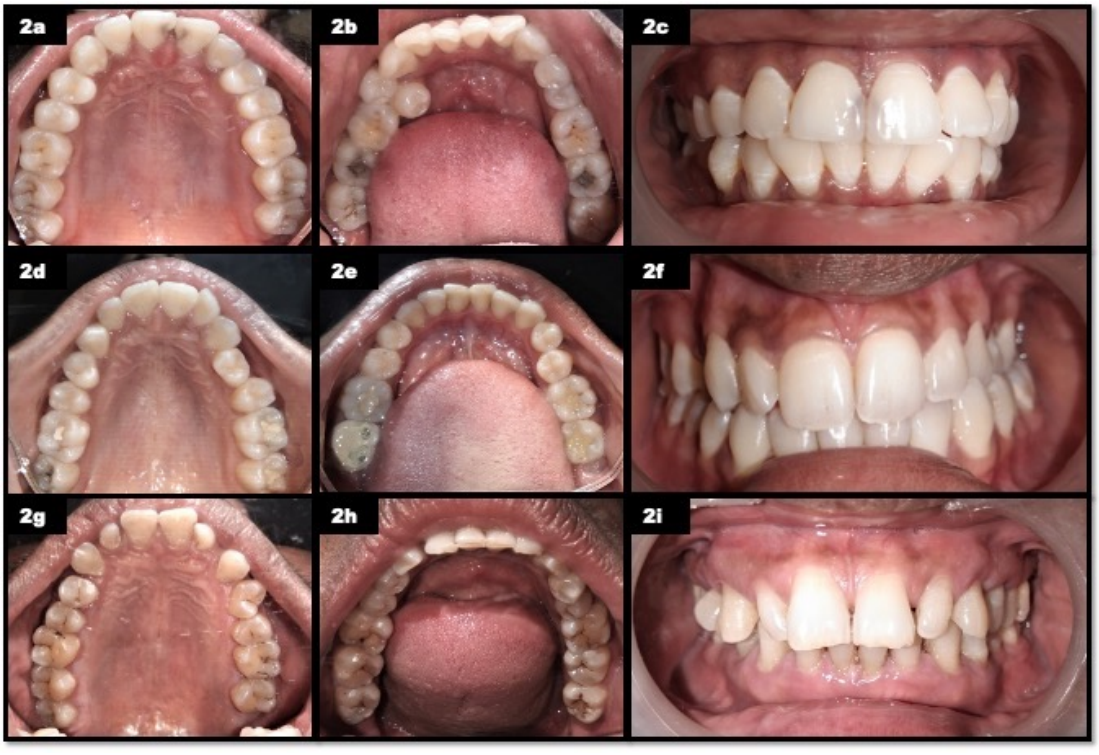

Fig 2. Clinical pictures of the three groups; 2a-2c) Intraoral pictures of healthy individual, 2d-2f) Intraoral pictures of thalassemic patients, 2g- 2i) Intraoral pictures of hemophilic patients.

test of association of patient group was done following cross tabulation procedure followed by Chi-square test of independence. The chi-Square test of independence was used to determine if there was a significant relationship between two categorical variables. The null hypothesis for this *test* was that there is no relationship between the categorical variables.

Comparison of age, decayed teeth, filled teeth, calculus, and fluoride levels among the three groups of patients was performed following nonparametric Kruskal-Wallis test, as these variables failed to pass the Shapiro Wilki normality test. The Kruskal-Wallis H test, a is the nonparametric analog of one-way analysis of variance and detects differences in distribution location. The mean, SD and quartiles were calculated following a descriptive statistics procedure. Colony-forming units (CFUs) is the estimate of the number of viable bacteria or fungal cells in a sample and have been classified into three groups: 10+ to 20+, 30+ to 50+, and 80+ to 150+. The level of significance was kept at $p<0.05$.

RESULTS

The demographic details are the mean age of patients in healthy individuals, thalassemic and hemophilic were 18.73 ± 2.59, 20.20 ± 8.91, 18.27 ± 4.23 years respectively. The difference in the distribution of age among the three groups was not significant (p=0.374). In hemophilic group all the patients were males. The male-female proportions in the control group were 46.7% and 53.3% and in the thalassemic group were 56.7% and 43.3%, respectively.

The mean debris index among groups A, B, and C was 0.55 ± 0.43, 0.61 ± 0.46, and 0.46 ± 0.47, respectively. The median debris among the three groups was in the range of 0.915 with IQR (interquartile range): 0.000 to 1.000 to 0.330 with an IQR: 0.00 to 1.00. The mean calculus index among groups A, B, and C was 0.33 ± 0.48, 0.18 ± 0.34, and 0.15 ± 0.34, respectively. The median calculus among the three groups was in the range of 0.000 with IQR: 0.000 with IQR: 0.00 to 0.000 to 0.000 with IQR 0.000 to 1.000. The OHI-S (debris and calculus) among the groups was stastistically insignificant (Tables 1&2).

The DMFT (decayed and filled) score for group A (control) was high (1.93 ± 1.86, 1.67 ± 1.92) compared to groups B (0.40 ± 0.77, 0.67 ± 1.37) and C (0.47 ± 0.68, 0.30 ± 0.54). The DMFT scores among Groups B and C were statistically insignificant compared to Group A (p=0.000). However, clinically Group C showed lower DMFT scores (Figs 3&4). The fluoride concentrations among the three groups were 0.06 ± 0.07, 0.12 ± 0.13, and 0.12 ± 0.13 ppm. The mean difference among the three groups was statistically insignificant (p=0.566) (Table 3).

TABLE 1. Comparison of Debris among groups.

Group	N	Mean ± SD	Q1	Q2 (Median)	Q3	Minimum	Maximum
Control	30	0.55 ± 0.43	0.000	0.580	1.000	0	1
Thalassemic	30	0.61 ± 0.46	0.000	0.915	1.000	0	1
Hemophilic	30	0.46 ± 0.47	0.000	0.330	1.000	0	1
Kruskal Wallis Test 'p' value				0.465			

TABLE 2. Comparison of Calculus among groups.

Group	N	Mean ± SD	Q1	Q2 (Median)	Q3	Minimum	Maximum
Control	30	0.33 ± 0.48	0.000	0.000	1.000	0	1
Thalassemic	30	0.18 ± 0.34	0.000	0.000	0.330	0	1
Hemophilic	30	0.15 ± 0.32	0.000	0.000	0.000	0	1
Kruskal Wallis Test 'p' value				0.288			

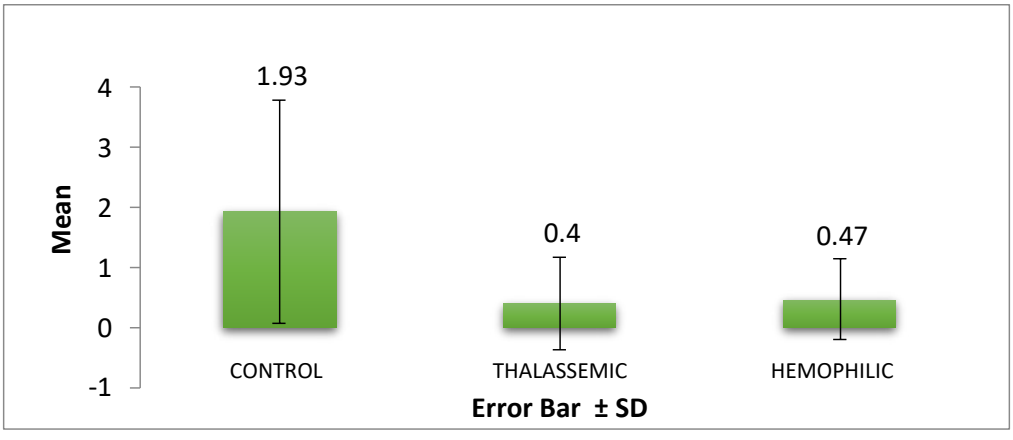

Fig 3. Comparison of mean Decayed tooth among groups.

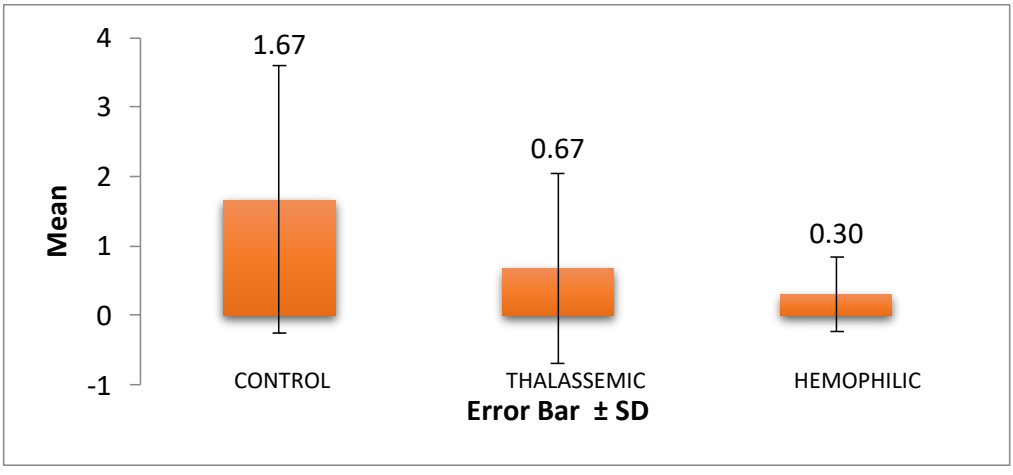

Fig 4. Comparison of mean Filled tooth among groups.

TABLE 3. Comparison of Fluoride concentration (in ppm) among groups.

Group	Fluoride level in ppm						
	N	Mean ± SD	Q1	Q2 (Median)	Q3	Minimum	Maximum
Control	30	0.06 ± 0.07	0.019	0.027	0.054	0.002	0.254
Thalassemic	30	0.12 ± 0.13	0.018	0.036	0.230	0.001	0.453
Hemophilic	30	0.10 ± 0.11	0.014	0.025	0.201	0.001	0.321
Kruskal Wallis Test 'p' value				0.566			

The proportions of *S. mutans* and *Lactobacillus* in group A were 86.7% and 10.0%, group B 93.3% and 6.7%, and group C were 80.0% and 20.0%, respectively. The predominant microorganisms did not have a significant association among the groups (p=0.323). The association between decayed teeth and different colony forming groups was 0.71± 0.95 in the 10+ - 20+ CFU group, which increased to 3.36± 2.20 in the 80+ - 150+ CFU group compared to the control group. In group B, 0.13 ± 0.35 in 10+ - 20+ CFU group which increased to 2.00 ± 1.00 in 80+ - 150+ CFU group and for group C was 0.00 ± 0.00 in 10+ -20+ CFU group which increased to 1.17 ± 0.75 in 80+ - 150+ CFU group. The number of colony-forming units was highest in healthy individuals and lowest in thalassemic patients. The increased CFU level has a significant association with a higher number of decayed teeth (Tables 4&5).

The correlation of age, number of decayed teeth and fluoride showed that age did not have a significant correlation with the number of decayed teeth or fluoride in the healthy and hemophillic groups. However, age had a significant positive correlation of 0.40 with fluoride in the thalssemic group (p<0.05). The number of decayed teeth showed no statistically significant correlation with fluoride in any of the three groups (p>0.05).

DISCUSSION

Saliva is an important predictor of oral health status. The preference for unstimulated saliva in this study is attributable to the fact that "stimulated saliva has increased flow rate, dilution, and change in pH".[11,4,15] During the collection of a saliva sample, it was observed that the salivary flow rate was higher in young individuals than in adults, which is in accordance with a meta-analysis that revealed that the maturing process is directly associated with a decreased salivary flow rate and is unaffected by medications.[16]

The hemophilic group had only male patients considering "hemophilia inherits in an x-linked recessive pattern that occurs primarily in males".[17] Females become

TABLE 4. Association of Predominant Microorganisms in groups.

PM	Group						Total		χ^2, p
	Control		Thalassaemic		Hemophilic				
	No.	%	No.	%	No.	%	No.	%	
S. Mutans	26	86.7	28	93.3	24	80	78	86.7	
Candida	1	3.3	0	0	0	0	1	1.1	χ^2 = 4.671
Lactobacillus	3	10	2	6.7	6	20	11	12.2	p=0.323
Total	30	100	30	100	30	100	90	100	

TABLE 5. Comparison of mean number of decayed teeth by CFUs within groups.

CFU	Group Decayed tooth Control			Thalassaemic			Hemophilic		
	N	Mean ± SD	Median (IQR)	N	Mean± SD	Median (IQR)	N	Mean ± SD	Median (IQR)
10+ - 20+	7	0.71±0.95	0(0,2)	15	0.13±0.35	0(0,0)	10	0.00±0.00	0(0,0)
30+ - 50+	12	1.33±0.89	1(1,2)	12	0.33±0.65	0(0,0.75)	14	0.50±0.65	0(0,1)
80+ - 150+	11	3.36±2.20	3(2,4)	3	2.00±1.00	2	6	1.17±0.75	1(0.75,2)
Total	30	1.93±1.86	2(0.75,3)	30	0.40±0.77	0(0,1)	30	0.47±0.68	0(0,1)
Kruskal Wallis Test 'p' value		0.004			0.003			0.003	

carriers and are usually asymptomatic, although in rare situations, they may develop hemophilia symptoms.[18,19] A case-control study found that children and adolescents with hemophilia had similar caries experiences and had no significant differences in oral hygiene or dietary habits.[20,21] Group B's age ranged from 15 to 54 years old, whereas group C's age ranged from 14 to 32 years old. Thalassemic patients have low IgA levels in their saliva and endocrine dysfunction, which increases their risk of decay.[22,23] The results of the present study are in accorandace with the aforementioned studies.

When compared to healthy persons, patients with blood disorders had compromised oral health, particularly poor periodontal conditions (gingival and plaque index) in - thalassemia and sickle cell anemia patients.[24,25] Individuals affected and their families' physical and psychological well-being was impacted (involves regular visit, chelation therapy, and uncertainties about the future), and studies have shown that thalassemia patients have a higher rate of caries, which could be attributed to aberrant tooth morphology, abnormal pits and fissures, and changes in salivary components and volume.[13,23] Despite the foregoing reasoning, the current investigation found a minor rise in mean clinical debris (0.61 ± 0.46), an improved calculus index (0.18 ± 0.34), and a lower DFMT score (0.40 ± 0.77) when compared to the control group. Among the groups (A; 0.06 ± 0.07, C; 0.10 ± 0.11), group B (0.12 ± 0.13) had a higher clinical fluoride level. The proportion of the predominant microorganisms *S.mutans* and *Lactobacillus* was slightly greater than that in the control group, but the difference was statistically insignificant (p=0.323). Only one patient in the control group exhibited Candida, whereas groups B and C had none.

In a study of hemopliliacs' oral and general health-related quality of life, researchers noted that psychological behavior and mental health were lower, but that self-assessing oral health state and regularly perceiving dental treatment needs were higher than in healthy people.[26] This is consistent with the findings of the current investigation, in which these patients were well-versed in the consequences of poor dental hygiene and the risk of caries. When compared to the thalassemia and control groups, the debris index (0.46 ± 0.47), calculus index (0.15 ± 0.32) and DMFT score (0.47 ± 0.68) were lower. The control group's DMFT scores were statistically significant (p=0.000).

Salivary fluoride concentration was clinically evident in groups C and D when compared to the control group. This could be because these patients are more aware of the importance of maintaining good dental hygiene. There was no test of gender association in the hemophilic group because all of the cases were males. In comparison to the thalassemic and control groups, the proportions of *S. mutans, Candida,* and *Lactobacillus* were lower (80.0%, 0%, and 20.0%, respectively) in the hemophilic group. Previous research has found that patients with blood problems had a greater *S. mutans* and *Lactobacillus* count in their saliva than healthy people.[27,28] The presence of a certain microorganism was not revealed by an increase

in the number of colony-forming units in the groups ($p \geq 0.05$).

The current study revealed that thalassemic and hemophilic patients were well aware of the conditions and potential problems associated with poor oral health. The majority of patients visited the dentist every six months for a routine dental examination, and the parents /gaurdian of patients under the age of 18 yrs. were well aware of the issue.[9] Any dental invasive surgery should be performed after factor replacement/ transfusion.[29,30] Hematologists should inform such patients about dental problems and treatments, and encourage them to visit the dentist on a frequent basis to avoid complications. Further studies into the impacts of various fluoride therapy methods, specific microbiological load, and pain perception during dental treatment can be considered for a large thalassemic and hemophilic population (different location, depending on socioeconomic status of the individual and their families).

CONCLUSION

The current study concludes that the OHI-S (debris & calculus) index and mean salivary fluoride concentration was statistically insignificant among the groups ($p>0.05$). DMFT scores were less in thalassemic and hemophilic patients compared to the healthy individuals. The number of colony-forming units was higher in healthy individuals and lowest in thalassemic patients. Dentists should be aware of and knowledgeable about the risks involved when treating thalassemic and hemophilic patients. Early detection and recognition of oral health concerns will help patients financially and in terms of reducing the risk. According to the current findings, the incidence of caries, gingivitis, and microorganism in thalassemic and hemophilic patients is clinically significant. To receive safe, comprehensive oral care, these patients' families, guardians, physicians, and dental clinicians must work collaboratively.

ACKNOWLEDGEMENT

None

Disclosure Statement

The authors have no conflicts of interest to declare.

Funding Sources

Have no such funding sources involved.

REFERENCES

1. Muddugangadhar BC, Sangur R, Rudraprasad IV, Nandeeshwar DB, Kumar BD. A clinical study to compare between resting and stimulated whole salivary flow rate and pH before and after complete denture placement in different age groups. J Indian Prosthodont Soc. 2015;15(4):356.
2. Schwartz E, Cohen A, Surrey S. Overview of the beta thalassemias: genetic and clinical aspects. Hemoglobin. 1988;12(5-6):551-64.
3. Fibach E, Rachmilewitz EA. Pathophysiology and treatment of patients with beta-thalassemia–an update. F1000Research. 2017;6.
4. Karim MA, Jamal CY. A review on hemophilia in children. Bangladesh J Child Health. 2013;37(1):27-40.
5. Chokshi A, Mahesh P, Sharada P, Chokshi K, Anupriya S, Ashwini BK. A correlative study of the levels of salivary Streptococcus mutans, lactobacilli and Actinomyces with dental caries experience in subjects with mixed and permanent dentition. J Oral Maxillofac Pathol. 2016;20(1):25.
6. Kianoush N, Adler CJ, Nguyen K-AT, Browne GV, Simonian M, Hunter N. Bacterial profile of dentine caries and the impact of pH on bacterial population diversity. PLoS One. 2014;9(3):e92940.
7. Zoitopoulos L, Brailsford SR, Gelbier S, Ludford RW, Marchant SH, Beighton D. Dental caries and caries-associated microorganisms in the saliva and plaque of 3-and 4-year-old Afro-Caribbean and Caucasian children in south London. Arch Oral Biol. 1996;41(11):1011.
8. Van Dis ML, Langlais RP. The thalassemias: oral manifestations and complications. Oral Surg Oral Med Oral Pathol. 1986;62(2):229-33.
9. Abrisham M, Tabrizizadeh M, Ghateh A. Knowledge of Oral Hygiene among Hemophilic Patients Referred to Iranian Hemophilia Society. J Dent Res Dent Clin Dent Prospects. 2009;3(2):60-63.
10. Boyd D, Kinirons M. Dental caries experience of children with haemophilia in Northern Ireland. Int J Paediatr Dent. 1997;7(3):149-53.
11. Meyers IA. Minimum intervention dentistry and the management of tooth wear in general practice. Aust Dent J. 2013;58:60-65.
12. Hattab FN, Hazza'a AM, Yassin OM, al-Rimawi HS. Caries risk in patients with thalassaemia major. Int Dent J. 2001;51(1):35-38.
13. Babu NSV, Shah S. Comparative Assessment of Salivary Flow Rate, Buffering Capacity, Resting PH and Dental Caries in Children with Beta Thalassemia. J Middle East North Afr Sci. 2018;10(5777):1-5.
14. Carver CD. Comparison of protein composition in stimulated vs. unstimulated whole human saliva. Published online 2007.
15. Kumar B, Kashyap N, Avinash A, Chevvuri R, Sagar MK, Kumar S. The composition, function and role of saliva in maintaining oral health: A review. Int J Contemp Dent Med Rev. 2017;2017.
16. Affoo RH, Foley N, Garrick R, Siqueira WL, Martin RE. Meta-analysis of salivary flow rates in young and older adults. J Am Geriatr Soc. 2015;63(10):2142-51.
17. Azhar S, Yazdanie N, Muhammad N. Periodontal status and IOTN interventions among young hemophiliacs. Haemoph Off J World Fed Hemoph. 2006;12(4):401-4.
18. Nair PS, Shetty S, Ghosh K. A homozygous female hemophilia A. Indian J Hum Genet. 2012;18(1):134.
19. Hirayama AB, Silva AKC da, Rocha JS, Roberti M do RF. Prevalence of symptoms in hemophilia carriers in comparison with the general population: a systematic review. Hematol Transfus Cell Ther. 2019;41:349-55.
20. Othman N a. A, Sockalingam SNMP, Mahyuddin A. Oral health status in children and adolescents with haemophilia. Haemoph

Off J World Fed Hemoph. 2015;21(5):605-11.
21. Jangra B, Goswami M. Assessment of Dental Caries Experience and Periodontal Health Status among Children with Haemophilia in New Delhi, India - A Case Control Study. Oral Health Prev Dent. 2017;15(2):131-7.
22. Siamopoulou-Mavridou A, Mavridis A, Galanakis E, Vasakos S, Fatourou H, Lapatsanis P. Flow rate and chemistry of parotid saliva related to dental caries and gingivitis in patients with thalassaemia major. Int J Paediatr Dent. 1992;2(2):93-97.
23. Al-Wahadni AM, Taani DQ, Al-Omari MO. Dental diseases in subjects with beta-thalassemia major. Community Dent Oral Epidemiol. 2002;30(6):418-22.
24. Amirabadi F, Saravani S, Miri-Aliabad G, Khorashadi-Zadeh M. The Association between Dental Health Status and Oral Health-Related Quality of Life of Children Diagnosed with beta-Thalassemia Major in Zahedan City, Iran. Int J Pediatr-Mashhad. 2019;7(2):8985-91.
25. Elangovan A, Mungara J, Joseph E, Guptha V. Prevalence of dentofacial abnormalities in children and adolescents with β-thalassaemia major. Indian J Dent Res. 2013;24(4):406.
26. Alpkiliç Baskirt E, Ak G, Zulfikar B. Oral and general health-related quality of life among young patients with haemophilia. Haemoph Off J World Fed Hemoph. 2009;15(1):193-8.
27. AlDhaher ZA, Alhadi LM. Comparison between severe haemophilic A and healthy children in Streptococcus mutans, oral Lactobacilli and Candida albicans counts. Sci J Publ Coll Dent Baghdad. Published online 2012:149.
28. Salem K, Seyyedkhamesi S, Aminian M. Evaluation of oral and dental health status in hemophilic children and adolescents in the city of Rasht. J Pediatr Res Internet. Published online 2018: 182-6.
29. Helmi N, Bashir M, Shireen A, Ahmed IM. Thalassemia review: features, dental considerations and management. Electron Physician. 2017;9(3):4003-8.
30. Kumar JN, Kumar RA, Varadarajan R, Sharma N. Specialty dentistry for the hemophiliac: Is there a protocol in place? Indian J Dent Res. 2007;18(2):48.

Correlation of Cerebral Atrophy and White Matter Hyperintensity Burden in MRI with Clinical Cognitive Decline

Priyam Agarwal, M.D., Adya Kinkar Panda, M.D., Satyaswarup Jena, M.D., SSG Mohapatra, M.D.

Department of Radio Diagnosis, IMS and SUM Hospital, Siksha 'O' Anusandhan Deemed to be University, Bhubaneswar, India.

ABSTRACT

Objective: Dementia is a disease of gradual memory and cognitive loss that affects an individual's day-to-day activities and is caused by permanent brain damage. Majority of patients are from the elderly population and only 2 to 10 % of affected population is less than 65 years.

Materials and Methods: We obtained a correlation of severity of white matter hyperintensity (WMH) burden in MRI with severity of clinically assessed cognitive decline. And also analysed the severity of cerebral atrophy in MRI with severity of clinically assessed cognitive decline.

Results: In our study Fazekas scoring for WMHs showed a sensitivity of 87.5% and specificity of 83.3% on correlation with clinical cognitive decline assessed by ADAS-Cog. Also, MTA scale for cerebral atrophy showed a sensitivity of 72% and specificity of 88% on correlation with clinical cognitive decline assessed by ADAS-Cog. Significant P-value have been obtained for both the above visual rating scales of MRI (Fazekas and MTA) by linear regression, on correlation with clinically assessed cognitive decline.

Conclusion: White matter disease assessed by Fazekas scale and cerebral atrophy by MTA scale on MRI brain correlated well with cognitive decline clinically assessed by neuropsychological tests.

Keywords: Cerebral atrophy; hyperintensity; MRI; clinical cognitive decline (Siriraj Med J 2022; 74: 323-329)

INTRODUCTION

Dementia is a syndrome of progressive cognitive and memory decline affecting an individual in his daily activities, due to irreversible neuronal damage. Dementia is predominantly a disease of the elderly population and only 2 to 10 % of affected population is less than 65 years.[1] According to an estimate, number of people affected by dementia will be reaching over 81 million by the year 2040 globally, doubling in every 20 years. There will be approximately 150 million elderly individuals (those aged over 60 years) constituting about 12.30% of total population by 2025 in India.[2-4]

The structure and function of the brain change as people become older. Memory, attention, executive cognitive function, language, and visuospatial ability are just a few of the cognitive functions that degrade as people become older.[5] There is grey matter and white matter volume loss.[6] Areas more prone to grey matter volume reduction are the prefrontal cortex and medial temporal lobe containing the hippocampus.[7,8] The frontal lobe's corpus callosum and white matter experienced the most dramatic volume reductions.[8,9] The white matter tract's integrity deteriorates with age, as seen by MRI diffusion tensor imaging.[10] As individuals age, the number

Corresponding author: Satyaswarup Jena
E-mail: docsatyaswarup@gmail.com
Received 30 November 2021 Revised 16 March 2022 Accepted 27 March 2022
ORCID ID: https://orcid.org/0000-0002-4591-2623
http://dx.doi.org/10.33192/Smj.2022.39

and length of dendrites decreases, as does the loss of dendritic spines and axons, as well as there is significant loss of synapses.[11] The loss of synapses is an important structural sign of ageing.[12,13]

Cognitive decline is most commonly diagnosed clinically. Clinical tests such as the Mini Mental State Examination (MMSE), the Alzheimer Disease Assessment Scale (ADAS cog), and the Verbal Fluency Test, Cognitive Abilities Screening Instrument, Clock drawing test etc. are often used. Risk factors of Dementia on Magnetic resonance imaging (MRI) include brain atrophy, cerebral microhaemorrhages, and cerebral small vessel disease. Alzheimer disease (AD) is characterized by atrophy in specific brain regions, which includes the hippocampus, Para hippocampal cortex, entorhinal cortex, inferior parietal lobule, precuneus, and cuneus.[14,15]

Microhaemorrhages, depending on their locations, play roles in both AD-related and vascular-specific pathology in dementia development.[16] Haemorrhages, particularly in deep gray and white matter, are more likely to be associated with hypertensive arteriolar disease and are therefore considered vascular sign.[17] White matter hyperintensities (WMHs) and lacunar infarcts are signs of small vessel disease.[18-22] They contribute to vascular dementia but may also be associated with the pathogenesis of AD.[23,24] WMHs are regions of increased intensity on T2-weighted and FLAIR MRI sequences that are usually assessed using rating systems based on ocular evaluation of the lesion nature and size.

The purpose of this research is to detect the continuing process of neurodegeneration as early as possible, when intervention options are most viable, as our understanding of the risk factors and treatment of dementia has improved.[25] Our aim here is to obtain a correlation of severity of WMH burden in MRI with severity of clinically assessed cognitive decline and to study severity of cerebral atrophy in MRI with severity of clinically assessed cognitive decline.

MATERIALS AND METHODS

The proposed study was a Hospital Based Retrospective Cross-Sectional Study and carried out in the department of Radiodiagnosis in collaboration with the Department of Psychiatry, IMS & SUM Hospital, Bhubaneswar, India.

The present study was done on 40 patients of age more than 45 years with an incidental finding of T2/FLAIR Hyperintensity & cerebral atrophy on MRI. They all underwent neuropsychiatric screening by MMSE (Mini Mental State Examination) test.[26] All patients having score less than 23 were included in the study. They were further evaluated by various visual rating scales like Fazekas scale, Medial Temporal Atrophy scale (MTA Scale) & Global Cerebral Atrophy scale (GCA scale) for grading the cortical atrophy and WMH. After assessing the atrophy and WMH in MRI, the patients were subjected to a battery of neuropsychiatric tests like Verbal fluency test, ADAS-Cog, Montreal Cognitive Assessment test.[27] Lastly after obtaining all the scores, a correlation between the MRI grading of atrophy & WMH with the severity of cognition decline assessed by neuropsychiatric tests was established with the help of statistical analysis. Exclusion Criteria was Post stroke patients; space occupying lesions in brain; history of depression, psychosis and substance use disorder excluding nicotine use; seizure disorder; and any contraindications to MRI.

RESULTS

The maximum number of patients in our study belonged to the age group of 65-69 years, making a total of 20 cases out of 40 (i.e., 50% of the total). Second largest number of patients (9 in number) belonged to the age group 60-64 years (i.e., 22.5% of the total), followed by 4 cases in 70-74 years age group (i.e., 10% of the total) and 3 cases in 50-59 age group. Also 10% of the cases (4 in number) were seen in >=75 years of age. The youngest patient of the study sample was 56 years old and the oldest patient of the study sample was 78 years old. Our study sample had 23 females (i.e., 55% of the total) and 17 males (i.e., 45% of the total). Among them 21 were diabetic (i.e., 52.5% of the total) & 19 were non-diabetic (i.e., 47.5% of the total) and 25 were hypertensive i.e., 62.5% of the total) & 15 were non-hypertensive (i.e., 37.5% of the total). Out of the 40 patients ,14 were both hypertensive and diabetic (i.e., 35% of the total) and 26 were either hypertensive or diabetic (i.e., 37.5% of the total).

Patients assessed for cognitive decline by MMSE (as the screening tool) showed about 22 of them (i.e., 55% of the total) had mild cognitive impairment; followed by 14 subjects who had moderate cognitive impairment (i.e., 35% of the total). Severe cognitive impairment was seen in only 4 study samples (10% of the total). On Fazekas visual rating scale, about 22 of them had mild WMH (grade 1) i.e., 55% of the total and about 14 of them had moderate WMH (grade 2) i.e, 35% of the total. Severe WMH (grade 3) was seen in 4 patients i.e, 10% of the total (Fig 1). Assessment on MTA scale showed no atrophy (Score 0) in 2 patients, i.e, 5% of the total. Score 1 atrophy was seen in 16 patients (i.e, 40% of the total). Score 2 atrophy was seen in 12 patients (i.e., 30% of the total). Score 3 atrophy was seen in 8 (i.e., 20% of the total) and Score 4 atrophy was seen in 2 (i.e., 5%

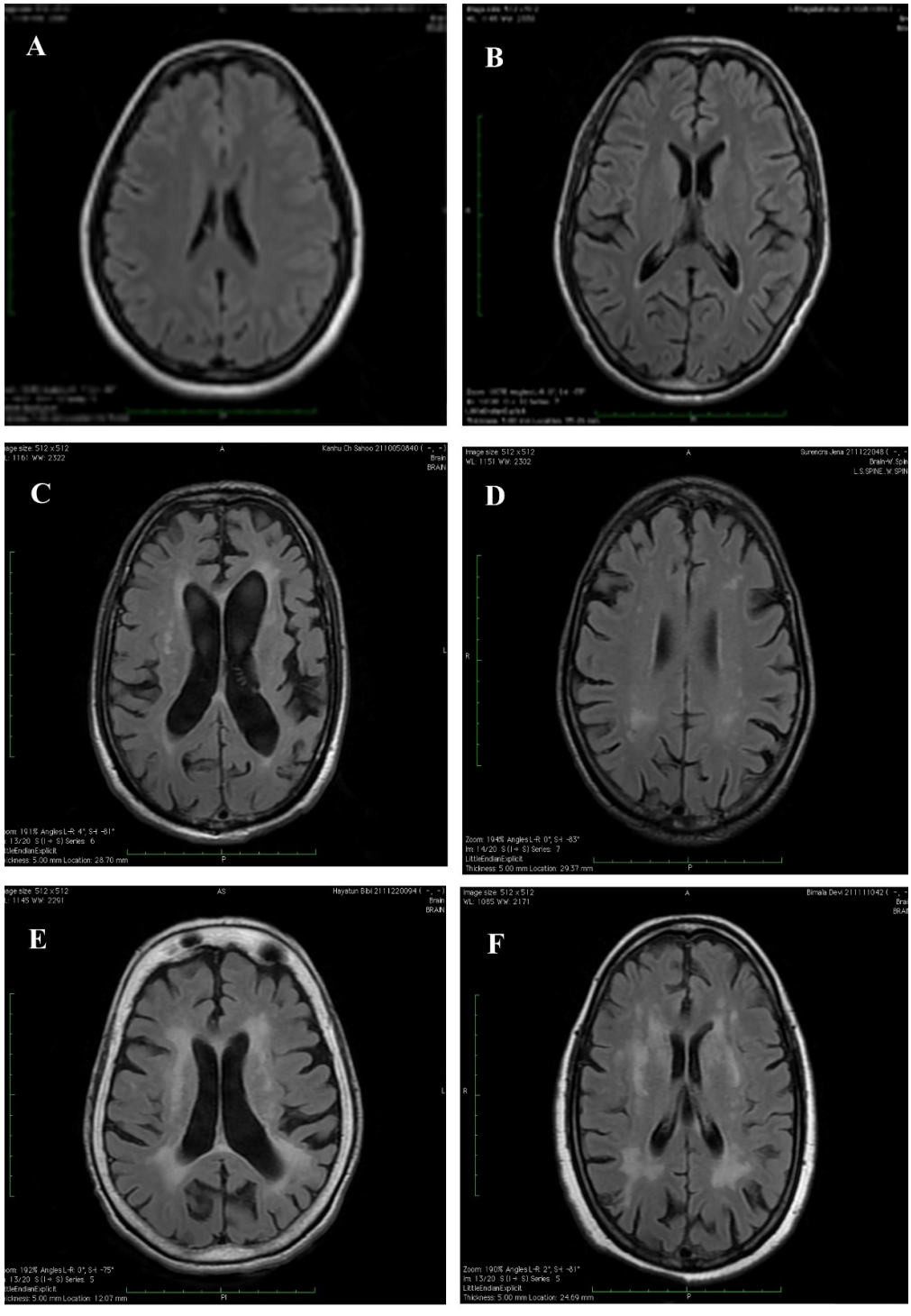

Fig 1. Grade of FAZEKAS scale; A,B) grade-1; C,D) grade-2; E,F) grade-3

of the total). Score >=2 was considered abnormal in less than 75 years of age and Score >=3 was considered abnormal in more than 75 years of age.

Out of 40 patients,Grade 0 (no atrophy) is seen in 22 patients in GCA scale, i.e., 55%of the total. Grade 1 atrophy is seen in 14 patients (i.e., 40% of the total). Grade 2 atrophy is seen in 4 patients (i.e., 10% of the total). However ,no cases show severe atrophy. Since GCA scoring showed inconclusive result in terms of assesment of severity of cognitive decline we use only MTA scoring for further assessment of sensivity and specificity. Further assessment for cognitive decline by neuropsychiatric test ADAS-Cog showed about 22 of them (i.e., 55 % of the total) had mild cognitive impairment, followed by 18 subjects who had moderate to severe cognitive impairment (i.e., 45% of the total).

The Sensitivity of Fazekas scoring in the assessment of severity of cognitive decline was 87.5%.The Specificity of Fazekas scoring in the assessment of severity of cognitive decline was 83.3%. P-value for fazeka scale correlation with clinical cognitive decline is 0.000013, which is significant. The Sensitivity of MTA scoring in the assessment of severity of cognitive decline was 72%. The Specificity of MTA scoring in the assessment of severity of cognitive decline was 88%. P-value of medial temporal lobe atrophy correlation with clinical cognitive decline by linear regression is 0.0006, which is significant. The Sensitivity of Combined Medial temporal atrophy (MTA) and Fazekas scoring in the assessment of severity of cognitive decline is 66.6%. The Specificity of Combined Medial temporal atrophy and Fazekas scoring in the assessment of severity of cognitive decline is 87.5% (Tables 1&2).

DISCUSSION

Dementia is a disease of elderly seen generally in age of more than 65 years. In the present study, the mean age of the participants was 66.15 years and 70% of the participants were more than 65 years of age. Aging is a very important risk factor for dementia as with advancing age the incidence of dementia increases exponentially between ages 65 to 90 and doubles approximately every 5 years.[28] With aging there is loss of grey as well as white matter volume manifesting as cerebral atrophy. In neurons, structural abnormalities include a decrease in the number, length and amount of dendrites, as well as an increase in segmental demyelination axons and a significant loss of synapses. Progressive dementia is also observed in patients having low serum vit B12 level, patients with carcinomatous meningitis, patients undergoing neurosurgical procedures; and among the caregivers of dementia patients.[29-35]

TABLE 1. Result of FAZEKAS, MTA scale and combined FAZEKAS+MTA scale in assessment of severity of cognitive decline.

Clinical (ADAS-COG) / FAZEKAS	Moderate to severe cognitive decline (>=2)	Percantage	Mild cognitive decline (<2)	Percantage
Moderate to severe cognitive decline	14		4	
Mild cognitive decline	2		20	
Clinical(ADAS-COG)/MTA				
Moderate to severe cognitive decline	16		2	
Mild cognitive decline	6		16	
Clinical(ADAS-COG)/MTA+FAZEKAS				
Moderate to severe cognitive decline	16	2		
Mild cognitive decline	8	14		

TABLE 2. Sensitivity and specificity of FAZEKAS, MTA scale and combined FAZEKAS+MTA scale in assessment of severity of cognitive decline.

	FAZEKAS	MTA scale	Combined FAZEKAS+MTA
Sensitivity	87.5%	72%	66.6%
Specificity	83.3%	88%	87.5%

The research group had a modest female majority with 57.5 percent of the participants being female. It has been proposed that due to loss of estrogen or other hormonal changes in association with other factors, there is increased risk in postmenopausal women, and estrogen replacement therapy has been shown to reduce the risk of AD in them.[36]

Diabetes and hypertension are important risk factors for dementia. In the study, 52.5% (21 out of 40 study subjects) were diabetic and 62.5% (25 out of 40) were hypertensive. Insulin receptors are abundant in cognition-related brain areas, as well as in the blood-brain barrier.[37] Insulin resistance reduces the quantity of glucose that enters the brain in diabetic individuals, resulting in neuronal damage.[38] It's also been suggested that a hyperglycemic state in the brain leads to the development of glycated end products, which may lead to neuroinflammation.[38] High SBP has been linked to decreased regional and overall brain sizes;[39-43] as well as brain volume declines over time.[44] When compared to normotensive people, hypertension people's brains have more amyloid plaques, atrophy, and neurofibrillary tangles.[45,46] Sustained rises in blood pressure may cause cerebral vascular remodeling and, as a consequence, cognitive impairment. Hypertension causes endothelial dysfunction, which disrupts the microvasculature's coordinated connection of neurons, glia, and cerebral blood flow.[47]

The majority of research individuals exhibited mild cognitive impairment (22 out of 40) and 45 percent had moderate to severe cognitive impairment, according to the MMSE and ADAS-COG assessments. It could be because our study group had the mean age of 66.1 years and majority of them were under the age group 60-70 years. According to the study conducted by Sengupta et al, 2014, Cognitive impairment among elderly people in India out of 268 total patients, 60% had mild cognitive impairment as the maximum number of the patients in the study were less than 70 years of age. The patients with increasing age had moderate to severe cognitive decline and lesser MMSE scores.[48]

In our study on assessment by Fazekas Scale for WMHs, 55% of the study subjects were rated as grade 1, suggesting that these subjects had mild cognitive decline. About 45% of the subjects were rated as grade 2 or grade 3 suggesting that these subjects had moderate to severe cognitive decline. WMH is associated with cognitive decline, especially in the domains of attention, executive function, and processing speed.[49,50] Hypoxic injury caused by atherosclerosis-induced hypoperfusion has been suggested as a possible etiological factor.[51] On correlation of data obtained by neuropsychological test ADAS-Cog and Fazekas scoring, we found sensitivity of 87.5% and specificity of 83.3%. Linear regression analysis between Fazekas and ADAS-Cog showed a P-value of < 0.001, which is highly significant. In the Landmark LADIS study, it was shown that the baseline severe white matter changes had an association with worse scores on MMSE and ADAS-Cog.[52] WMH has also been connected to poor performance on global cognitive evaluations, executive abilities, speed and motor control, attention, naming, and vasoconstriction praxis, and is an independent predictor of dementia and cognitive decline.[53]

MTA Scale is also used in the present study for assessment of severity of cognitive decline by MRI. Out of 40 patients, 55 % of the total study subjects had moderate to severe atrophy (Score >=2) and 45% had mild atrophy (Score <2). The MTA scale shows a good correlation with manual hippocampal assessments when utilised in combination with cognitive function, as well as increased clinical importance. Automated volume measurement and volume of cortical thickness estimates have the same sensitivity and specificity.[54,55] On correlation of data obtained by neuropsychological test ADAS-COG and MTA scoring, we found sensitivity 72 % and specificity of 88%. Linear regression analysis between MTA and ADAS-COG showed a P-value of <0.001 which is highly significant. In a study done by Jules j Claus et al on 1165 patients of Alzheimer disease and subjective cognitive impairment, it was seen that optimal MTA cut-off values for the age ranges <65, 65–74, 75–84 and ≥85 years were ≥1.0, ≥1.5, ≥ 2.0 and ≥2.0 and Corresponding sensitivity & specificity values were 83.3%, 86.4%; 73.7%, 84.6% and 73.7%, 76.2%, 84.0%, 62.5% respectively.[56]

Limitations of the study: The data in this study came from a cross-sectional survey and, there was no follow up. Confounding factors like diabetes and hypertension may have affected the results interpretation in our study as scale of dementia will vary according to duration of both illnesses.

CONCLUSION

Cognitive impairment, which is a typical sign of ageing, is often considered as a precursor to more serious disorders like Alzheimer's disease, dementia and depression. The role of white matter disorders and brain shrinkage in cognitive decline and dementia is becoming more generally recognised. White matter disease assessed by Fazekas scale and cerebral atrophy by MTA scale on MRI brain correlated well with cognitive decline clinically assessed by neuropsychological tests. In our

study Fazekas scoring for WMHs showed a sensitivity of 87.5% and specificity of 83.3% on correlation with clinical cognitive decline assessed by ADAS-Cog. Also, MTA scale for cerebral atrophy showed a sensitivity of 72% and specificity of 88% on correlation with clinical cognitive decline assessed by ADAS-Cog. Significant P-value have been obtained for both the above visual rating scales of MRI (Fazekas and MTA) by linear regression, on correlation with clinically assessed cognitive decline.

REFERENCES

1. World Alzheimer Report 2014. Available from: URL: https://www. alz.co.uk/research/WorldAlzheimerReport2014.pdf
2. Bose A, Shankardass MK. Growing old in India: voices reveal, statistics speak. New Delhi: BR Publishing Corporation; 2000. p.244-6.
3. Tantanokit T, Bosittipichet T, Leesri T. The Study of Prevalence and Associated Factors of Dementia in the Elderly. Siriraj Med J. 2021;73(4):224-35.
4. Sukhatunga K, Phattarayuttawat S, Luchom M, Chantra J, Chaiyasit W, Bunnagulrote K. Depression and Dementia in Thai Elderly in Urban and Rural Communities. Siriraj Med J. 1999;51(4):232-43.
5. Lezak MD, Howieson DB, Bigler ED, Tranel D. Neuropsychological Assessment. 5th ed. New York, NY: Oxford University Press; 2012.
6. Harada CN, Natelson Love MC, Triebel KL. Normal cognitive aging. Clin Geriatr Med. 2013;29(4):737-52.
7. Raz N, Gunning FM, Head D, Dupuis JH, McQuain J, Briggs SD, et al. Selective aging of the human cerebral cortex observed in vivo: differential vulnerability of the prefrontal gray matter. Cereb Cortex. 1997;7(3):268-82.
8. Salat DH, Kaye JA, Janowsky JS. Prefrontal gray and white matter volumes in healthy aging and Alzheimer disease. Arch Neurol. 1999;56(3):338-44.
9. Madden DJ, Spaniol J, Costello MC, Bucur B, White LE, Cabeza R, et al. Cerebral white matter integrity mediates adult age differences in cognitive performance. J Cogn Neurosci. 2009;21(2):289-302.
10. Dennis EL, Thompson PM. Functional brain connectivity using fMRI in aging and Alzheimer's disease. Neuropsychol Rev. 2014;24(1):49-62.
11. Pannese E. Morphological changes in nerve cells during normal aging. Brain Struct Funct. 2011;216(2):85-89.
12. Terry RD, Masliah E, Salmon DP, Butters N, DeTeresa R, Hill R, et al. Physical basis of cognitive alterations in Alzheimer's disease: synapse loss is the major correlate of cognitive impairment. Ann Neurol. 1991;30(4):572-80.
13. Masliah E, Mallory M, Hansen L, DeTeresa R, Terry RD. Quantitative synaptic alterations in the human neocortex during normal aging. Neurology. 1993;43(1):192-7.
14. Galton CJ, Patterson K, Graham K, Lambon-Ralph MA, Williams G, Antoun N, et al. Differing pattern soft emporal atrophyin Alzheimer's disease and semantic dementia. Neurology. 2001;57(2):216-25.
15. Reitz C, Mayeux R. Alzheimer disease: epidemiology, diagnostic criteria, risk factors and biomarkers. Biochem Pharmacol. 2014;88(4):640-651.
16. Romero JR, Beiser A, Himali JJ, Shoamanesh A, DeCarli C, Seshadri S. Cerebral microb leed sand risk ofi ncident dementia: the Framingham Heart Study. Neurobiol Aging. 2017;54:94-99.
17. Graff-Radford J, Simino J, Kantarci K, Mosley TH Jr, Griswold ME, Windham BG, et al. Neuroimaging correlates of cerebral microbleeds: the ARIC Study (Atherosclerosis Risk in Communities). Stroke. 2017;48(11):2964-72.
18. Poungvarin N, Prayoonwiwat N, Senanarong V, Chaisevikul R, Danchaivijitr C, Nilanont Y. Siriraj Acute Stroke Unit: The Experience of 614 Patients. Siriraj Med J. 2002;54(3):151-8.
19. Kuller LH, Lopez OL, Newman A, Beauchamp NJ, Burke G, Dulberg C, et al. Risk factors for dementiaint he cardiovascular health cognition study. Neuroepidemiology. 2003;22(1):13-22.
20. Barnes DE, Covinsky KE, Whitmer RA, Kuller LH, Lopez OL, Yaffe K. Predicting risk of dementia in older adults: the late-life dementia risk index. Neurology. 2009;73(3):173-79.
21. Debette S, Beiser A, DeCarli C, Au R, Himali JJ, Kelly-Hayes M, et al. Association of MRI markers of vascular brain injury with incident stroke, mild cognitive impairment, dementia, and mortality: the Framingham Offspring Study. Stroke. 2010;41(4):600-6.
22. Knopman DS, Griswold ME, Lirette ST, Gottsman RF, Kantarci K, Sharrett AR, et al. ARIC Neurocognitive Investigators. Vascular imaging abnormalities and cognition: mediation by cortical volume in nondemented individuals: atherosclerosis risk in communities-neurocognitive study. Stroke. 2015;46(2):433-40.
23. Gottesman RF, Schneider AL, Zhou Y, Coresh J, Green E, Gupta N, et al. Association between midlife vascular risk factors and estimated brain amyloid deposition. JAMA. 2017;317(14):1443-50.
24. Chawalparit O, Saenanarong V, Chiewvit P. CT Criteria in Vascular Dementia: A Study in Thai Population. Siriraj Med J. 2006;58(2):644-7.
25. Barkhof F, Hazewinkel M, Binnewijzend M, Smithuis R. Dementia - Role of MRI updated version. [Internet] Alzheimer Centre and Image Analysis Centre, Vrije Universiteit Medical Center, Amsterdam and the Rijnland Hospital, Leiderdorp, The Netherlands. Available from: https://radiologyassistant.nl/neuroradiology/dementia/role-of-mri
26. Folstein MF, Folstein SE, McHugh PR. Mini-mental state: A practical method for grading the cognitive state of patients for the clinician. J Psychiatr Res. 1975;12:189-98.
27. Zainal NH, Silva E, Lim LL, Kandiah N. Psychometric Properties of Alzheimer's Disease Assessment Scale-Cognitive Subscale for Mild Cognitive Impairment and Mild Alzheimer's Disease Patients in an Asian Context. Ann Acad Med Singap. 2016;45(7):273-83.
28. Jorm AF, Jolley D. The incidence of dementia: a meta-analysis. Neurology. 1998;51(3):728-33.
29. Sotthibundhu A, Buntup D, Sanghirun C, Cherdchu K, Cheeramakara C, Chansirikarnjan S, et al. Low Serum Vitamin B12 in AlzheimerÃ»s Patients as Detected by a Solid Phase Radioimmunoassay. Siriraj Med J. 2008;60(1):66-68.
30. Muangpaisan W. Rapidly Progressive Dementia due to Carcinomatous Meningitis Associated with Gastric Cancer. Siriraj Med J. 2016;68(1):47-50.
31. Suesat H, Srinonprasert V, Limpawattana P, Nakyos S, Poontananggul J, Jiraphorncharas C, et al. Detection of Postoperative Cognitive Dysfunction by Telemedicine Among Octogenarian Patients Who Underwent Minor Elective Surgery;

Prospective Cohort Study. Siriraj Med J. 2022;74(2):126-33.
32. Piyapittayanan S, Segsarnviriya C, Ngamsombat C, Witthiwej T, Cheunsuchon P, Chawalparit O. Comparison between Dynamic Contrast-Enhanced MRI and Dynamic Susceptibility Contrast MRI in Glioma Grading. Siriraj Med J. 2017;69(6): 369-76.
33. Yossie Susanti Eka Putri, Sitthimongkol Y, Wirojratana V, Chansatitporn N. Predictors of Depressive Symptoms among Family Caregivers of Patients with Dementia in Java, Indonesia. Siriraj Med J. 2021;73(8):549-58.
34. Piyapittayanan S, Segsarnviriya C, Ngamsombat C, Witthiwej T, Cheunsuchon P, Chawalparit O. Comparison between Dynamic Contrast-Enhanced MRI and Dynamic Susceptibility Contrast MRI in Glioma Grading. Siriraj Med J. 2017;69(6): 369-76.
35. Ananwattanasuk J, Chiewvit P, Nilanont Y. Imaging Findings of CNS Lymphoma in Siriraj Hospital. Siriraj Med J. 2006;58(8): 967-72.
36. Paganini-Hill A, Henderson VW. Estrogen replacement therapy and risk of Alzheimer's disease. Arch Intern Med. 1996;156: 2213-17.
37. Stephen CW, Randy JS, Denis GB, Michael WS. Insulin and the Blood-Brain Barrier. Curr Pharm Des. 2003;9:795-800.
38. Convit A. Links between cognitive impairment in insulin resistance: An explanatory model. Neurobiol Aging. 2005;26: 31-35.
39. Leritz EC, Salat DH, Williams VJ, Schnyer DM, Rudolph JL, Lipsitz L, et al. Thickness of the human cerebral cortex is associated with metrics of cerebrovascular health in a normative sample of community dwelling older adults. Neuroimage. 2011; 54:2659-71.
40. Nagai M, Hoshide S, Ishikawa J, Shimada K, Kario K. Ambulatory blood pressure as an independent determinant of brain atrophy and cognitive function in elderly hypertension. J. Hypertens. 2008;26:1636-41.
41. Glodzik L, Mosconi L, Tsui W, de Santi S, Zinkowski R, Pirraglia E, et al. Alzheimer's disease markers, hypertension, and gray matter damage in normal elderly. Neurobiol Aging. 2012;33: 1215-27.
42. Gianaros PJ, Greer PJ, Ryan CM, Jennings JR. Higher blood pressure predicts lower regional grey matter volume: Consequences on short-term information processing. Neuroimage. 2006;31: 754-65.
43. Firbank MJ, Wiseman RM, Burton EJ, Saxby BK, O'Brien JT, Ford GA. Brain atrophy and white matter hyperintensity change in older adults and relationship to blood pressure. Brain atrophy, WMH change and blood pressure. J Neurol. 2007;254:713-21.
44. Jennings JR, Mendelson DN, Muldoon MF, Ryan CM, Gianaros PJ, Raz N, et al. Regional grey matter shrinks in hypertensive individuals despite successful lowering of blood pressure. J Hum Hypertens. 2012;26:295-305.
45. Petrovitch H, White LR, Izmirilian G, Ross GW, Havlik RJ, Markesbery W, et al. Midlife blood pressure and neuritic plaques, neurofibrillary tangles, and brain weight at death: the HAAS. Neurobiol. Aging. 2000;21:57-62.
46. Ashby EL, Miners JS, Kehoe PG, Love S. Effects of Hypertension and Anti-Hypertensive Treatment on Amyloid-ß Plaque Load and Aß-Synthesizing and Aß-Degrading Enzymes in Frontal Cortex. J Alzheimers Dis. 2016;50:1191-203.
47. Girouard H, Iadecola C. Neurovascular coupling in the normal brain and in hypertension, stroke, and Alzheimer disease. J Appl Physiol. 2006;100:328-35.
48. Sengupta P, Benjamin AI, Singh Y, Grover A. Prevalence and correlates of cognitive impairment in a north Indian elderly population. WHO South East Asia J Public Health. 2014;3(2): 135-43.
49. Verdelho A, Madureira S, Moleiro C, Ferro JM, Santos CO, Erkinjuntti T, et al. White matter changes and diabetes predict cognitive decline in the elderly: the LADIS study. Neurology. 2010;75:160-7.
50. Debette S, Markus HS. The clinical importance of white matter hyperintensities on brain magnetic resonance imaging: systematic review and meta-analysis. BMJ. 2010;341:c3666.
51. Roman GC, Erkinjuntti T, Wallin A, Pantoni L, Chui HC. Subcortical ischaemic vascular dementia. Lancet Neurol. 2002; 1:426-36.
52. Van der Flier WM, van Straaten EC, Barkhof F, Verdelho A, Madureira S, Pantoni L, et al. Small vessel disease and general cognitive function in nondisabled elderly: the LADIS study. Stroke. 2005;36:2116-20.
53. Verdelho A, Madureira S, Ferro JM, Basile AM, Chabriat H, Erkinjuntti T, et al. Differential impact of cerebral white matter changes, diabetes, hypertension and stroke on cognitive performance among non-disabled elderly. The LADIS study. J Neurol Neurosurg Psychiatry. 2007;78:1325-30.
54. Cavallin L, Bronge L, Zhang Y, Oksengard, AR, Wahlund LO, Fratiglioni L, et al. Comparison between visual assessment of MTA and hippocampal volumes in an elderly, non-demented population. Acta Radiol. 1987;53:573-9.
55. Westman E, Cavallin L, Muehlboeck J-S, Zhang Y, Mecocci P, Vellas B, et al. Sensitivity and specificity of medial temporal lobe visual ratings and multivar- iate regional MRI classification in Alzheimer's disease. PLoS One. 2011;6:e22506.
56. Claus JJ, Staekenborg SS, Holl DC, Roorda JJ, Schuur J, Koster P, et al. Practical use of visual medial temporal lobe atrophy cut-off scores in Alzheimer's disease: Validation in a large memory clinic population. Eur Radiol. 2017;27(8):3147-55.

Consideration of Accuracy and Observational Error Analysis in Pelvic Sex Assessment: A Study in a Thai Cadaveric Human Population

Napakorn Sangchay, M.D., Ph.D.*, Veronika Dzetkuličová, Ph.D., Micol Zuppello, Ph.D.***, Jirapa Chetsawang, M.D., Ph.D.***

**Department of Anatomy, Faculty of Medicine, Siriraj Hospital, Mahidol University, Bangkok, Thailand, **Department of Anatomy, Faculty of Medicine, Masaryk University, Czech Republic, ***Institute of Clinical Sciences, College of Medical and Dental Sciences, University of Birmingham, Edgbaston, Birmingham, UK.*

ABSTRACT

Objective: In situations where skeletal human remains are recovered, pelvic bone morphology has been demonstrated to have an essential role in forensic sex identification. Determination of sex is one of the four pillars used to construct a biological profile of unidentified skeletal remains. Such analysis has mainly been confined to direct visual inspection or morphometric analysis of pelvic elements available. This study evaluates the identification accuracy and classification error established based on a morphometric sex determination of this bone either by direct observation or digital image analysis.

Materials and Methods: We used morphometric analysis of human pelvic bone from modern Thai samples to clarify the effect of variation in pelvic morphometric parameters on prediction accuracy. A total number of 408 pelvic bones (Male, n=249 and Female, n=159) were examined. Pelvic morphometric variables were measured in multiple regions for each bone.

Results: We found statistically significant differences in the pelvic morphometric parameters measured between the two sexes with considerably accurate classification and unavoidable errors by all means of analytical assessment.

Conclusion: Our findings suggest that it is not only variation of pelvic morphometric parameters between the two sexes in this population, but also the selection of analytical approach that can impact prediction accuracy and thus may contribute to the effect on the determination of sex. Ethical approval was not required for this study.

Keywords: Morphometric analysis; forensic anthropology; sex estimation; technical error of measurement (Siriraj Med J 2022; 74: 330-339)

INTRODUCTION

Forensic examiners must establish a biological profile when identifying unknown human remains, including sex, age, stature, and ancestry. This information can be compared with antemortem records and other information contributing to the identification process. Analysis of skeletal remains should be organized promptly to assess sex. Skeletal sex estimation is crucial for forensic anthropologists and forensic osteologists in developing a biological profile since sex assessment serves as a foundation for developing other aspects of a biological profile.[1-4] As part of a significant step to establishing a biological profile and personal identification, this process requires experience and needs accurate decision-making.

Corresponding author: Jirapa Chetsawang
E-mail: napakorn.sac@mahidol.ac.th
Received 3 February 2022 Revised 31 March 2022 Accepted 2 April 2022
ORCID ID: https://orcid.org/0000-0002-7776-6456
http://dx.doi.org/10.33192/Smj.2022.40

The manifestations of sex characteristics within bones are different in both sexes under genetic influence and hormonal regulations.[5] They make up their skeletal components and these distinctive skeletal traits can be used to differentiate males from females.[6,7] A reliable and less subjective technique for assessing sex should be conducted and documented to emphasise the identification performed.

Accurate and valid assessments of sex are used in field and laboratory settings for determining sex from skeletal remains.[8] Many studies have focused on gross skeletal features, utilizing cranial or postcranial bones.[9-11] In general, the selection of pelvic bone from unidentified human remains is preferable to estimate sex because of a high level of certainty and validity due to the sexual dimorphism demonstrated within this bone.[12,13] Studies have examined the utility of human pelvic bone to estimate sex, and in many cases, these lack intra- and inter-observer comparisons of observational error.[14,15] The estimation of sex can be established by visual assessment based on observing sexual dimorphic differences.[10] This method to estimate sex from the os pubis evaluates the different degrees of morphological traits to differentiate between the two sexes. It can be performed by using various morphologic characteristics, such as the subpubic concavity and the medial aspect of the ischio-pubic ramus.[16]

Alternatively, several morphological features of the pelvic complex can indicate the biological sex of individuals, including the size and shape of the os pubis, greater sciatic notch, obturator foramen, the existence or absence of the preauricular sulcus and evidence of parturition scars. However, sex estimation utilizing gross pelvic morphology requires complete or nearly complete skeletal elements. When the pelvic complex is less damaged, this method is achievable. However, morphological assessment becomes more challenging when these bones appear fragmented or severely damaged by taphonomic factors. For these reasons, an alternative method for sex estimation utilizing digital images of the specific characteristics from pelvic bone should be considered.[17]

Despite the acceptable accuracy, an estimation of sex utilizing gross morphology has several limitations. This method creates both intra- and inter-observer errors causing variation between observers and is non-reproducible. The decision-based observational method is highly subjective. It can be especially problematic when it appears to be undetermined or unclassified. Accordingly, sex estimation using pelvic morphometrics by direct measurements has been introduced to increase the certainty and accuracy.[18]

This method of sex estimation from the pelvis is problematic because it is regionally dependent.[19,20] Complete pelvic elements are required when determining the sex of unknown skeletal remains using either the non-metric method or metric analysis. This means that the degree of certainty in establishing sex from severely damaged pelves due to taphonomic causes is reduced. Consideration of an alternative pelvic landmark to establish sex identification is essential, especially when encountering fragmented pelvic bones. A morphologic analysis is mainly focused on the pubic region. Such analysis relies on either the presence or absence of morphological traits or the degree of expression.[21] When comparing anterior and posterior regions of the pelvic bone, it is clear that the pubis, being located anteriorly, has a high possibility of being exposed to postmortem changes. As a result, it can be impossible to establish sex. In terms of pelvic anthropometric sex assessment, this method relies on measuring observational characteristics. It utilizes individual measurements or combinations of measurements to differentiate the two sexes. The accuracy rate of prediction depends on the selection of skeletal landmarks utilized in this analytical method. The posterior region of the pelvic bone is more robust than the anterior border, and measurements of skeletal landmarks from this area are achievable.[22]

Metric sex estimation using the pelvic bone is more precise than visual morphological analyses and can exceed an accuracy rate of 90%. However, this approach requires a complete or nearly complete pelvic complex to assess all the landmarks proposed by current literature. The ischio-pubic index provided the most accurate sex estimation of 96.5%.[23] Supportive results of the ischio-pubic index as a sex indicator from pubic measurements were analyzed and achieved 90% accuracy.[24]

It is necessary to consider that either the non-metric or metric analytical methods using pelvic elements depend upon identifiable morphologic features, which in turn depend upon the bones being intact or nearly intact. Currently, sex estimation methods are mainly established from the pelvis samples from specific (black and white American) skeletal collections, whereas morphological traits for Asian and other ethnic groups are limited.[25,26] Several authors suggested that population-specific databases and classification analysis for sex estimation in heterogeneous populations are crucially required.[27]

This research will focus on the prediction accuracy and intra- and inter-observer observational errors from three different sex estimation methods, including estimating sex from gross morphological sex characteristics, digital images, and a measured analytical approach in a modern Thai population utilizing human pelvic dry bones.

MATERIALS AND METHODS

The study was conducted on 408 human pelvic bone samples from the Siriraj Bone collection, Department of Anatomy, Faculty of Medicine Siriraj hospital, Mahidol University. For each bone, three gross morphologies based on the Phenice method, including the presence of ventral arc, inferior pubic ramus and subpubic concavity, were used to determine sex. Subsequently, three digital images were taken from each bone to determine an inter-observer accuracy and error of sex assessment using the Phenice criteria. Pelvic morphometric parameters (Fig 1) were measured from each bone. The usefulness of iliac associated bony landmarks for assessing sex was examined. This was done by analysing sex discriminant functions for sex indicators of those measurements taken from prominent posterior foci to the anterior iliac bony landmarks. The parameters measured in this method are located on the anterior and posterior border of the ilium, including ASIS, AIIS, PSIS, and PIIS. Additional parameters were measured from those two iliac borders to other skeletal landmarks: the pubic tubercle and ischial spine. Pelvic landmarks and morphometric measurements were described as shown in Table 1. The mean and standard deviations were calculated for each parameter. Statistical analyses using paired student's t-tests were performed to evaluate the differences between each group. The null hypothesis was rejected where the difference between groups was 0. A p-value of <0.05 was interpreted as being statistically significant. Inferential statistics were used to determine discriminant function analysis (total analytical sample) and evaluate the probability of sex prediction and classification accuracy for those variables that revealed statistically significant differences. The best discriminant functions were compared and selected based on positive prediction accuracy.

Observational error and reliability analysis

Intra-observer error of measurement evaluation (Table 3).

Two measures were used in this observational study to investigate intra-observer measurement error rates between two separate measurements taken by the same investigator. The measurements were taken by the researcher who did this study, who first measured morphometric characteristics from pooled human pelvic samples, then took a second measurement. The interval between the first and second measurements was two weeks. To quantify intra-observer error, researchers measured pelvic bone-related data. Six variables were measured: PL, IL, vertical and horizontal Acetabular diameters, and obturator foramen diameters. The statistical difference between the two measurements was analysed using the student t-test.

Inter-observer error of measurement evaluation (Table 3).

Two observers conducted two sets of measurements independently to investigate an inter-observer technical error of measurement between two independent investigators. The researcher who conducted this current investigation and analysed bone samples was the first witness. Each of the six parameters was assessed. The second observer was a ten-year anatomical academic staff member who evaluated the pelvic parameters using the same pelvic samples. The objective of this study was to quantify the inter-observer measurement error and the repeatability. The instructions and descriptions for data collection were supplied to the second observer. Before conducting the inter-observer inquiry, the observers were given definitions for six criteria. A brief session was provided to measure the variables with the anthropometric tools. For non-bias considerations,

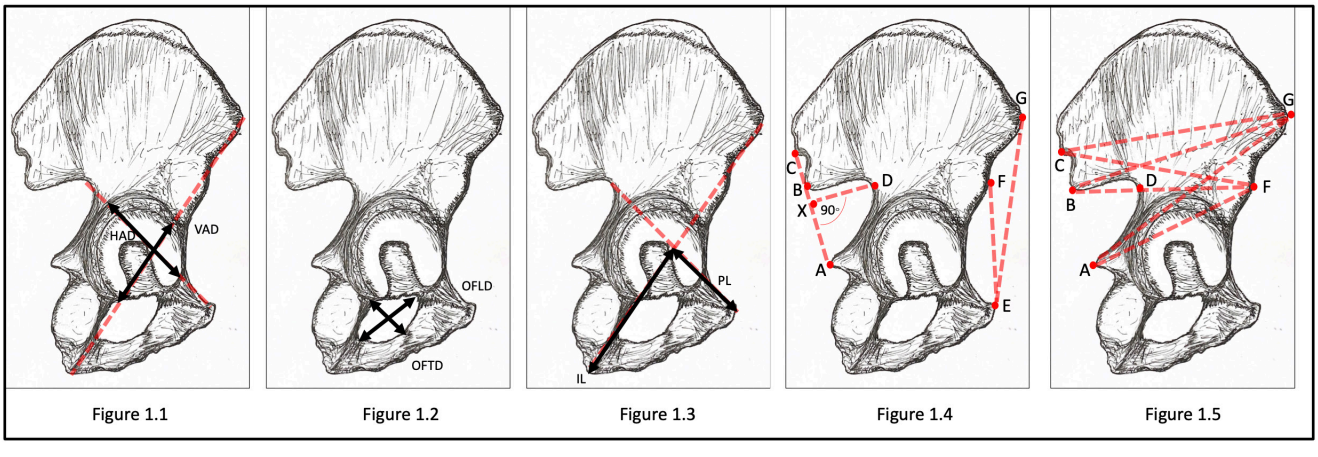

Fig 1. Diagrams illustrating pelvic morphometric landmarks and dimensional measurements.

TABLE 1. Description of pelvic landmarks and morphometric measurements.

	Pelvic morphometric landmarks and descriptions
VAD	Vertical Acetabular Diameter
HAD	Horizontal Acetabular Diameter
MAD	Mean Acetabular diameter
OFLD	Obturator Foramen Longitudinal Diameter
OFTD	Obturator Foramen Transverse Diameter
MOFD	Mean Obturator Foramen diameter
OF index	Obturator Foramen index
PL	Pubic Length
IL	Ischial Length
P/I index	Pubic/Ischial length index
A	Ischial spine
B	Posterior inferior iliac spine (PIIS)
C	Posterior superior iliac spine (PSIS)
D	Highest point of greater sciatic notch
E	Pubic tubercle
F	Anterior inferior iliac spine (AIIS)
G	Anterior superior iliac spine (ASIS)
AB	Distance between ischial spine and PIIS
BC	Distance between PSIS and PIIS
XD	Maximal greater sciatic notch heigth
EF	Distance between pubic tubercle and AIIS
EG	Distance between pubic tubercle and ASIS
BG	Distance between PIIS and ASIS
CG	Distance between PSIS and ASIS
AG	Distance between ischial spine and ASIS
BF	Distance between PIIS and AIIS
AF	Distance between ischial spine and AIIS
CF	Distance between PSIS and AIIS

the measurement was carried out without knowing the sample's demographic characteristics. The statistical difference between the two observers was investigated using a paired student t-test. The intra-observer error rates for two measures and the inter-observer error rates for two observers were calculated for the conventional morphometric measurement. Repeatability between observations/observers was assessed, calculating the technical error of measurement (TEM), relative technical error of measurement (rTEM) and coefficient of reliability (R). These values indicate the repeatability between two observations.[28] TEM is calculated as follows,

$$TEM=\sqrt{(\Sigma D^2)/2N}$$

(D = difference between the two observers or measurements 1 and 2, and N = the total number of tested samples. Subsequently, the relative TEM (rTEM) was calculated using the formula as shown below:

$$rTEM= (TEM/ mean) \times 100$$

An agreement threshold between observations is accepted at a 5% cut off value.[29] This study assesses the coefficient of reliability (R) to determine a repeatability in anthropometric measurement.[30] It was calculated using the formula as shown below:

$$R= 1 - ((TatalTEM)2/SD^2)$$

The value of coefficient of reliability (R) ranges from 0 to 1. Levels of reliability coefficient (R) are accepted when the values were > 0.95.[27]

The relationship between pelvic morphometric variables and known sex were examined using discriminant function analysis. The entire dataset was utilised at this stage of the analysis (N = 408). Ten discriminant functions were created (Table 4) shows a summary of all functions and parameters.

RESULTS

Descriptive statistics for the pelvic measurements are summarized in Table 2, including group means, standard deviations, variances and minimum and maximum values. Means of all pelvic measurements were significantly different between males and females ($p < 0.05$), except for obturator foramen transverse diameter (OFTD).

Table 3 shows the summary of descriptive statistics and intra- and inter-observer technical error of measurement values and the reliability coefficient obtained from all six measurements. Among the six variables, the results

TABLE 2. Descriptive statistics of pelvic landmarks and morphometric variables (* represented no statistical difference).

Variables	Male (n=249)					Female (n=159)					*P-value*
	Mean	*Std Dev*	*Variance*	*Minimum*	*Maximum*	*Mean*	*Std Dev*	*Variance*	*Minimum*	*Maximum*	
VAD	49.05	2.88	8.28	40.36	57.28	44.14	2.74	7.52	34.14	51.98	< 0.05
HAD	49.99	2.85	8.10	39.88	59.79	45.11	2.97	8.81	36.33	64.84	< 0.05
MAD	49.52	2.72	7.39	40.12	58.54	44.62	2.67	7.10	35.24	55.73	< 0.05
OFLD	50.61	3.69	13.64	39.08	63.63	46.62	3.51	12.30	38.57	58.74	< 0.05
OFTD	32.96	3.44	11.85	21.70	44.66	33.32	3.36	11.29	21.69	43.27	0.29*
MOFD	41.78	3.19	10.19	30.64	54.15	39.97	3.06	9.35	31.80	47.75	< 0.05
OF index	65.17	5.54	30.72	47.63	80.84	71.54	5.93	35.17	51.75	87.92	< 0.05
PL	70.44	5.69	32.39	54.88	86.55	68.10	5.52	30.44	55.92	81.69	< 0.05
IL	87.96	6.03	36.31	64.21	119.40	79.63	5.04	25.36	67.58	91.52	< 0.05
P/I index	80.23	6.00	36.04	67.18	99.94	85.67	6.74	45.48	69.54	105.49	< 0.05
AB	54.52	5.70	32.53	37.42	70.01	60.97	7.10	50.44	43.08	84.43	< 0.05
BC	36.79	5.35	28.67	21.30	51.11	32.64	4.71	22.21	18.24	45.41	< 0.05
AB+BC	91.31	7.68	58.97	72.78	112.68	93.61	8.79	77.20	70.23	129.18	< 0.05
XD	35.84	3.20	10.27	27.69	44.51	33.70	3.70	13.68	24.96	45.77	< 0.05
EF	85.77	6.07	36.90	61.24	105.79	83.40	6.31	39.83	69.66	99.79	< 0.05
EG	119.34	9.69	93.86	78.01	149.48	116.75	8.60	73.88	96.53	146.62	< 0.05
BG	13.20	0.75	0.56	10.60	15.50	12.65	0.85	0.72	10.20	14.90	< 0.05
CG	14.61	0.83	0.69	11.00	16.80	14.22	0.86	0.74	12.00	16.50	< 0.05
AG	13.16	0.74	0.54	11.00	15.50	12.30	0.70	0.49	10.50	14.50	< 0.05
BF	11.25	0.72	0.52	8.50	13.60	10.79	0.80	0.64	8.70	12.90	< 0.05
AF	10.11	0.69	0.48	7.80	13.50	9.20	0.62	0.39	7.50	11.00	< 0.05
CF	13.36	0.76	0.58	10.00	15.70	12.84	0.81	0.66	10.20	14.80	< 0.05

TABLE 3. Comparisons of intra- and inter-observer technical errors of measurement (TEM) and Reliability coefficient (SD – standard deviation, Ab TEM – Absolute TEM, rTEM – relative TEM, R – Reliability coefficient).

	Intra-observer error								Inter-observer error							
	Mean		SD		p value	Ab TEM	rTEM	R	Mean		SD		p value	Ab TEM	rTEM	R
	Measurement1	Measurement2	Measurement1	Measurement2					Observer1	Observer2	Observer1	Observer2				
VAD	47.137	47.301	3.704	3.596	0.112	1.473	3.120	0.837	47.137	47.288	3.704	3.490	0.200	1.68	3.558	0.782
HAD	48.090	48.191	3.748	3.701	0.044	0.71	1.475	0.964	48.090	48.185	3.748	3.201	0.392	1.57	3.261	0.797
OFLD	49.056	49.202	4.109	4.115	0.105	1.29	2.626	0.901	49.056	49.257	4.109	4.192	0.126	1.86	3.784	0.799
OFTD	33.096	33.179	3.411	3.385	0.282	1.39	3.289	0.832	33.096	33.167	3.411	3.260	0.569	1.78	5.372	0.715
PL	69.524	69.316	5.732	5.608	0.032	1.38	1.988	0.941	69.524	68.893	5.732	5.258	0.000	2.55	3.685	0.786
IL	84.714	84.708	6.963	6.766	0.961	1.66	1.960	0.941	84.714	84.647	6.963	6.554	0.649	2.11	2.492	0.903

TABLE 4. Comparisons of Canonical discriminant function coefficients for pelvic dimensions, discriminant classification function and classification matrix.

Canonical discriminant function coefficients for pelvic dimensions

Functions and parameters		Raw Canonical Coefficients	Standardized Canonical Coefficients (Pooled Within-Class)	Total Canonical Structure	Group Centroids		Discriminant Classification Function								Classification Matrix				
Function1	OFLD	0.343	1.242	0.819	F	-0.887	Group	OFLD	OFTD	Constant					Group \ Predicted	F	M	Total	Percent Correct
	OFTD	-0.238	-0.812	-0.089	M	0.566	F	3.018	0.956	-86.266					F	90	69	159	56.604%
	Constant	-8.933					M	3.516	0.61	-99.016					M	37	212	249	85.141%
															Total	127	281	408	74.02%
															Number of correct = 302				
Function2	MAD	0.393	1.062	0.994	F	-1.12	Group	MAD	MOFD	Constant					F	126	33	159	79.245%
	MOFD	-0.051	-0.161	0.407	M	0.715	F	5.024	2.117	-154.411					M	26	223	249	89.558%
	Constant	-16.63					M	5.746	2.023	-184.549					Total	152	256	408	85.539%
															Number of correct = 349				
Function3	PL	0.149	0.836	0.335	F	-0.926	Group	PL	IL	PII	Constant				F	115	44	159	72.327%
	IL	0.034	0.19	0.98	M	0.591	F	-248.775	207.126	210.282	-8,783.987				M	32	217	249	87.149%
	PII	-0.164	-1.031	-0.652			M	-248.549	207.177	210.034	-8,783.306				Total	147	261	408	81.373%
	Constant	0.282													*Number of correct = 332*				
Function4	VAD	110.349	311.844	0.97	F	-1.109	Group	VAD	HAD	MAD	Constant				F	124	35	159	77.987%
	HAD	110.33	319.357	0.964	M	0.708	F	3.719	3.594	-1.188	-136.813				M	27	222	249	89.157%
	MAD	-220.308	-594.476	1.			M	4.242	4.016	-1.453	-168.813				Total	151	257	408	84.804%
	Constant	-17.645													*Number of correct = 346*				
Function5	AB	0.118	0.741	0.77	F	0.894	Group	AB	BC	XD	Constant				F	103	56	159	64.78%
	BC	-0.102	-0.522	-0.633	M	-0.571	F	1.423	1.098	2.554	-104.329				M	37	212	249	85.141%
	XD	-0.132	-0.448	-0.504			M	1.25	1.248	2.746	-106.251				Total	140	268	408	77.206%
	Constant	1.475													*Number of correct = 315*				
Function6	BG	0.331	0.26	0.61	F	-0.768	Group	BG	CG	AG	Constant				F	62	96	158	39.241%
	CG	-0.662	-0.557	0.413	M	0.488	F	4.569	9.442	13.432	-178.746				M	38	211	249	84.739%
	AG	1.559	1.125	0.955			M	4.985	8.61	15.39	-197.064				Total	100	307	407	67.076%
	Constant	-14.726													*Number of correct = 273*				
Function7	AF	1.82	1.211	0.976	F	-0.865	Group	AF	BF	CF	Constant				F	108	51	159	67.925%
	BF	-0.325	-0.244	0.502	M	0.552	F	6.594	4.758	14.186	-147.09				M	39	210	249	84.337%
	CF	-0.178	-0.139	0.54			M	9.174	4.297	13.933	-163.599				Total	147	261	408	77.941%
	Constant	-11.803													*Number of correct = 318*				
Function8	MAD	-0.297	-0.8	-0.911	F	1.327	Group	MAD	MOFD	OFI	PII	Constant			F	136	23	159	85.535%
	MOFD	-0.008	-0.024	-0.373	M	-0.847	F	5.824	1.166	1.574	1.958	-293.442			M	20	229	249	91.968%
	OFI	0.077	0.437	0.659			M	6.469	1.182	1.408	1.87	-305.777			Total	156	252	408	89.461%
	PII	0.04	0.255	0.534											*Number of correct = 365*				
	Constant	5.913																	
Function9	AB	-0.138	-0.87	-0.769	F	-0.895	Group	AB	BC	EF	EG	Constant			F	109	50	159	68.553%
	BC	0.092	0.47	0.633	M	0.572	F	0.922	0.841	1.387	0.359	-120.523			M	32	217	249	87.149%
	EF	0.064	0.393	0.317			M	0.719	0.975	1.48	0.378	-123.615			Total	141	267	408	79.902%
	EG	0.013	0.138	0.257											*Number of correct = 326*				
	Constant	-2.27																	
Function10	VAD	0.161	0.456	0.889	F	-1.328	Group	VAD	HAD	OFLD	OFTD	PL	IL	Constant	F	136	23	159	85.535%
	HAD	0.12	0.347	0.873	M	0.848	F	1.524	2.012	1.317	0.481	0.737	0.606	-166.936	M	19	230	249	92.369%
	OFLD	0.105	0.381	0.651			M	1.875	2.273	1.546	0.148	0.64	0.717	-198.467	Total	155	253	408	89.706%
	OFTD	-0.153	-0.522	-0.071											*Number of correct = 366*				
	PL	-0.044	-0.25	0.274															
	IL	0.051	0.29	0.801															
	Constant	-14.728																	

demonstrated statistically significant differences in HAD and PL between the two measurements (p-value of < 0.05). HAD demonstrated intra-observer error rates with R value > 0.95. This finding indicates high repeatability with only the HAD not exceeding the 5% acceptance threshold. In terms of inter-observer error analysis, statistical analysis demonstrated that only PL examined by the two observers was statistically significantly different (p-value of < 0.05). The six pelvic parameters demonstrated inter-observer error rates with R value < 0.95. These findings indicate low repeatability with all measured variables not exceeding the 5% acceptance threshold.

When accuracy for estimating sex by direct observation using Phenice's characteristic was compared with sex assessment using Phenice's pelvic morphologies digital images, 91.42% accuracy was achieved from sex estimation based on gross pelvic examination (373/408). Similar figures were obtained from two observers (90.32%, 84/93 and 87.09%, 81/93) using pelvic morphologies digital images approach based on Phenice's characteristics with the mean accuracy of 88.71%.

Table 4 shows the standard, structure and unstandardized coefficients, the group centroids, results, and the discriminant function analysis results from the study data. For all of the ten discriminant functions produced for sex determination, sex was correctly assessed with an accuracy between 67.07% and 89.46%. Using the discriminant function analysis of pelvic dimensions, the lowest accuracy in the prediction was observed from Function 6 when using a combination of BG, CG and AG as a sex predictor with an accuracy of 67.07%. The best discriminator between the sexes with the highest predicted accuracy was achieved using VAD, HAD, OFLD, OFTD, PL and IL with an accuracy of 89.71%.

For the function using only acetabular-related variables, average accuracy was 84.8%; using only obturator foramen-related variables classification accuracy was 74.02%. Function 5, where sciatic notch measurements were assessed, performed an average accuracy of 81.37%. Functions established from distances measuring ASIS and AIIS to the posterior pelvic landmark achieved an accuracy of 67.08% and 77.94%, respectively.

DISCUSSION

Skeletal sex estimation can be assessed by visual observation of morphological variation in the bones because of sexual dimorphism.[32] Skeletal size and robusticity, attributed by extrinsic factors such as biomechanics, interact with bones, and intrinsic factors including genetic and sex hormones, are the preferable sex indicator. Cranial and postcranial skeletal elements exhibit sexual dimorphism observed in adult skeletons.[8] Non-metric analysis of pelvic morphology, along with metric methods, is the most reliable sex indicator for adult skeletons.[8] Within the pelvis, the morphology of the pubic region is thought to establish the most reliable indicators for sex estimation. Existence of the ventral arc, the subpubic

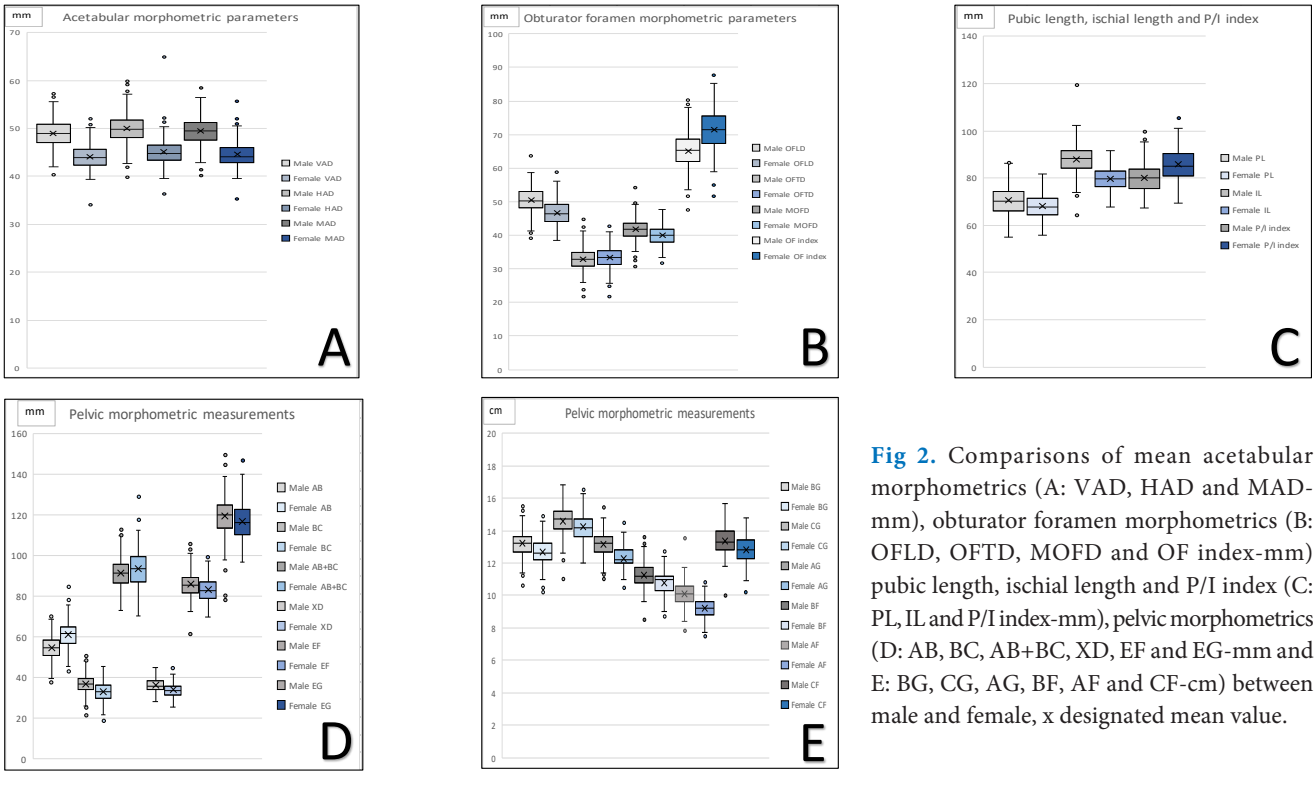

Fig 2. Comparisons of mean acetabular morphometrics (A: VAD, HAD and MAD-mm), obturator foramen morphometrics (B: OFLD, OFTD, MOFD and OF index-mm) pubic length, ischial length and P/I index (C: PL, IL and P/I index-mm), pelvic morphometrics (D: AB, BC, AB+BC, XD, EF and EG-mm and E: BG, CG, AG, BF, AF and CF-cm) between male and female, x designated mean value.

concavity, and the morphology of the medial surface of the ischiopubic ramus was introduced by Phenice as an accurate method for sex estimation. Phenice's pelvic morphological traits have been further validated with improved accurate prediction and reduced classification errors.[15,24,33,34]

The morphologies of the acetabulum, the size of the obturator foramen, and the pubic and ischial lengths can reveal sex differences. In addition, studies report other morphological features that are possible for sex indicators within the pelvic bone, including the acetabulum and the greater sciatic notch.[35] These anatomical regions have a durability that potentially endures destructive processes more readily than the pubis. The use of morphometric measurement incorporated with stepwise-selected discriminant functions can yield more accurate classification than observational morphometric approaches. Nonetheless, analysis using a digital image is achievable. This study found that this method can provide less accuracy than direct observational sex differentiation.

While most adult skeletons demonstrate sexually dimorphic characteristics, the validity of sex assessment is also influenced by other factors: population variations, age, and pathological and taphonomic changes. The expression of sexual dimorphism is variable among and across populations. Therefore, it is necessary to consider comparative data from a specific population when applying these techniques in forensic circumstances.[36] Sexual dimorphism and the differences between the sexes vary in other populations. In addition, different methodologies, including morphological and metric features, may analyze skeletal remains for sex estimation. Skeletal differences in morphological attributes vary by shape, morphological traits, and relative size between the sexes. Methods based on the shape and size of the pelvis and the presence or absence of pelvic characteristics are favoured. Other morphological features may represent sex differences. However, they are usually less accurate than methods using distinct morphological features with substantial sexual dimorphism and observations. Instruments, standards, appropriate analytical software and a combination of measurements and multivariate approaches can increase reliability in sex evaluations, although a single measurement may provide reasonably reliable sex estimation.

It is well acknowledged that intra- and inter-observer error caused by visual or metric variables can lead to disparities in sexual dimorphism evaluation and sex determination. Current studies, however, have shown that visual assessment is associated with significant levels of inter-observer error due to imprecise variable definitions, substantial reliance on previous observer experience, and the seriation process employed to sort the individuals. This error measurement analysis reveals that geometric morphometrics produces good intra- and inter-observer agreement.

Pelvic morphologies can be differentiated consistently even among observers with no prior experience. However, those with obscure morphologies are exceedingly difficult to determine consistently. Our findings show that even observers familiar with pelvic analysis using sexual dimorphism have an inconsistent interpretation of coordinative landmarks for assessing sex; even though the presence of the ventral arc is the best sex indicator for females, determination of sex from digital images still establishes various degrees of prediction accuracy among observers. This shows that descriptive anatomical landmarks may be misinterpreted in the ischiopubic regions.[24,35] It is worth describing the quantitative methodologies utilizing the pelvic characteristics which show sexual dimorphism variance. These methodologies are relevant and applicable to every forensic practitioner. The effect of sex estimation utilizing pubic length, ischial length and P/I index on classification accuracy is critical. The description of anatomical landmarks for these measurements, especially the pubic length, is diverse among current literature. In this study, measurement of pubis length and ischial length between the two observers revealed lower reliability than results from an intra-observer error of measurement, indicating a low reproducibility.

Additionally, the definition of a specific landmark being measured within the acetabulum is identical to a problematic issue occurring in the ischiopubic region.[37,38] All measurements should be repeatable and independent. Therefore, future research should incorporate an assessment of the interobserver error in these dimensions to avoid sex misinterpretation.

The integration of the iliac landmark measurement and the assessment of pubic sex characteristics should be considered when dealing with skeletal parts and severely fragmented skeletal remains to improve sex prediction accuracy. The range of prediction accuracy from discriminant functions utilizing these measurements in this study was 67.08% (Function6)-79.9% (Function9), indicating that those measurements are potentially reliable in estimating the sex, as highlighted in previous studies.[22,39,40] Thus, sex discrimination utilizing iliac measurement can be conducted independently.[41] However, a correct estimation between an isolated morphometric measurement analysis and the morphological assessment showed that the former established a less favourable outcome and provided a lower prediction accuracy than the latter

method. Sex dimorphism of pelvic morphological traits has been documented across different human populations, and it is also considered as a sex-determining method. This study shows that the utilization of iliac associated morphological characteristic measurements is less reliable when applied to sex assessment because the attribution of sex dimorphism is demonstrated less within this bony segment. As a result, these measurements require further investigation and the expansion of this analytical method into the different populations to validate the usefulness of these sex indicators in a forensic application.[26]

The effect of sample size is another aspect to consider in this situation. The requirement of cross-validation study using different populations is necessary to evaluate the discriminant outcomes established from these present classification functions. The use of approximately 400 individuals in this study can affect prediction accuracy and increase technical errors. As a result, it is feasible that increased samples will reduce undesirable errors and improve efficiency.

In summary, the consideration of factors affecting prediction accuracy and classification errors for pelvic sex estimation is critical because this bone is under hormonal regulation rather than mechanical influence. These functions may be beneficial where the population of origin of the unidentified skeleton is unknown. Further research is required on cooperative group data from other divergent populations, both in the pelvis region and other skeletal parameters that express sexually dimorphic characteristics.

CONCLUSION

Identifying sex from skeletal remains is a crucial step in human identification. Although human pelvic bone has been the most crucial determinant in this process, only a few anthropologic methods can influence sex determination accuracy. Promoting alternative morphological assessment methods, such as digital evaluation and direct morphometric measurement, as well as direct morphological interpretation from this bone, may be shown to be the most accurate methods. It is critical to recognize instruments that influence correct prediction in sex discrimination. The selection of an appropriate analytical method is essential because it can affect the whole process of forensic human identification. Therefore, it can minimize the possibility of misidentification.

Conflicts of interest: None

Funding: None

Ethics/IRB approval: Yes, SIRB Protocol No. (Si 625/2020)

REFERENCES

1. Christensen AM, Crowder CM. Evidentiary standards for forensic anthropology. J Forensic Sci. 2009;54(6):1211-6.
2. Christensen AM, Passalacqua NV. Introduction to Forensic Anthropology. In: A Laboratory Manual for Forensic Anthropology. London: Academic Press, 2018.
3. Christensen AM, Passalacqua NV, Bartelink EJ. Forensic Anthropology: Current Methods and Practice. London: Academic Press, 2014.
4. Krishan K, Chatterjee PM, Kanchan T, Kaur S, Baryah N, Singh RK. A review of sex estimation techniques during examination of skeletal remains in forensic anthropology casework. Forensic Sci Int. 2016;261:165.e1-8.
5. Kirkham GR, Cartmell SH. Genes and Proteins Involved in the Regulation of Osteogenesis. Genes Osteogenes. 2007;3(0): 1-22.
6. Durić M, Rakočević Z, Donić D. The reliability of sex determination of skeletons from forensic context in the Balkans. Forensic Sci Int. 2005;147(2-3):159-64.
7. White T, Folkens P. The Human Bone Manual. Oxford: Academic, 2005.
8. Spradley MK, Jantz RL. Sex estimation in forensic anthropology: skull versus postcranial elements. J Forensic Sci. 2011;56(2):289-96.
9. Guyomarc'h P, Bruzek J. Accuracy and reliability in sex determination from skulls: A comparison of Fordisc® 3.0 and the discriminant function analysis. Forensic Sci Int. 2011;208 (1-3):180.e1-6.
10. Bruzek J. A method for visual determination of sex, using the human hip bone. Am J Phys Anthropol. 2002;117(2):157-68.
11. Sangvichien S, Boonkaew K, Chuncharunee A. Sex Determination in Thai Skulls by Using Craniometry: Multiple Logistic Regression Analysis. Siriraj Med J. 2007;59:216-21.
12. Austin D, King RE. The Biological Profile of Unidentified Human Remains in a Forensic Context. Acad Forensic Pathol. 2016;6(3):370-90.
13. Rösing FW, Graw M, Marré B, Ritz-Timme S, Rothschild MA, Rötzscher K, et al. Recommendations for the forensic diagnosis of sex and age from skeletons. Homo. 2007;58(1):75-89.
14. González PN, Bernal V, Ivan Perez S, Barrientos G. Analysis of dimorphic structures of the human pelvis: its implications for sex estimation in samples without reference collections. J Archaeol Sci. 2007;34(10):1720-30.
15. Lesciotto KM, Doershuk LJ. Accuracy and Reliability of the Klales et al. (2012) Morphoscopic Pelvic Sexing Method. J Forensic Sci. 2018;63(1):214-20.
16. Phenice TW. A newly developed visual method of sexing the os pubis. Am J Phys Anthropol. 1969;30(2):297-301.
17. Ali SHM, Omar N, Shafie MS, Ismail NAN, Hadi H, Nor FM. Sex estimation using subpubic angle from reconstructed three-dimensional computed tomography pelvic model in a contemporary Malaysian population. Anat Cell Biol. 2020;53(1):27-35.
18. Mahakkanukrauh P, Ruengdit S, Tun SM, Case DT, Sinthubua A. Osteometric sex estimation from the os coxa in a Thai population. Forensic Sci Int. 2017;271:127.e1-127.e7.
19. Bytheway JA, Ross AH. A geometric morphometric approach to sex determination of the human adult os coxa. J Forensic Sci. 2010;55(4):859-864.
20. Gonzalez PN, Bernal V, Perez SI. Geometric morphometric approach to sex estimation of human pelvis. Forensic Sci Int.

2009;189(1–3):68-74.
21. Chanapa P, Kijkuokool P, Singsuwan P, Mahakkanukrauh P. The most accurate sex determination using three morphologies in the pubis. Int Med J. 2018;25(3):189-192.
22. Rmoutilová R, Dupej J, Velemínská J, Brůžek J. Geometric morphometric and traditional methods for sex assessment using the posterior ilium. Leg Med. 2017;26:52-61.
23. Thieme F, Schull W. Sex determination from the skeleton. Hum Biol an Int Rec Res. 1957;29(3):242-73.
24. Drew R. A review of the ischium-pubis index: Accuracy, reliability, and common errors. Hum Biol. 2013;85(4):579-96.
25. Patriquin ML, Loth SR, Steyn M. Sexually dimorphic pelvic morphology in South African whites and blacks. HOMO- J Comp Hum Biol. 2003;53(3):255-62.
26. Patriquin ML, Steyn M, Loth SR. Metric analysis of sex differences in South African black and white pelves. Forensic Sci Int. 2005;147(2-3 SPEC.ISS.):119-27.
27. Sierp I, Henneberg M. The Difficulty of Sexing Skeletons from Unknown Populations. J Anthropol. 2015;2015:1-13.
28. Perini TA, de Oliveira GL, dos Santos Ornellas J, Palha de Oliveira F. Technical error of measurement in anthropometry. Rev Bras Med do Esporte. 2005;11(1):81-90.
29. Purkait R. Anthropometric landmarks: How reliable are they? Anthropometric landmarks. Medico-Legal Updat. 2004;4(4):133-40.
30. Ulijaszek SJ, Kerr DA. Anthropometric measurement error and the assessment of nutritional status. Br J Nutr. 1999;82(3):165-77.
31. Goto R, Mascie-Taylor CGN. Precision of measurement as a component of human variation. J Physiol Anthropol. 2007;26(2):253-6.
32. Jeyashree T, Sangeetha S, Premavathy D. Quantitative and qualitative morphometry of hip bone for determining sex. Drug Invent Today. 2019;11(10):2590-2.
33. Ubelaker DH, Volk CG. A Test of the Phenice Method for the Estimation of Sex. J Forensic Sci. 2002;47(1):19-24.
34. Kenyhercz MW, Klales AR, Stull KE, McCormick KA, Cole SJ. Worldwide population variation in pelvic sexual dimorphism: A validation and recalibration of the Klales et al. method. Forensic Sci Int. 2017;277:259.e1-259.e8.
35. Antony M, Mohanraj KG. Sex determination using geometric dimensions of greater sciatic notch and subpubic angle of human pelvic bone: A morphometric study. Drug Invent Today. 2019;12(10):2199-202.
36. Oikonomopoulou EK, Valakos E, Nikita E. Population-specificity of sexual dimorphism in cranial and pelvic traits: evaluation of existing and proposal of new functions for sex assessment in a Greek assemblage. Int J Legal Med. 2017;131(6):1731-8.
37. James MacAluso P. Sex determination from the acetabulum: Test of a possible non-population-specific discriminant function equation. J Forensic Leg Med. 2010;17(6):348-51.
38. Mary DJ, Mohanraj KG. Morphometric analysis of acetabulum and pubis of pelvic bone using acetabulopubic index. Drug Invent Today. 2019;12(10):2206-8.
39. Kanabur V. Identification of the sex of human hip bone by metric analysis of its anterior border. Biomed Res. 2012;23(2):211-214.
40. Brůžek J, Santos F, Dutailly B, Murail P, Cunha E. Validation and reliability of the sex estimation of the human os coxae using freely available DSP2 software for bioarchaeology and forensic anthropology. Am J Phys Anthropol. 2017;164(2):440-449.
41. Akshaya K, Mohanraj KG. Sex determination using the distance between posterior inferior iliac spine and ischial spine in dry human innominate bone. Drug Invent Today. 2019;11(9):2246-2249.

Ocular Manifestations in Rheumatoid Arthritis

Sutasinee Boonsopon, M.D.*, Swetha Dhanireddy, M.D., Ambika Manhapra, BA.**,***, C. Stephen Foster, M.D.**,***,****

**Department of Ophthalmology, Faculty of Medicine Siriraj Hospital, Mahidol University, Bangkok 10700, Thailand, **Massachusetts Eye Research and Surgery Institution, Waltham, MA, USA, ***Ocular Immunology and Uveitis Foundation, Waltham, MA, USA, ****Harvard Medical School, Department of Ophthalmology, Boston, MA, USA.*

ABSTRACT

Rheumatoid arthritis (RA) is an inflammatory rheumatic disease that generally damages synovial-line joints. Extra-articular manifestations of RA have been reported in cases of multiorgan involvement. These manifestations can occur in the hematologic and cardiovascular system, lungs, kidneys, and eyes. Various ocular manifestations of RA have been previously reported including keratoconjunctivitis sicca, conjunctivitis, uveitis, scleritis, retinal vascular occlusion, optic neuritis, and amaurosis fugax. It is important to recognize these ocular issues as manifestations of RA since they can sometimes be a response marker for the onset of an immune reactivation. Urgent management of ocular complications is essential to manage sight-threatening complications and prevent further damage to the eyes.

Keywords: Rheumatoid arthritis; connective tissue disease; autoimmune disease; ocular manifestations; eye involvement (Siriraj Med J 2022; 74: 340-349)

List of abbreviations

AION; anterior ischemic optic neuropathy
C; complement
CCP; cyclic citrullinated peptide
CD; cluster of differentiation
DMARDs; disease-modifying antirheumatic drugs
FDA; Food and Drug Administration
HLA; human leukocyte antigen
Ig; immunoglobulin
IL; interleukin
JIA; juvenile idiopathic arthritis
KCS; keratoconjunctivitis sicca
MMP; matrix metalloproteinases
MTX; methotrexate
NSAIDs; non-steroidal anti-inflammatory drugs
PUK; peripheral ulcerative keratitis
RA; rheumatoid arthritis
RF; rheumatoid factor
SMIs; small molecule inhibitors
SS; Sjögren's syndrome
TNF-α; tumor necrosis factor-alpha

Corresponding author: C. Stephen Foster
E-mail: sfoster@mersi.com
Received 27 January 2021 Revised 6 March 2022 Accepted 11 March 2022
ORCID ID: https://orcid.org/0000-0002-6612-5653
http://dx.doi.org/10.33192/Smj.2022.41

Rheumatoid arthritis (RA)

Introduction of ocular manifestation of rheumatoid arthritis

Origin/history of the ocular manifestation of rheumatoid arthritis

Rheumatoid arthritis (RA) is a chronic progressive autoimmune disease characterized by polyarticular synovitis. Ocular complications, which are caused by inflammatory mediators such as immune complex depositions and upregulation of pro-inflammatory cytokines such as tumor necrosis factor-α (TNF-α) and interleukin (IL) 6, are commonly associated with dry eye, peripheral ulcerative keratitis (PUK), and scleritis.[1-3]

Epidemiology

RA is reported to be the most common systemic autoimmune disease. It affects roughly 1% of the general population.[4] Previously, extra-articular manifestations of RA were believed to occur in the late stages of the disease, following joint inflammation[5], but we now know that extra-articular complications can present at any stage of the disease.[3] Extra-articular manifestations often present as hematologic and cardiovascular complications, while ocular complications are less common.[3]

Pathophysiology

TNF-α, IL-1, and IL-6, as proinflammatory cytokines, are believed to be involved in the inflammatory pathway.[3] Prada J et al. investigated specific gene probes for TNF-α and IL-6 from paraffin corneal sections from seven patients who had corneal ulcerations/perforations with RA. The results revealed TNF-α expression in 71% and IL-6 expression in 100% of the analysed tissue samples.[6] Unfortunately, there was no control group in their study. The authors concluded that collagenolytic corneal damage was caused by the production of metalloproteinases as a result of the upregulation of the proinflammatory cytokines. RA patients who presented with necrotizing scleritis and/or PUK were involved in one of our studies. Conjunctival and/or scleral biopsy samples revealed microangiopathy with fibrinoid necrosis, vessel invasion by neutrophils, and/or vascular immunodeposits with immunoglobulin (Ig) A, IgG, IgM, complement (C) 3 and C4 in all patients with PUK and in 83% of patients with necrotizing scleritis.[7] Moreover, RA patients who experienced dry eye were found to have high levels of IL-17 in their tears.[8] A prospective case-control study among 72 RA patients revealed that there was no correlation between joint activity and the severity of keratoconjunctivitis sicca (KCS) symptoms.[9]

Ocular manifestation of RA (Table 1)

Definition/criteria for diagnosis

Secondary Sjögren's syndrome (SS) and KCS

RA is one of the most common autoimmune disorders associated with KCS.[10] Lymphocytic infiltration and destruction of acini in the lacrimal glands results in secondary SS.[10] This lymphocyte infiltration from pathological sections of lacrimal glands obtained from patients with primary SS and secondary SS cannot be distinguished. The severity of dry eye symptoms and corneal fluorescein dye staining were similar in both primary SS and secondary SS. These features suggest autoimmune mechanisms as a cause of dry eye, which is fairly common in many systemic autoimmune diseases.[10]

Pathophysiology

Lymphocyte and plasma cell infiltration is generally found in the tubuloacinar glands of lacrimal gland lobules.[11-13]

Symptoms and signs

The most common clinical presentation of secondary SS is dry eye. In addition, patients may also experience redness, light sensitivity, ocular burning sensation, foreign body sensation, and painful superficial keratitis. Punctate erosion, which can be detected through fluorescein, rose bengal, or lissamine green staining, is also common. Moreover, some patients can present with visual deficiencies, corneal epitheliopathy, filament keratopathy, and plaque formation. Diagnosis of secondary SS can also be confirmed through objective measures such as a decrease in lacrimal secretion (hyposecretion) through Schirmer's test and a decrease in lacrimal stability, measured by a decrease in tear break-up time.[14,15]

Episcleritis

Episcleritis is the inflammation of episcleral tissue over the sclera. The frequency of episcleritis in RA patients was reported to be 0.17-3.7%.[16]

Pathophysiology

Increased inflammation associated with RA can lead to the infiltration of white blood cells to the episcleral tissue and result in episcleritis. This causes the anterior ciliary arteries to become congested and more prominent. In addition, the dysregulation of levels of cytokines such as transforming growth factor b in tear fluid and the subsequent loss in tear integrity are believed to be related to episcleritis.[14]

TABLE 1. Comparison of mean number of decayed teeth by CFUs within groups.

Ocular manifestations	Frequency among RA individuals	References
Keratoconjunctivitis sicca	18-90%	14
Episcleritis	1-5%	14
Scleritis	1-6%	14
Anterior uveitis	14-42%	14
Peripheral ulcerative keratitis	1-2%	44
Retinal vasculitis	18% (subclinical)	36
Choroiditis	rare	
Optic neuropathy	rare	

Abbreviations: RA; rheumatoid arthritis

Symptoms and signs

Episcleritis patients generally present with red eyes as a result of vasodilation of superficial radial episcleral vessels, which can be sectoral, diffuse, or nodular. Bilateral involvement was found in 40% of episcleritis cases.[16] The disease itself is painless and visual loss has not been reported. In order to differentiate between episcleritis and scleritis, 10% phenylephrine drops can be instilled to assess if the characteristic constricting and blanching of episcleral vessels associated with episcleritis occurs.[14]

Scleritis

The most common systemic association with scleritis that has been reported is RA.[17,18] About one-fifth to one-fourth of patients with scleritis have RA and conversely, 0.2-6.3% of RA patients suffer from scleritis.[19] Most RA patients develop articular manifestations preceding the onset of scleritis. Necrotizing scleritis, which is the most severe form of scleritis, is caused by vascular occlusion of the affected area, shown in Fig 1. Associated uveitis and peripheral ulcerative keratitis may be associated with scleral inflammation. Complicated cataract and secondary glaucoma are frequently found in patients with scleritis, especially in those patients with severely inflamed eyes.[17] On the other hand, patients can also develop anterior scleritis without inflammation, known as scleromalacia perforans (Fig 2). Thinning of the sclera and visible uveal tissue gradually develops as a late complication of the inflammatory processes; however spontaneous perforation is rare. Posterior scleritis can also be associated with RA. In these cases, subretinal fluid, macular edema, papillitis,

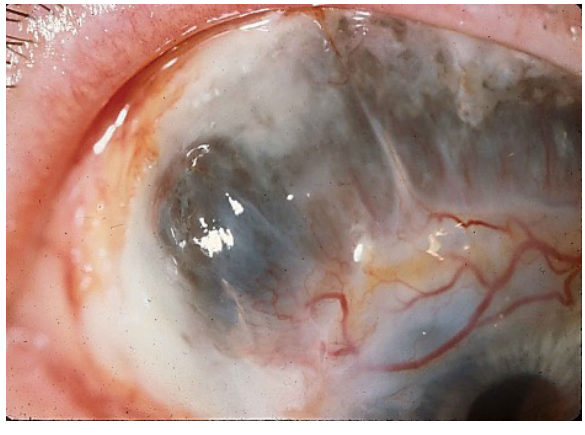

Fig 1. Necrotizing scleritis with associated peripheral ulcerative keratitis in rheumatoid arthritis patient.

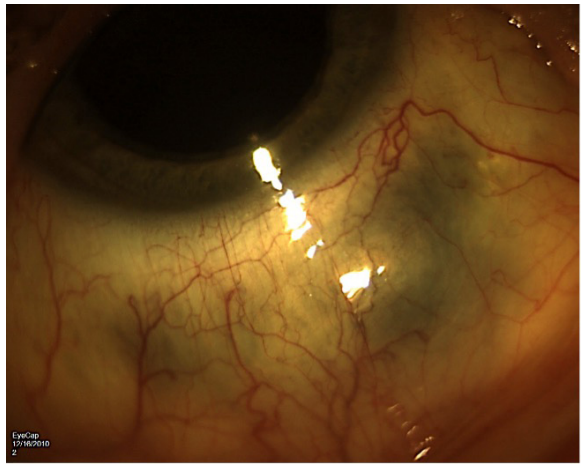

Fig 2. Scleral thinning with exposure of the choroid covered by healthy conjunctiva without inflammation, which is also known as scleromalacia perforans.

or uveal inflammation can result in the deterioration of vision (Fig 3). RA-associated scleritis is typically classified as a condition of intermediate severity.[20]

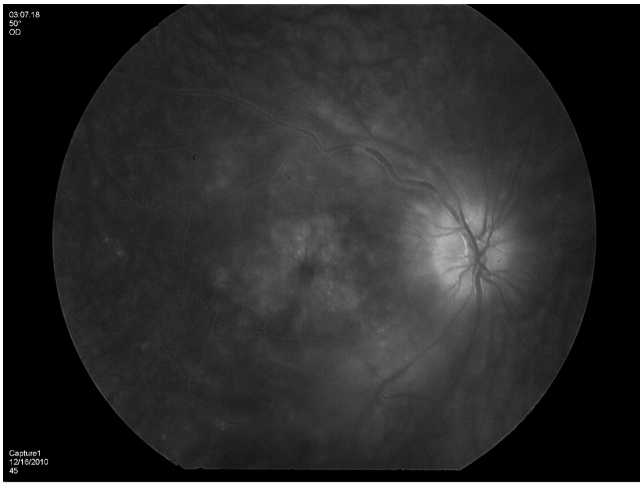

Fig 3. Fundus fluorescein angiogram of rheumatoid arthritis patient who had posterior uveitis with papillitis, retinal vasculitis and cystoid macular edema in the right eye.

Pathophysiology

Histopathological examination of scleral tissue of patients with scleritis has shown fibrinoid necrosis and vascular infiltration, specifically infiltration of macrophages and T-lymphocytes. These findings are similar to what is found in patients with occlusive retinal vasculitis.[21,22] Furthermore, collagenase matrix metalloproteinase-3 (MMP-3), MMP-8, and MMP-9 are speculated to be responsible for collagen breakdown, in combination with the imbalance of MMP and tissue inhibitors of MMPs.[14,23]

Symptoms and signs

Severe eye pain is the main symptom of scleritis. Bilateral involvement was found in half of cases.[24] Redness (deep violaceous hue) with scleral edema and dilation of the superficial and deep episcleral vascular plexuses are important signs of scleritis. Tearing, photophobia, and decreased visual acuity can also be found.[14]

Classification regarding anatomical location

The location of inflammation compared to the insertion of the rectus muscles is used to classify scleritis to either anterior scleritis and posterior scleritis. Anterior scleritis is more commonly found compared to posterior scleritis.[15,16] The diagnosis of posterior scleritis is more challenging. Ocular examination in the early stages of inflammation may sometimes show no abnormalities, while more severe cases may reveal optic disc swelling, retinal fold, retinal exudates, subretinal fluid and macular edema.[15] Ocular pain is an important feature that should alert the physician to assess if scleritis is present. Blurred vision is commonly associated with scleritis, as a result of refractive shift from thickened posterior sclera or from the inflammatory processes itself. Patients may experience metamorphopsia from macular fold and macular edema.[25] B-scan ultrasonography is the most useful diagnostic tool, which confirms the diagnosis of posterior scleritis by showing scleral thickening and demonstrating any scleral nodules, if present.[26] (Fig 4)

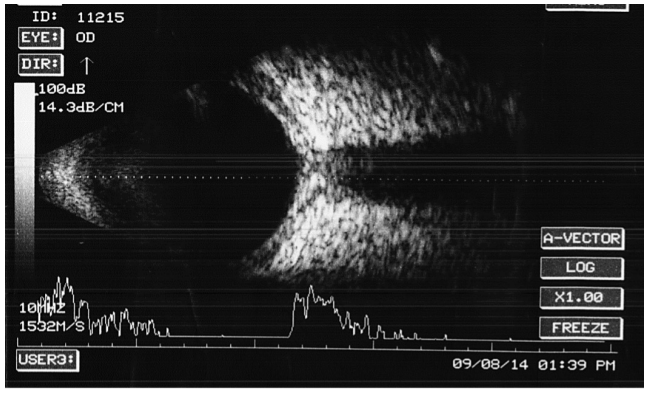

Fig 4. B-scan ultrasonography of the right eye shows chorioretinal thickening with classicT-sign, which represent subtenon fluid in patient with posterior scleritis.

Classification regarding the pattern of scleral inflammation

Scleritis can be classified into diffuse scleritis, nodular scleritis and necrotizing scleritis with or without inflammation. Diffuse anterior scleritis is the most common type of RA associated scleritis, followed by nodular anterior, necrotizing, and posterior scleritis.[27] Diffuse scleritis is more benign than other types of scleral inflammation.[28] Necrotizing scleritis with inflammation is a type of inflammation that increases the probability of other ocular complications such as marginal keratitis, anterior uveitis, and secondary ocular hypertension, and disease associations include connective tissue diseases and vasculitic diseases with infectious diseases, rosacea, and foreign body.[16] Scleromalacia perforans is characterized by the bluish-grey hue of the sclera without any sign of inflammation. It was believed to be a result of scleral thinning.[25]

Peripheral ulcerative keratitis

PUK is relatively common in patients with connective tissue diseases, especially among RA patients.[17] PUK can lead to corneal melt syndrome and ocular perforation, and may be associated with scleritis.[17] Corneal perforation is the most severe ocular complication in RA patients.[24] We

reported the mortality rate of RA patients' concurrence with PUK and/or necrotizing scleritis was approximately 50% at 10 years without immunosuppressive medication. The major cause of death in that study was rheumatoid vasculitis.[29] When PUK is found in RA patients, urgent multidisciplinary management is required.[24]

Pathophysiology

Both cellular and humoral immunity are involved in the inflammation process. T- and B-lymphocytes play an important role in increasing antibody production and immune-complex deposition around the peripheral cornea.[30,31] Inflammatory cells, specifically neutrophils and macrophages, are recruited to the cornea by C activation.[24] Collagenases and other proteases, secreted from those inflammatory cells, cause corneal melting and eventually perforation.[32] Abnormal MMP-2 production and the presence of MMP-9[33,34], and possibly other MMPs have been thought to be related to PUK progression.

Symptoms and signs

Symptoms and signs of PUK include ocular pain and redness, photophobia, tearing, visual deterioration from corneal astigmatism or corneal opacity, peripheral corneal thinning, and ulceration[15] (Fig 5).

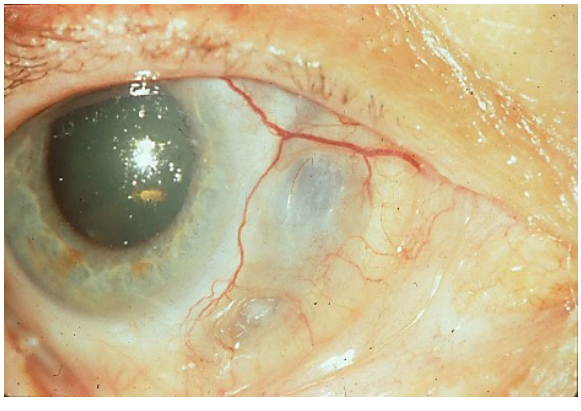

Fig 5. Anterior segment photograph showing an extensive area of peripheral corneal thinning with abnormal feeding vessel in a patient with peripheral ulcerative keratitis associated with rheumatoid arthritis.

Retinal vasculitis

Retinal vasculitis, which describes inflammation of retinal blood vessels can result in poor visual outcome[35] and is associated with several connective tissue diseases, including RA.[36]

Pathophysiology

Rheumatoid vasculitis is believed to be related to longstanding rheumatoid factor (RF) positive cases.[37] Circulating immune complex, co-stimulatory molecule (CD28) on naive T cells, and proinflammatory cytokines are involved in the inflammatory processes.[38] Intraocular inflammation, more specifically retinal vasculitis (despite its rare presentation), PUK and necrotizing scleritis, is considered as a clinical manifestation of rheumatoid vasculitis.[36,39]

Symptoms and signs

Most RA patients with retinal vasculitis are asymptomatic and show no clinical signs of retinal vasculitis. However subclinical retinal vasculitis with retinal vascular leakage on fundus fluorescein angiogram has been reported in 18% of RA patients.[40]

Optic neuritis and anterior ischemic optic neuropathy (AION)

Optic neuritis and AION occur at a lower frequency compared to PUK, corneal melt, and scleritis.[10] Optic disc swelling can occur secondary to posterior scleritis.[17]

Risk factors

Predisposing genetic factors such as the human leukocyte antigen (HLA)-DR4 allele, and inappropriate immune mechanisms leading to immune complex deposition and microvasculitis in the joint play a pivotal role in the pathogenesis and joint destruction of RA.[7] High titers of RF, circulating immune complexes, cryoglobulinemia and hypocomplementemia are strongly associated with rheumatoid systemic vasculitis.[41] These laboratory parameters also have been abnormal in a high percentage of patients with RA who developed necrotizing scleritis and/or PUK, observed in our study.[7] Patients who were both anticyclic citrullinated peptide (anti-CCP) and RF positive tend to have more severe ocular disease.[42-44]

Treatment

Indications for treatment

Most RA patients have dry eye symptoms, which is generally mild to moderate in severity. Treatment for these patients comprise of lubricating eye drops, and in some instances, topical cyclosporine eye drops.[24] The use of autologous serum tear drops is typically reserved for more severe cases of dry eye.[45] Systemic medications such as doxycycline can inhibit MMP and induce T cell apoptosis, which is also useful in decreasing the inflammatory cascade associated with dry eye syndrome.[46,47] For the more severe cases of dry eye, such as dry eye with corneal epitheliopathy, scleritis, and PUK, the previously mentioned therapy is generally inadequate

to control the disease[10] (Fig 5). Almost every type of scleritis eventually requires systemic therapy such as non-steroidal anti-inflammatory drugs (NSAIDs) and corticosteroids.[28] Immunomodulatory therapy is indicated in PUK or scleritis patients who fail to respond to oral corticosteroid therapy. Therapy failure is defined as having persistent inflammation, disease progression, intolerability to corticosteroid side effects, or unable to taper prednisolone to physiologic doses.[27] The treatment modalities for ocular manifestations in RA is summarized in Table 2.

Medical treatment

Non-steroidal anti-inflammatory medications

Oral NSAIDs are considered useful in mild forms of scleritis.[25] They can be used as a first-line therapy for patients with non-necrotizing scleritis.[48] Necrotizing scleritis, which is the more severe form of scleritis, and posterior scleritis, where the inflammatory site located at the back of the eye, require systemic corticosteroid therapy, and eventually immunomodulatory therapy.[25]

Corticosteroids

Initial treatment that is effective at controlling active inflammation is high doses of systemic corticosteroids. For the more severe cases such as necrotizing scleritis or PUK with impending corneal perforation, methylprednisolone infusion is recommended. During maintenance therapy, slow taper of the medication is required. Relapsed inflammation can often occur during the tapering of medication.[25,49] Topical steroids can be used as an adjunctive treatment for scleritis with anterior uveitis.[25]

Immunosuppressant medications

About ¼ of scleritis patients require immunomodulatory therapy to control their inflammation.[19] In RA associated scleritis, the indication for immunosuppressants is broad.[7]

Antimetabolite

Methotrexate (MTX) has proved to be highly beneficial.[7] MTX has less potential toxicity compared to cytotoxic agents and is used as a first-line medication in the chemotherapeutic management of PUK and necrotizing scleritis in most patients with RA. Azathioprine is a second-line medication for chemotherapeutic management in RA.[7]

Calcineurin inhibitor

Cyclosporine is a second line drug, which may be successful in select cases.[31]

Cytotoxic agent

Chlorambucil has been used as a treatment option for RA, but its efficacy related to extra-articular manifestation is rarely reported. Cyclophosphamide has been the most effective, but[7] is associated with higher toxicity.

Biologic agents

Biologic agents are usually reserved for the treatment of RA that is refractory to conventional therapy. They have a favorable safety profile as compared to cytotoxic agents but their use must be closely monitored to avoid the reactivation of latent infections such as mycobacterium tuberculosis and to avoid the risk of opportunistic infections.[44,50]

TNF inhibitors

TNF inhibitors that are approved by the U.S. Food and Drug Administration (FDA) for the treatment of RA are etanercept (Enbrel®), infliximab (Remicade®), adalimumab (Humira®)[3], certolizumab pegol (Cimzia®) and golimumab (Simponi®).[51] TNF inhibitors can decrease inflammation and corneal destruction by decreasing the products of MMP, such as MMP-9, which halts the destruction of corneal epithelial basement membrane and the degradation of extracellular matrix of the corneal stroma.[34,52,53] MTX may have synergistic effects when combined with TNF inhibitors.[54] Etanercept and adalimumab were also reportedly successful in select cases.[55,56] Infliximab is the more favorable treatment option, especially in uveitis, because of its successful outcomes.[57,58] On the other hand, some reports suggested that etanercept may induce intractable scleritis or is ineffective in treating scleritis.[59,60] Certolizumab pegol, a newer TNF-α inhibitor, has been used to treat extra-articular manifestations of RA, but very few reports have been published on this medication.[61] This medication differs from the older TNF-α inhibitors in that it has a longer half-life with less toxicity.[62] The use of golimumab in several case reports and case series demonstrate successful control of recalcitrant uveitis associated with juvenile idiopathic arthritis (JIA), Adamantiades-Behçet's disease, idiopathic retinal vasculitis, spondyloarthropathies, and HLA-B27 positivity.[63-67]

IL-1 inhibitor

Anakinra (Kineret®) is approved by the FDA.[3] In scleritis, both TNF-α and IL-1 released by the local inflammatory cell infiltrate have been associated with scleral destruction.[68] An observation by C. Botsios et al. demonstrates the efficacy of anakinra in RA associated diffuse scleritis.[69]

TABLE 2. Treatment modalities for ocular complications in rheumatoid arthritis.

Medications	Route of administrations	Indications	Evidence
Artificial tears	ED	KCS	
Autologous serum	ED	KCS	
Topical cyclosporine	ED	KCS	
Doxycycline	Oral	KCS	
NSAIDs	ED/ oral	Episcleritis/ scleritis (mild form)	
Corticosteroids	ED/ oral/ IV	Episcleritis/ scleritis/ PUK/ uveitis	
Immunosuppressant			
Antimetabolite			
Methotrexate	Oral/ SC	Scleritis/ PUK/ uveitis	First line
Azathioprine	Oral	Scleritis/ PUK/ uveitis	Second line
Mycophenolate mofetil	Oral	Scleritis/ PUK/ uveitis	-
Calcineurin inhibitor			
Cyclosporine	Oral	Scleritis/ PUK/ uveitis	Second line
Cytotoxic agents			
Cyclophosphamide	Oral/ IV	Scleritis/ PUK/ uveitis	Recommended in severe and/ or refractory cases
Chlorambucil	Oral	Uveitis	-
Biologic agents			
TNF inhibitors			
Infliximab	IV	Scleritis/ PUK/ uveitis	RCT
Adalimumab	SC	Scleritis/ PUK/ uveitis	FDA-approved
Certolizumab pegol	SC	Uveitis	Case reports
Golimumab	SC	Uveitis	Case reports
Etanercept	SC	Not recommended (less effective)	Phase II/III
IL-inhibitors			
Anakinra	SC	Scleritis	Case reports
Tocilizumab	SC/ IV	Scleritis/ PUK/ uveitis	Case reports
Gevokizumab	SC	Scleritis	Phase I/II
B-cell depletion			
Rituximab	IV	Scleritis/ PUK/ uveitis	Phase I/II
Cytotoxic T-lymphocyte antigen 4			
Abatacept	SC/ IV	Scleritis/ uveitis	Case reports
Small molecules inhibitors			
Janus kinase			
Tofacitinib	Oral	Scleritis/ uveitis	Phase II
Baricitinib	Oral	Uveitis	Case reports
Filgotinib	Oral	NA	NA
Peficitinib	Oral	NA	NA
Decernotinib	Oral	NA	NA
Other new medications			
ACTH gel	SC	Scleritis	Phase II
Sirolimus	Subconjunctival	Scleritis	Case reports

Abbreviations: ED; eye drops, KCS; keratoconjunctivitis sicca, NSAIDs; non-steroidal anti-inflammatory drugs, IV; intravenous, PUK; peripheral ulcerative keratitis, SC; subcutaneous, TNF; tumor necrosis factor, RCT; randomized controlled trial, FDA; food and drug administration, IL; interleukin, NA; not applicable, ACTH; adrenocorticotropic hormone

IL-6 inhibitor

Tocilizumab (Actemraâ) is approved for the treatment of RA and JIA.[70] Successful suppression of PUK in RA patient with tocilizumab has been reported.[71]

B-cell depletion

Rituximab (Rituxanâ) is a chimeric monoclonal antibody against cluster of differentiation (CD) 20 aimed at depleting B cells. It is reported as a successful treatment for many connective tissue diseases, including RA. T-cell activation in scleritis and PUK might be associated with the existence of B lymphocytes surrounding blood vessels, resulting in immediate action of rituximab.[72,73]

Cytotoxic T-lymphocyte antigen 4 (CTLA 4)

Abatacept (Orenciaâ) is a recent yet widely utilized therapeutic option in RA.[74] Its efficacy to treat extra-articular manifestations is under investigation. One patient developed PUK while on abatacept, and the treatment was switched to tofacitinib citrate (Xeljanzâ) combined with corneal gluing within one week, which led to a successful treatment of the PUK.[75] Several reports demonstrated its efficacy to control or improve refractory JIA related uveitis.[76-79]

Surgical treatment

Surgical indication for scleritis and PUK is corneoscleral melting with impending perforation or perforation, both of which require immediate surgical intervention. Surgery can also be used as an adjunctive treatment to decrease or halt the progression of active inflammation in some instances.[25] Surgical interventions include cyanoacrylate adhesive, tectonic corneal graft, conjunctival flap, and scleral grafting. Conjunctival resection may also be done to enhance the healing process of PUK by decreasing the number of inflammatory cells and cytokines surrounding the cornea and thus, promoting corneal epithelialization.[7,80] A combination treatment of immunomodulatory medication and adjuvant surgical intervention can generally preserve the eyeball in most of the RA patients, but visual outcome is sometimes unsatisfied.[7]

Future direction

Recently, there has been development of small molecule inhibitors (SMIs) for RA as a new generation of targeted synthetic disease-modifying antirheumatic drugs (DMARDs). These medications can block pro-inflammatory pathways such as Janus kinase, mitogen-activated protein kinase, and spleen tyrosine kinase.[81] The therapeutic treatment of SMIs for ocular manifestations related to RA is yet to be investigated.[44]

ACKNOWLEDGEMENTS

None

Funding disclosure

This was an unfunded study.

Conflict of interest

S Boonsopon, S Dhanireddy and A Manhapra report no conflict of interest. C. Stephen Foster reports no conflict of interest, but declares consultancies with Aldeyra Therapeutics, Allakos, Bausch & Lomb Surgical, Inc, Eyegate Pharma, Genentech, Novartis, pSivida; grants or grants pending with Aciont, Alcon, Aldeyra Therapeutics, Bausch & Lomb, Clearside Biomedica, Dompé pharmaceutical, Eyegate Pharma, Mallinckrodt pharmaceuticals, Novartis Pharmaceuticals, pSivida, Santen; payment for lectures including service on speaking bureaus: Alcon, Allergan, Mallinckrodt pharmaceuticals; stock or stock options: Eyegate Pharma.

REFERENCES

1. Harper SL, Foster CS. The ocular manifestations of rheumatoid disease. Int Ophthalmol Clin. 1998;38(1):1-19.
2. Thomas DC, Kohli D, Chen N, Peleg H, Almoznino G. Orofacial manifestations of rheumatoid arthritis and systemic lupus erythematosus: a narrative review. Quintessence Int. 2021;52(5):454-66.
3. Moreland LW, Curtis JR. Systemic nonarticular manifestations of rheumatoid arthritis: focus on inflammatory mechanisms. Semin Arthritis Rheum. 2009;39(2):132-43.
4. Widdifield J, Paterson JM, Bernatsky S, Tu K, Tomlinson G, Kuriya B, et al. The epidemiology of rheumatoid arthritis in Ontario, Canada. Arthritis Rheumatol. 2014;66(4):786-93.
5. Feldmann M, Brennan FM, Maini RN. Rheumatoid arthritis. Cell. 1996;85(3):307-10.
6. Prada J, Noelle B, Baatz H, Hartmann C, Pleyer U. Tumour necrosis factor alpha and interleukin 6 gene expression in keratocytes from patients with rheumatoid corneal ulcerations. Br J Ophthalmol. 2003;87(5):548-50.
7. Messmer EM, Foster CS. Destructive corneal and scleral disease associated with rheumatoid arthritis. Medical and surgical management. Cornea. 1995;14(4):408-17.
8. Kang MH, Kim MK, Lee HJ, Lee HI, Wee WR, Lee JH. Interleukin-17 in various ocular surface inflammatory diseases. J Korean Med Sci. 2011;26(7):938-44.
9. Fujita M, Igarashi T, Kurai T, Sakane M, Yoshino S, Takahashi H. Correlation between dry eye and rheumatoid arthritis activity. Am J Ophthalmol. 2005;140(5):808-13.
10. Tong L, Thumboo J, Tan YK, Wong TY, Albani S. The eye: a window of opportunity in rheumatoid arthritis? Nat Rev Rheumatol. 2014;10(9):552-60.
11. Pepose JS, Akata RF, Pflugfelder SC, Voigt W. Mononuclear cell phenotypes and immunoglobulin gene rearrangements in lacrimal gland biopsies from patients with Sjogren's syndrome. Ophthalmology. 1990;97(12):1599-605.
12. Fox RI. Sjogren's syndrome: evolving therapies. Expert Opin Investig Drugs. 2003;12(2):247-54.

13. Usuba FS, de Medeiros-Ribeiro AC, Novaes P, Aikawa NE, Bonfiglioli K, Santo RM, et al. Dry eye in rheumatoid arthritis patients under TNF-inhibitors: conjunctival goblet cell as an early ocular biomarker. Sci Rep. 2020;10(1):14054.
14. Bhamra MS, Gondal I, Amarnani A, Betesh S, Zhyvotovska A, Scott W, et al. Ocular Manifestations of Rheumatoid Arthritis: Implications of Recent Clinical Trials. Int J Clin Res Trials. 2019;4(2).
15. Murray PI, Rauz S. The eye and inflammatory rheumatic diseases: The eye and rheumatoid arthritis, ankylosing spondylitis, psoriatic arthritis. Best Pract Res Clin Rheumatol. 2016;30(5):802-25.
16. Sainz de la Maza M, Molina N, Gonzalez-Gonzalez LA, Doctor PP, Tauber J, Foster CS. Clinical characteristics of a large cohort of patients with scleritis and episcleritis. Ophthalmology. 2012;119(1):43-50.
17. Young S. Ocular involvement in connective tissue disorders. Curr Allergy Asthma Rep. 2005;5(4):323-6.
18. Boonsopon S, Choopong P, Wongwijitsook W, Sopitviriyaporn W, Tesavibul N. Non-Infectious Scleritis and Systemic Collagen Vascular Disease Association. Siriraj Med J. 2020;72(4):352-60.
19. Smith JR, Mackensen F, Rosenbaum JT. Therapy insight: scleritis and its relationship to systemic autoimmune disease. Nat Clin Pract Rheumatol. 2007;3(4):219-26.
20. Sainz de la Maza M, Foster CS, Jabbur NS. Scleritis associated with systemic vasculitic diseases. Ophthalmology. 1995;102(4):687-92.
21. Fong LP, Sainz de la Maza M, Rice BA, Kupferman AE, Foster CS. Immunopathology of scleritis. Ophthalmology. 1991;98(4):472-9.
22. Bernauer W, Watson PG, Daicker B, Lightman S. Cells perpetuating the inflammatory response in scleritis. Br J Ophthalmol. 1994;78(5):381-5.
23. Di Girolamo N, Lloyd A, McCluskey P, Filipic M, Wakefield D. Increased expression of matrix metalloproteinases in vivo in scleritis tissue and in vitro in cultured human scleral fibroblasts. Am J Pathol. 1997;150(2):653-66.
24. Artifoni M, Rothschild PR, Brezin A, Guillevin L, Puechal X. Ocular inflammatory diseases associated with rheumatoid arthritis. Nat Rev Rheumatol. 2014;10(2):108-16.
25. Sims J. Scleritis: presentations, disease associations and management. Postgrad Med J . 2012;88(1046):713-8.
26. McCluskey PJ, Watson PG, Lightman S, Haybittle J, Restori M, Branley M. Posterior scleritis: clinical features, systemic associations, and outcome in a large series of patients. Ophthalmology. 1999;106(12):2380-6.
27. Jabs DA, Mudun A, Dunn JP, Marsh MJ. Episcleritis and scleritis: clinical features and treatment results. Am J Ophthalmol. 2000;130(4):469-76.
28. Sainz de la Maza M, Molina N, Gonzalez-Gonzalez LA, Doctor PP, Tauber J, Foster CS. Scleritis therapy. Ophthalmology. 2012;119(1):51-8.
29. Foster CS, Forstot SL, Wilson LA. Mortality rate in rheumatoid arthritis patients developing necrotizing scleritis or peripheral ulcerative keratitis. Effects of systemic immunosuppression. Ophthalmology. 1984;91(10):1253-63.
30. Murray PI, Rahi AH. Pathogenesis of Mooren's ulcer: some new concepts. Br J Ophthalmol. 1984;68(3):182-7.
31. Messmer EM, Foster CS. Vasculitic peripheral ulcerative keratitis. Surv Ophthalmol. 1999;43(5):379-96.
32. Riley GP, Harrall RL, Watson PG, Cawston TE, Hazleman BL. Collagenase (MMP-1) and TIMP-1 in destructive corneal disease associated with rheumatoid arthritis. Eye. 1995;9 (Pt 6):703-18.
33. Smith VA, Rishmawi H, Hussein H, Easty DL. Tear film MMP accumulation and corneal disease. Br J Ophthalmol. 2001;85(2):147-53.
34. Smith VA, Hoh HB, Easty DL. Role of ocular matrix metalloproteinases in peripheral ulcerative keratitis. Br J Ophthalmol. 1999;83(12):1376-83.
35. Boonsopon S, Anesi S. Retinal Vasculitis: Fundamentals, Diagnostics, and Management. Siriraj Med J. 2021;73:493-500.
36. Androudi S, Dastiridou A, Symeonidis C, Kump L, Praidou A, Brazitikos P, et al. Retinal vasculitis in rheumatic diseases: an unseen burden. Clin Rheumatol. 2013;32(1):7-13.
37. Wilkinson M, Torrance WN. Clinical background of rheumatoid vascular disease. Ann Rheum Dis. 1967;26(6):475-80.
38. Turesson C, Matteson EL. Vasculitis in rheumatoid arthritis. Curr Opin Rheumatol. 2009;21(1):35-40.
39. Matsuo T, Masuda I, Matsuo N. Geographic choroiditis and retinal vasculitis in rheumatoid arthritis. Jpn J Ophthalmol. 1998;42(1):51-5.
40. Giordano N, D'Ettorre M, Biasi G, Fioravanti A, Moretti L, Marcolongo R. Retinal vasculitis in rheumatoid arthritis: an angiographic study. Clin Exp Rheumatol. 1990;8(2):121-5.
41. Vollertsen RS, Conn DL, Ballard DJ, Ilstrup DM, Kazmar RE, Silverfield JC. Rheumatoid vasculitis: survival and associated risk factors. Medicine. 1986;65(6):365-75.
42. Itty S, Pulido JS, Bakri SJ, Baratz KH, Matteson EL, Hodge DO. Anti-cyclic citrullinated peptide, rheumatoid factor, and ocular symptoms typical of rheumatoid arthritis. Trans Am Ophthalmol Soc. 2008;106:75-81; discussion 81-3.
43. Vignesh AP, Srinivasan R. Ocular manifestations of rheumatoid arthritis and their correlation with anti-cyclic citrullinated peptide antibodies. Clin Ophthalmol. 2015;9:393-7.
44. Promelle V, Goeb V, Gueudry J. Rheumatoid Arthritis Associated Episcleritis and Scleritis: An Update on Treatment Perspectives. J Clin Med. 2021;10(10).
45. Petznick A, Tong L, Chung R, Wang JC, Koh M, Salleh R, et al. Autologous plasma eyedrops prepared in a closed system: a treatment for dry eye. Eye. 2013;27(9):1102.
46. Dogru M, Tsubota K. Pharmacotherapy of dry eye. Expert Opin Oharmacother. 2011;12(3):325-34.
47. Liu J, Kuszynski CA, Baxter BT. Doxycycline induces Fas/Fas ligand-mediated apoptosis in Jurkat T lymphocytes. Biochem Biophys Res Commun. 1999;260(2):562-7.
48. Watson PG. The diagnosis and management of scleritis. Ophthalmology. 1980;87(7):716-20.
49. Okhravi N, Odufuwa B, McCluskey P, Lightman S. Scleritis. Surv Ophthalmol. 2005;50(4):351-63.
50. Gomez-Reino JJ, Carmona L, Valverde VR, Mola EM, Montero MD, Group B. Treatment of rheumatoid arthritis with tumor necrosis factor inhibitors may predispose to significant increase in tuberculosis risk: a multicenter active-surveillance report. Arthritis Rheum. 2003;48(8):2122-7.
51. Jinesh S. Pharmaceutical aspects of anti-inflammatory TNF-blocking drugs. Inflammopharmacology. 2015;23(2-3):71-7.
52. St Clair EW. Infliximab treatment for rheumatic disease: clinical and radiological efficacy. Ann Rheum Dis. 2002;61(Suppl 2):ii67-9.

53. Li DQ, Lokeshwar BL, Solomon A, Monroy D, Ji Z, Pflugfelder SC. Regulation of MMP-9 production by human corneal epithelial cells. Exp Eye Res. 2001;73(4):449-59.
54. Fox DA. Cytokine blockade as a new strategy to treat rheumatoid arthritis: inhibition of tumor necrosis factor. Arch Intern Med. 2000;160(4):437-44.
55. Ashok D, Ayliffe WH, Kiely PD. Necrotizing scleritis associated with rheumatoid arthritis: long-term remission with high-dose infliximab therapy. Rheumatology. 2005;44(7):950-1.
56. Hernandez-Illas M, Tozman E, Fulcher SF, Jundt JW, Davis J, Pflugfelder SC. Recombinant human tumor necrosis factor receptor Fc fusion protein (Etanercept): experience as a therapy for sight-threatening scleritis and sterile corneal ulceration. Eye Contact Lens. 2004;30(1):2-5.
57. Theodossiadis PG, Markomichelakis NN, Sfikakis PP. Tumor necrosis factor antagonists: preliminary evidence for an emerging approach in the treatment of ocular inflammation. Retina. 2007;27(4):399-413.
58. Galor A, Perez VL, Hammel JP, Lowder CY. Differential effectiveness of etanercept and infliximab in the treatment of ocular inflammation. Ophthalmology. 2006;113(12):2317-23.
59. Sassa Y, Kawano Y, Yamana T, Mashima T, Ishibashi T. A change in treatment from etanercept to infliximab was effective to control scleritis in a patient with rheumatoid arthritis. Acta Ophthalmol. 2012;90(2):e161-2.
60. Smith JR, Levinson RD, Holland GN, Jabs DA, Robinson MR, Whitcup SM, et al. Differential efficacy of tumor necrosis factor inhibition in the management of inflammatory eye disease and associated rheumatic disease. Arthritis Rheum. 2001;45(3):252-7.
61. Tlucek PS, Stone DU. Certolizumab pegol therapy for rheumatoid arthritis-associated scleritis. Cornea. 2012;31(1):90-1.
62. Nesbitt A, Fossati G, Bergin M, Stephens P, Stephens S, Foulkes R, et al. Mechanism of action of certolizumab pegol (CDP870): in vitro comparison with other anti-tumor necrosis factor alpha agents. Inflamm Bowel Dis. 2007;13(11):1323-32.
63. Cordero-Coma M, Salom D, Diaz-Llopis M, Lopez-Prats MJ, Calleja S. Golimumab for uveitis. Ophthalmology. 2011;118(9):1892 e3-4.
64. William M, Faez S, Papaliodis GN, Lobo AM. Golimumab for the treatment of refractory juvenile idiopathic arthritis-associated uveitis. J Ophthalmic Inflamm Infect. 2012;2(4):231-3.
65. Miserocchi E, Modorati G, Pontikaki I, Meroni P, Gerloni V. Golimumab treatment for complicated uveitis. Clin Exp Rheumatol. 2013;31(2):320-1.
66. Mesquida M, Victoria Hernandez M, Llorenc V, Pelegrin L, Espinosa G, Dick AD, et al. Behcet disease-associated uveitis successfully treated with golimumab. Ocul Immunol Inflamm. 2013;21(2):160-2.
67. Faez S, Lobo AM, Sobrin L, Papaliodis GN. Treatment of seronegative spondyloarthropathy-associated uveitis with golimumab: retrospective case series. Clin Exp Ophthalmol. 2014;42(4):392-5.
68. Wakefield D, Lloyd A. The role of cytokines in the pathogenesis of inflammatory eye disease. Cytokine. 1992;4(1):1-5.
69. Botsios C, Sfriso P, Ostuni PA, Todesco S, Punzi L. Efficacy of the IL-1 receptor antagonist, anakinra, for the treatment of diffuse anterior scleritis in rheumatoid arthritis. Report of two cases. Rheumatology (Oxford). 2007;46(6):1042-3.
70. Pasadhika S, Rosenbaum JT. Update on the use of systemic biologic agents in the treatment of noninfectious uveitis. Biologics. 2014;8:67-81.
71. Wendling D, Dernis E, Prati C, Frisch E, Delbosc B. Onset of inflammatory eye disease under tocilizumab treatment for rheumatologic conditions: a paradoxical effect? J Rheumatol. 2011;38(10):2284.
72. Iaccheri B, Androudi S, Bocci EB, Gerli R, Cagini C, Fiore T. Rituximab treatment for persistent scleritis associated with rheumatoid arthritis. Ocul Immunol Inflamm. 2010;18(3):223-5.
73. Bonnet I, Rousseau A, Duraffour P, Pouchot J, Nguyen CD, Gabison E, et al. Efficacy and safety of rituximab in peripheral ulcerative keratitis associated with rheumatoid arthritis. RMD Open. 2021;7(1):e001472.
74. Selmi C, Generali E, Massarotti M, Bianchi G, Scire CA. New treatments for inflammatory rheumatic disease. Immunol Res. 2014;60(2-3):277-88.
75. Meadow PB, Nguyen J, Kesavarapu K. Tofacitinib citrate for ulcerative keratitis in a patient with rheumatoid arthritis. Case reports in rheumatology. 2014;2014:403452.
76. Angeles-Han S, Flynn T, Lehman T. Abatacept for refractory juvenile idiopathic arthritis-associated uveitis- a case report. J Rheumatol. 2008;35(9):1897-8.
77. Zulian F, Balzarin M, Falcini F, Martini G, Alessio M, Cimaz R, et al. Abatacept for severe anti-tumor necrosis factor alpha refractory juvenile idiopathic arthritis-related uveitis. Arthritis Care Res. 2010;62(6):821-5.
78. Elhai M, Deslandre CJ, Kahan A. Abatacept for refractory juvenile idiopathic arthritis-associated uveitis: two new cases. Comment on the article by Zulian et al. Arthritis Care Res. 2011;63(2):307-8; author reply 308.
79. Kenawy N, Cleary G, Mewar D, Beare N, Chandna A, Pearce I. Abatacept: a potential therapy in refractory cases of juvenile idiopathic arthritis-associated uveitis. Graefes Arch Clin Exp Ophthalmol. 2011;249(2):297-300.
80. Acharya M, Dave A. Commentary: Corneal involvement in rheumatoid arthritis. Indian J Ophthalmol. 2021;69(1):73-4.
81. Ho LJ, Lai JH. Small-molecule inhibitors for autoimmune arthritis: Success, failure and the future. Eur J Pharmacol. 2015;747:200-5.